2018 Changwon International Conference on Intelligent Robot and Convergence Industry (CICIRO 2018)

December 13(Thusday) ~ December 14(Friday), 2018

Changwon International Hotel, Changwon, Korea

Organized by

Korean Society of Industry Convergence(KSIC)

Robotics Research Center for Robot Intelligent Technology, Kyungnam university, Korea

Technically Co-sponsored by

Institute of Control, Robotics and Systems (ICROS)

The Korean Society of Manufacturing Technology Engineers (KSMTE)

Korea Association of Robot Industry (KAR)

Gyeongnam Robot Industry Associaition (GRIA)

Gyeongnam Robot Land Foundation (GRF)

Artificial Life and Robotics (AROB)

I. Welcome Messeges

■□ Invitation Text □■

Sung-Hyun Han, Ph.D
General Chair of CICIRO 2018

Dear distinguished scholars, ladies and gentlemen, I feel very honored and privileged to welcome all the participants to Changwon city, Korea, for the 2018 international Conference on intelligent robot and convergence industry(CICIRO 2018). As the General Chair of the conference, I an very happy and honored to open the CICIRO2018 here in Changwon.

The CICIRO2018 will bring together academicians and professionals from around the world to exchange ideas, discuss novel findings and new methods, reacquaint with colleagues, and broaden their knowledge. This conference covers a wide range of fields from robotics and intelligent control technology to convergence industry. Especially, many research papers on artificial intelligence, advanced mechatronics, smart factories, as well as technical fields such as intelligent robots, IT and NT, which are the core fields of the fourth industrial revolution, are presented in the 2018 Changwon International Intelligent Robotics Conference. This will greatly contribute to the establishment of policies to foster the nation's future new growth engine industry and local specialized industries.

It is our great honor to have world-class scholars as plenary and Invited lectures in CICIRO2018. They are Prof. Jae-Won Choi(Univ. USA), Prof. H.Y. Lee(Waseda Univ., Japan), Prof. Ju-Jang Lee(KAIST. Korea) and Prof. Nguyen Chi hung(Hanoi Univ.,Vietnam). They will share their new resear results and informations on the fields of intelligent robotics, and convergence industry technology.

In addition, the 2018 International Intelligent Robotics Conference will provide a more efficient international industry-university cooperation network, and play a pivotal role in the development of the future new industry through international technology information exchange for advanced convergence industry.

Finally, I hope all of you who have visited on this Conference will have good and rewarding time with the presentation of academic papers in this conference.

Thank you very much.

II. Conference Organization

A. Organizing Committee

General Chair :	Sung-Hyun Han, Kyungnam Univ., Korea
General Co-Chairs :	Jae-Won Choi, Univ of Akron, Ohio, USA Ju-Jang Lee, KAIST,Korea Fumitoshi Matsuno, Kyoto Univ., Japan Sung-Wan Kim, Seoul Nat'l Univ., Korea
Organizing Co-Chairs :	In-Hyeok Song, Texas State Univ., USA Guoying Gu, Shanghai Jiao Tong Univ., China Young-Hoon Park, ADD, Korea Hee-Hyeol Lee, Waseda Univ., Japan Balan Pillai, Helsingki Univ., Finland Nguyen Chi Hung, Hanoi Univ., Vietnam
Program Co-Chairs :	Kang-Hyun Jo, Ulsan Univ., Korea Min-Cheol Lee, Pusan Nat'l Univ., Korea Kyung-Soo Kim, KAIST, Korea Jae-Sil Kim, Changwon Nat'l Univ. Korea Soo-hee Han, Postech, Korea Young-Im Cho, Gachon Univ., Korea
Regional Organizing Co-Chair :	Young-Jin Moon, Asan Hospital, Korea Kang-bak Park, Korea Univ., Korea Han-Sung Kim, Kyungnam Univ., Korea Kyung-Chang Lee, Pukyong Nat'l Univ., Korea Ho Lee, Kyungbuk Nat'l Univ., Korea
Regional Program Co-chair :	Jang-sik Park, Kyungsung Univ., Korea Won-gu Lee, Kyunghee Univ., Korea
	Sung-jun Park, chonnam Nat'l Univ., Korea Dang Bao Lam, Hanoi Univ., Vietnam Seok-Jo Go, Dongeui Institute of Technology, Korea
Publicity Chair :	Ha-Young Kim, Pusan National Univ., Korea Yang-Keun Jung, Shinla tech Co., Ltd., Korea
Finance Chair :	Young-Hwa Jeong, Daeho Tec., Korea Kyu-Hyun Jung, SEYOUNG INDUSTRY Co., Ltd.,Korea
General secretary :	Chul-Kyu Jin, kyungnam Univ., Korea

B. International Organizing Committee

Man Hyung Lee, Pusan National Univ., Korea
Hussein Abbass, Univ. of New South Wales, Australia
Hajime Asema, Tokyo Univ., Japan
Hideki Hashimoto, Chuo Univ., Japan
Mark A. Bedau, Reed College, United States
Malachy Eaton, Univ. of Limerick, Ireland
Joshua M. Epstein, The Johns Hopkins Univ., United States
Takayasu Fuchida, Kagoshima Univ., Japan
Adam Grzech, Wroclaw Univ. of Technology, Poland Maki K. Habib, The American Univ. in Cairo, Egypt
Yoshiteru Ishida, Toyohashi Univ. of Technology, Japan
David John Glyndwyr James, Coventry Univ., United Kingdom
Takashi Kohno, The Univ. of Tokyo, Japan
Man Hyung Lee, Pusan National Univ., Korea
Kenneth James Mackin, Tokyo Univ. of Information Sciences, Japan
Fumitoshi Matsuno, Kyoto Univ., Japan
Kaoru Mogushi, Juntendo Univ., Japan
Fusaomi Nagata, Tokyo Univ. of Science, Yamaguchi, Japan
Ken Naitoh, Waseda Univ., Japan
Masatoshi Nakamura, Research Institute of Systems Control, Japan Kazushi Nakano, The Univ. of Electro-Communications, Japan
Masanori Nishibori, International Univ. of Health and Welfare, Japan Nobuhiro Okada, The Univ. of Kitakyushu, Japan
Chintae Choi, RIST, Korea
Hyeungsik Choi, Korea Maritime Univ., Korea
Jae Weon Choi, Pusan Nat'l Univ., Korea
Kwan-ho Chun, Chungnam Univ., Korea
Carl Crane, Univ. of Florida, USA
Baocang Ding, Jiaotong Univ., China
Junping Du, Beijing Univ. of Sci. and Tech., China
Guangren Duan, Harbin Inst. of Tech., China
Yongsoon Eun, DGIST, Korea
Antonio Franchi, LAAS-CNRS, France
Anna Friesel, Technical Univ. of Denmark, Denmark
Li-Chen Fu, Nat'l Taiwan Univ., Taiwan
Toshio Fukuda, Nagoya Univ., Japan
Furong Gao, Hong Kong Univ. of Sci. and Tech., Hong Kong
Luis Gomes, Univ. Nova Lisbon, Portugal
Jerzy Świątek, Wroclaw Univ. of Technology, Poland
Yuichiro Taira, Sojo Univ., Japan
Charles E. Taylor, Univ. of California-Los Angeles, United States
Marion Oswald, Vienna Univ. of Technology, Austria
Steen Rasmussen, Univ. of Southern Denmark, Denmark
Thomas S. Ray, Univ. of Oklahoma, United States
Shinichi Sagara, Kyushu Institute of Technology, Japan
Katsunori Shimohara, Doshisha Univ., Japan
Hideyuki Suzuki, The Univ. of Tokyo, Japan
Reiji Suzuki, Nagoya Univ., Japan
Jian Chen, City Univ. of Hong Kong, Hong Kong
Kwang-Hyun Cho, KAIST, Korea
Kyoungrae Cho, Dong Seoul College, Korea
Toshio Tsuji, Hiroshima Univ., Japan
Masafumi Uchida, The Univ. of Electro-Communications, Japan
Fumio Uchikoba, Nihon Univ., Japan Shinjiro Umezu, Waseda Univ., Japan
Keigo Kunihito Yamamori, Univ. of Miyazaki, Japan
Kazuko Yamasaki, Tokyo Univ. of Information Sciences, Japan
Masao Yokota, Fukuoka Institute of Technology, Japan
Changshui Zhang, Tsinghua Univ., China
Kyung-Seok Byun, Mokpo Nat'l Univ., Korea

C. International Program Committee

Shyi-Ming Chen, National Taiwan Univ. of Science and Technology, Taiwan
Kazuyuki Aihara, The Univ. of Tokyo, Japan
Hiroshi Kinjo, Univ. of the Ryukyus, Japan
Kentarou Kurashige, Muroran Institute Technology, Japan
Yong Liu, Univ. of Aizu, Japan
Tomoharu Nakashima, Osaka Prefecture Univ., Japan
Trung Dung Ngo, Univ. of Prince Edward Island, Canada
Walter Nistico, Univ. of Dortmund, Germany
Harutoshi Ogai, Waseda Univ., Japan
Yangmin Li, Univ. of Macau, China
Der-Cherng Liaw, Nat'l Chiao Tung Univ., Taiwan
Myo Taeg Lim, Korea Univ., Korea
Fei Liu, Jiangnan Univ., China
Tao Liu, Dalian Univ. of Tech., China
Stefano Longo, Cranfield Univ., United Kingdom
Eric T. Matson, Purdue Univ., USA
Yoshifumi Morita, Nagoya Inst. of Tech., Japan
Shigeru Omatu, Osaka Institute of Technology, Japan Luigi Pagliarini, Technical Univ. of Denmark, Denmark
Rolf Pfeifer, Univ. of Zurich-Irchel, Switzerland
Mohd Rizon, Univ. of Malaysia Perlis, Malaysia
Peter S. Sapaty, National Academy of Sciences of Ukraine, Ukraine
Jeong Yon Sim, Kangnam Univ., Korea
Ken Sugawara, Tohoku Gakuin Univ., Japan
Mikhail Svinin, Kyushu Univ., Japan
Ivan Tanev, Doshisha Univ., Japan
Hiroshi Umeo, Osaka Electro-Communication Univ., Japan
Katsuji Uosaki, Fukui Univ. of Technology, Japan
Mutsumi Watanabe, Kagoshima Univ., Japan
Hidekazu Yanagimoto, Osaka Prefecture Univ., Japan
Ikuo Yoshihara, Univ. of Miyazaki, Japan
Yong Yu, Kagoshima Univ., Japan
Tao Zhang, Tsinghua Univ., China
Jordi Albo, La Salle – Ramon Llull Univ., Spain
Takaya Arita, Nagoya Univ., Japan
Nikos Aspragathos, Univ. of Patras, Greece
Juhoon Back, Kwangwoon Univ., Korea
Hyochoong Bang, KAIST, Korea
Young-bong Bang, Seoul Nat'l Univ., Korea
Pinhas Ben-Tzvi, George Washington Univ., USA
Young Jae Lee, Konkuk Univ., Korea
Donghai Li, Tsinghua Univ., China
Hongbo Li , Tsinghua Univ., China
Hyun Myung, KAIST, Korea
Nobuaki Nakazawa, Gunma Univ., Japan
Quang Hieu Ngo, Can Tho Univ., Vietnam
Quoc Chi Nguyen, Ho Chi Minh City Univ. of Tech., Vietnam
Yoshimasa Ochi, Nat'l Defense Academy, Japan
Yasuaki Ohataki, Kanagawa Inst. of Tech., Japan
Hyung-Soon Park, KAIST, Korea
Jaehyun Park, Inha Univ., Korea
Jong Hyeon Park, Hanyang Univ., Korea
Young Im Cho, The Univ. of Suwon, Korea
Mo-Yuen Chow, North Carolina State Univ., United States Yueyue Fan, Univ. of California-Davis, United States
Rintaro Haraguchi, Mitsubishi Electric Corporation, Advanced Technology R&D Center, Japan
Noriyasu Homma, Tohoku Univ., Japan
Dong Hyuk Cha, Korea Polytechnic Univ., Korea
Chwan Hsen Chen, Yuan Ze Univ., Taiwan

III. Local Information

A. Host Province, GyeongSangnam-do

The Best Investment location

Realize your dream in Gyeongsangnam-do
where the perfect infrastructure awaits you!

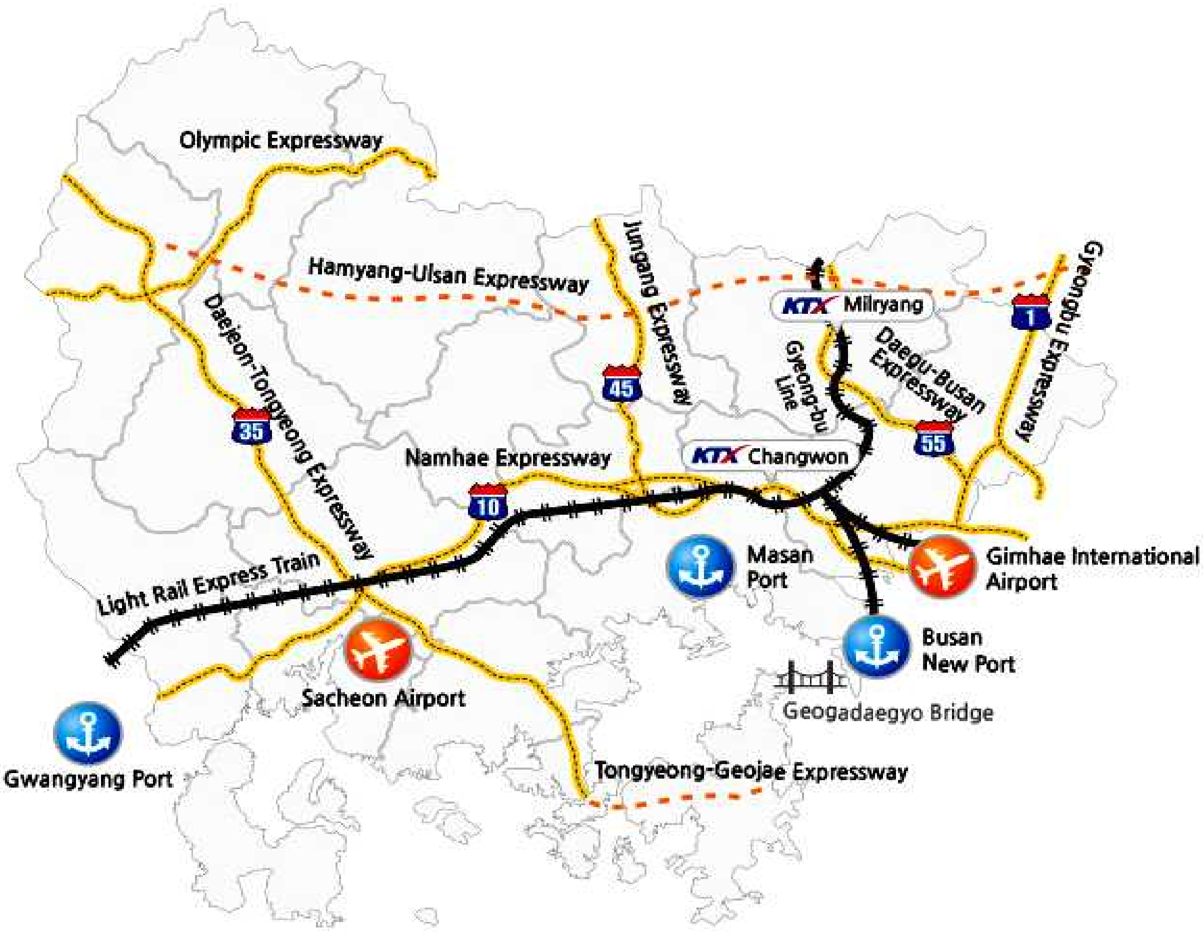

Airport
Gimhae International Airport and Sacheon Airport

Port
International ports (Busan Port, Gwangyang Port, and Masan Port)

Traffic Network
7 stations in expressway and 2 stations in KTX (Korea Train eXpress)

Industrial Complex
4,874 companies residing in 7 national industrial complexes and 158 General industrial complexes

Economic Zone
2 Free Economic Zones, 2 Foreign Investment Zones, and 1 Free Trade Zone

Gyeongnam

As of December 2012

Population	3.334 million (As of December 2013) ※ Number of foreigners registered: 69,126
Area	10,535㎢ (10.5% of Republic of Korea)
GRDP (Gross Regional Domestic Product)	KRW 95 trillion and 634.5 billion (the 3rd highest GRDP among all provinces of the Republic of Korea)
GRDP per capital	USD 26,134 (the 6th highest rate among all provinces of the Republic of Korea)
Economically active population	1.653 million (6.4% of entire economically active population in the Republic of Korea)
Total Enterprises / Number of Employees	242,123 Enterprises / 1,250,462 Employees
Trade Balance	Export: USD 51.9 billion (9.3% of entire export of the Republic of Korea) Import: USD 28.5 billion (5.5% of the entire import of the Republic of Korea)
Foreign-Invested Company	200 Companies Number of Employees: 28,762 / Production: USD 34.991 million Export: 20,724 million

CICIRO 2018

B. Host City, Changwon City

Status of tourism in Changwon City

16,088

Foreigners

6,544,353

Koreans

Tourism environment

A multitude of transportation modes

City Tour Bus

The City Tour Bus takes the tourists to major attractions of the city on circular courses and 12 selective courses. Throughout the courses, all of the city tour buses will be accompanied by a guide to provide stories about major tourist spots

Nubija Bikes

Changwon, an active advocate of eco-friendly transportation, has introduced the bike lending program to promote the use of bikes. Tourists can get a one-day pass to use Nubija bikes.

Coastal Cruise

The Coastal Cruise departs from Masan Port Cruise Terminal (Pier 2) and sails to Dotseom Islet, Machang Bridge, Makgaedo Island, Namdo Island, Modo Island and back to Machang Bridge, providing panoramic sea views along the voyage

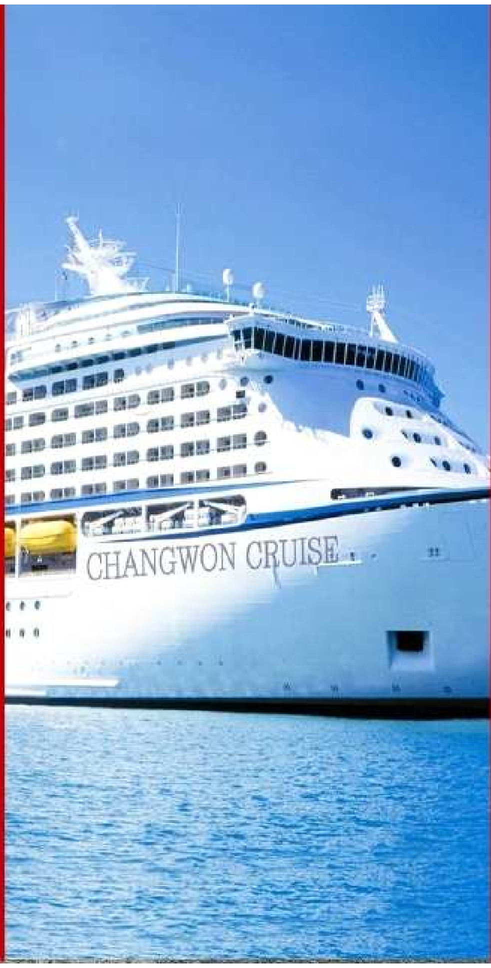

TRANSPORTATION

CICIRO 2018

C. Changwon Exhibition Convention Center(CECO)

1. Superior Industrial Infrastructure

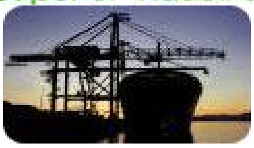

- The production base for global companies in high value-added industries including machinery, heavy industry, shipbuilding, aerospace, and robotics
- Arrangement for technical tour programs to companies that are relevant to conventions

2. EcoCity & Fantastic Tourist Resources

- Successfully holding prestigious environment conventions, RAMSAR COP 10
- A scenic and natural location
- UNESCO World Cultural Heritage(The Tripitaka Koreana)

3. Convention All-Inclusive Service

- State-of-the-art convention facilities
- Convention multi-functional complex (Hotel, Shopping&Entertainment facilities)
- Customizable menu and global level of service

4. Solid and Professional Support

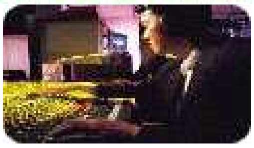

- Thorough support from beginning to end
- Experienced professionals
- Arranging systematic financial support program with Gyeongnam Convention Bureau

5. Easy Access & Various Accommodations

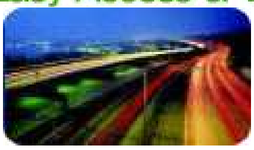

- 30 minutes(by car) from Gimhae Int'l Airport
- Regular operation of KTX, high speed train, between Seoul and Changwon
- More than 10,000 rooms from luxurious hotels within 30 minutes from CECO

-10-

D. Transportation

1. Air Transportation

Incheon Int'l Airport → Kimhae(Busan) Airport (50min.) Kimhae(Busan) Airport → CECO (30~40 min.)	There are about 5 flights per day.
Kimpo Int'l Airport → Kimhae(Busan) Airport (50min.) Kimhae(Busan) Airport → CECO (30~40 min.)	There are about 30 flights per day with 1 hour intervals.

Incheon Int'l Airport	http://www.airport.kr/eng/
Kimpo Int'l Airport	http://www.airport.co.kr/mbs/gimpoeng/
Kimhae Int'l Airport	http://www.airport.co.kr/mbs/gimhaeeng/

2. Train(KTX : High Speed Train)

Seoul → Changwon : 2 Hours 50 Minutes Station : Chanwon, Changwon Central, Masan(Within 15 Minutes from CECO)

KORAIL website	http://www.letskorail.com/ebizbf/EbizBfIndex_eng.do

3. Express Bus

Seoul(Gangnam Express Terminal or East Seoul Bus Terminal) → Changwon(5 hr) Busan → Changwon(45 min.~1 hr) (20 minute intervals from Sasang, Haeundae terminals)

IV. Program Schedule & Session Timetable

A. Program Schedule

☐ DECEMBER 14th(FRI.), 2018

<table>
<tr><td rowspan="2">10:00 ~ 11:40</td><td>< Room 3A ></td><td>< Room 3B ></td></tr>
<tr><td>ORAL SESSION (Ⅰ)</td><td>POSTER SESSION (Ⅰ)</td></tr>
<tr><td rowspan="2">13:00 ~ 14:40</td><td>< Room 3A ></td><td>< Room 3B ></td></tr>
<tr><td>ORAL SESSION (Ⅱ)</td><td rowspan="3">POSTER SESSION (Ⅱ)</td></tr>
<tr><td rowspan="2">14:40 ~ 16:00</td><td>< Room 3A ></td></tr>
<tr><td>ORAL SESSION (Ⅲ)</td></tr>
<tr><td rowspan="3">16:00 ~ 16:30</td><td colspan="2">2018 Internal Intelligent Robot Techuology Forum</td></tr>
<tr><td>< Room 3B ></td><td>< Room 3B ></td></tr>
<tr><td>Plenary Lecture
Jae-Won Choi
Univ of Akron, Ohio, USA

<Topic>
CONFORMAL 3D PRINTING OF
SMART STRUCTURES</td><td>POSTER SESSION (Ⅲ)</td></tr>
</table>

<table>
<tr><td rowspan="2">16:30 ~ 16:50</td><td>< Room 3B ></td><td>< Room 3C ></td></tr>
<tr><td>Invited Lecture (I)
Prof. Ju-Jang Lee
KAIST, Korea

<Topic>
Robust Fault-Tolerant Control for Underactuated Robot Manipulators</td><td rowspan="3">POSTER SESSION (IV)</td></tr>
<tr><td rowspan="2">16:50 ~ 17:10</td><td>< Room 3B ></td></tr>
<tr><td>Invited Lecture (II)
Prof. Kang Hyun Jo
University of Ulsan, Korea

<Topic>
Intelligent Robot Control Systems for Human Supportive Technology</td></tr>
<tr><td rowspan="2">17:10 ~ 17:50</td><td>< Room 3A ></td><td>< Room 3B ></td></tr>
<tr><td>WorkShop
Topic intelligent Technology</td><td>POSTER SESSION (V)</td></tr>
<tr><td rowspan="2">17:50 ~ 18:20</td><td>< Room 3A ></td><td>< Room 3B ></td></tr>
<tr><td>Panel Discussion</td><td>POSTER SESSION (VI)</td></tr>
<tr><td>18:20 ~ 20:00</td><td colspan="2">Welcome Reception</td></tr>
</table>

Ⅰ. Keynote Speech

December 14th(Friday) XX:XX ~ XX:XX

Professor JAE-WON CHOI

Affiliation: The University of Akron, Ohio, USA

Title :CONFORMAL 3D PRINTING OF SMART STRUCTURES

Abstract: Additive manufacturing, also called 3D printing, was originally regarded as a rapid prototyping tool since its advent in 1980's but nowadays it is beyond prototyping. Use of 3D printing technology spreads gradually into many industries as well as educations and research. This talk includes a brief history of 3D printing and its state of the art. Although 3D printing processes and materials are mature in producing 3D structures, there is lack in creating 3D smart structures including sensors, actuators, and electronics. Recently, the speaker's group at The University of Akron successfully developed a unique process and materials for producing stretchable tactile sensors. The developed process enables 3D printing of a tactile sensor on a freeform surface. In this process, a polymeric material is printed layer by layer by considering varying surface angles, where a series of algorithm for freeform slicing, offsetting, and tool path generation have been developed. In addition to the process, rheology-controlled polymers have been intensively investigated for the tactile sensor. These materials include stretchable and conductive electrodes using carbon nanotubes; stretchable and piezoresistive polymeric material using ionic liquids; and various photopolymers, whose viscosity changes under shear stress. Various stretchable tactile sensors will be highlighted as an outcome of the developed process and materials. Several applications with the developed tactile sensors will be introduced, including smart tires, smart insoles and robotic fingers. Other processes such as microstereolithography and vat-free photopolymerization developed by the speaker's group will be also introduced.

Keywords: 3D Printing, Additive Manufacturing, Smart Structure, Tactile Sensor, Piezoresistive Polymer, Stretchable Sensor

November 30(THU) 15:20 ~ 16:10 **[Chair : Kang-Hyun Jo]**

Professor Ju-Jang Lee

Affiliation: Dept. of Electrical Engineering, KAIST

Title : Robust Fault-Tolerant Control for Underactuated Robot Manipulators

Abstract: **The Development of Future Intelligent Robot Systems**

The applications of the development of “Intelligent Robot Systems” are existed various fields, such as “Silver Robot”, “Space and Military Robot”, “Ubiquitous Robot”, and “Genetic Robot”. The silver robot can improve the quality of our life and productive. The technology could promote the welfare of the aged (silver) people through the health monitoring and the assistiveequipment.

Future plans from NASA and the military call for we of space robotics. Space robotics is still a relatively small market with the potential to grow, however the government is currently the only customer. Ubiquitous Robot Systems will be the function of Intelligent Robots and internet networks.

Ubiquitous Robots(UbiBot) can be used by anyone for any service through any device and any network at anytime and anywhere in u-space. In case of Genetic Robot (Genebot), some artificial creatures which have its own genesand behaves autonomously according to internal state such as motivation and emotion.

Finally, Professor Hans Moravec predicts that machines will attain human levels of intelligence by the year 2040, and that by 2050, they will surpass we. “Machines, which will grow from us, learn our skills, and share our goals and values, can be viewed as “Child of Minds” ”, he also said.

III. Invited Lecture

December 14(FRI) 17:30 ~ 17:50 **[Chair : S.J. Park]**

Professor Kang Hyun Jo

Affiliation: University of Ulsan, Korea

Title : Intelligent Robot Control Systems for Human Supportive Technology

Abstract : Computer vision technology has been investigated for decades to search out the theoretical and application topics. Therefore it is widely challenged to use in the different fields as the real application solutions nowadays. In the presentation, it is outlined and considered the status of Vision based Intelligent Systems research and its some application widely tackled in the ICT(information communication technology) fields. While the IoT based technology is widely spoken recently, the computer vision-based technology still is major technology to lead the hot issues in the artificial intelligence and its application because of its straight forward and intuitive understanding in the predefined domains and its neighboring coverage. Here these belonging contents will be discussed and shown with some examples like intelligent surveillance system, vision application to autonomous driving car systems and robotic application for human supportive technology. In the presentation, some of the current research topics are also introduced with the real application.

Biography : Kanghyun Jo received the BS degree from Busan National University and MS and Ph.D from Osaka University, in 1989, 1993, 1997, respectively. He worked in ETRI (Electro-Telecommunication Research Center) as a Post-Doc. Research Fellow during 1997-1998. Since March of 1998, he has been with University of Ulsan, as a Faculty member, now as a Professor, in charging of an Intelligent Systems Lab.

He had served as the vice dean of e-Vehicle Graduate Institute during 2007-2009 and continuously the vice dean of College of Engineering during 2009-2011. He experienced as visiting Professor/Researcher Kyushu University and KIST during 2005-2006 and also in Oregon State University during 2008-2009 and UC Riverside during 2013-2014.

He has been also serving as a director of many societies, like ICROS (Institute of Control, Robotics and Systems), KMMS (Korean Multimedia Society), SICE (Society of Instrumentation and Control Engineers, Japan), as well as IEEE IES. He is currently contributing as an editorial member for a few renowned international journals, such as IJCAS(International Journal of Control, Automation and Systems) and TCCI (Transactions on Computational Collective Intelligence) or a guest editor of IEEE TII(Transactions on Industrial Informatics).

VII. Program Table

DECEMBER 14th(FRI.), 2018 [Session]

Oral Session I [10:00 ~ 11:40] : Room

□ Session I	Chair : Sung-Hyun Han
10:00~10:20	**A Study on Robusty Control of Humanoid Type Robot with Three-Wheel Driving Based on Voice Recognition for FA** Hee-jin Kim[1],Hyeon-wo Song[1], Du-Beum Kim[2], Yang-Keun Jeong[3], Sung-Hyun Han[4]
10:20~10:40	**A Study on A Robust Control of Mobile Robot for Physical Distribution Automation** Hee-jin Kim[1],Ho-YoungBae[2], O-Deuk Im[3],Hyun-Seok Sim[4] ,Eun-Tae Ha[5], Sung-Hyun Han[6]
10:40~11:00	**A Study on Robust Control of Intelligent Hand Gripper for Unmanned FA** Ho-young Bea[1],Jae-ik Paeng[1], Woo-Song Lee[2],Sung-HyunHan[3]
11:00~11:20	**A Study on Intelligent Control of Bipped Robot Based on voice Recoguition for Smart Factort** Jae-ik Paeng[1],Gyeong-HwaYoon[2],Du-BeumKim[3],Geun-HanDong[1],Sung-HyunHan[5]
11:20~11:40	**A Study on Intelligent Control of Robot with Four Wheel for Smart Factory** Sang-hyun Kim[1],Geun-HanDong[1],Hee-JinKim[2],Du-BeumKim[3],Sung-HyunHan[4]

Postor Session I [10:00 11:40] : Room

□ Session I	Chair : Yang-Geun Jeong
Poster 1	**A Orientation Control of Robot Arm Based on Image Feedback** Hee-Jin Kim1, Woo-Song Lee2, Sang-Hyun Kim3, Sung-Hyun Han4
Poster 2	**A Precise Position and Velocity Control of Horizontal Type Robot Arm with Five D.O.F** Jae-Ik Paeng1, Hee-Jin Kim2, Jeong-Suk Kang3, Nam-Il Yoon3, Jong-Bum Won3, Sung-Hyun Han4
Poster 3	**A Study on Learning Control of Mobile Robot** Woo-Song Lee1 Ki-Young Ko2, Ho-Young Bae3, Mun-Keun Cho4, Ki-Hyun Kim5, and Sung-Hyun Han6
Poster 4	**A Study on Motion Control of Humanoid Robot by Voice Command for Stable Walking** Yang-Geun Jeong1, Jae-Ik Paeng2, Yeon-Guk Noh3, and Sung-Hyun Han4

Oral Session II [13:00 ~ 14:40] : Room

□ Session II	Chair : Won-Sik Choi
13:00~13:20	**Growth Performance of chinese cabbage in different cultivation substrate** Wonsik Choi[1*], Jinkyu Park[2], Ji-Hee Woo[1],Eunsuk Lee[1],Jaeyoung Byun[1], Keefe Dimas Harris Sean[1]
13:20~13:40	**The adverse effects of clover grass and large crabgrass overtime of exposure in 1, 2, 3, and 4 days in saline water.** Okechukwu Nnaemeka Nicholas[1], Ji-Hee Woo[1], Jae –Young Byun[1], Eunsuk Lee[1],Choi Won Sik[1*]
13:40~14:00	**CHARACTERISTIC CONDITIONS OF CHINESE BUSH-CLOVER (*Sericea lespedeza*) FERMENTATION BY YINKIN FERMENTED POWDER** Maynanda Brigita Chrysta, Eun Suk Lee, Ji Hee Woo, Destiani Supeno, Mi Kyung Nam, Won Sik Choi
14:00~14:20	**Characteristics of Yellow Onion (*Allium cepa)* Fermentation with Uinkin for Fermentation Starter** Destiani Supeno[1], Ji-Hee Woo[1], Eunsuk Lee[1], Won Sik Choi[1]
14:20~14:40	**Performance Comparison of Cutter Head Shapes in Soybean Crusher Machine** Pandu Sandi pratama[1],Jaeyoung Byun[1],Ji-Hee Woo[1],Eunsuk Lee[1],Mi Kyung Nam, Okechukwu Nnaemeka Nicholas[1], Ji-Ung Yang[1], Won Sik Choi[1]

Oral Session III [14:40 ~ 15:40] : Room

□ Session II	Chair : Sung-Jun Pak
14:40~15:10	**An Image Anaysis for Classification of Alzheimer with Deep Learning** Marshall Wiranegara, Sanghup Lee, Baris Bardargil, Jangsik Park, Do-Young Kang
15:00~15:40	**A Feature of Biometry for Human Activity Recognition** Serkan Serdaroglu, Faruk Ince, Jangsik Park

Postor Session II [13:00 ~ 16:00] : Room

□ Session II	Chair : Sung-Jun Pak
Poster 1	**A Study on Motion Control of Bipped Robot for Human-Robot Interaction** Sang-Hyun Kim1, Byeong-Gap Moon2, Kyu-Hyun Jung3, Ju-Jang Lee5, Sung-Hyun Han6
Poster 2	**A Study on Motion Control of Three Wheel Driving Mobile Robot for Smart Factory** Ki-Won Jang1, Ho-Young Bae 2, Woo-Song Lee 3and Sung-Hyun Han4
Poster 3	**A Robust Control of Robot System with 7 Joints for Casting Trimming Automation** Jae-Ik Paeng1, Jong-Hun Kim1, Sung-Hun Noh2, Jeong-Suk Kang4, Jong-Bum Won4and Sung-Hyun Han5

- 18 -

Postor Session III [16:00 ~ 16:50] : Room

□ Session V — Chair : Kang-Hyun Jo

Poster 1	**Analysis of Traffic Sign Classification using Multiple Image Preprocessing Methods** Qing Tang1 and Kang-Hyun Jo2
Poster 2	**Exploiting Different Shape Features for Fall Action Classification** Sowmya Kasturi1 and Kang-Hyun Jo2
Poster 3	**A Study on Stable Control of Hymanoid Robot for Smart Factory** Un-Tae Ha1, Min-Seong Kim2, Byung-Suk Yoon3, Jung-Eup Gye4, Jong-Gyo Jung5 and Sung-Hyun Han6
Poster 4	**A Study on Optimal Trajectory Control of Robot System for FA** Du-Beum Kim1, Young-Hwa Jeong2, Sung-Hyun Han3

Postor Session IV [16:50 ~ 17:30] : Room

□ Session I — Chair : Woo-Song Lee

Poster 1	**A Study on Robust Control of Hand with 10 Joints** Jae-Jong Kim 1 , In-Man Park 2 , Hyun-Suk Sim 3, Sung-Hyun Han 4
Poster 2	**A Study on Stable Control of Walking Robot by Voice Command** Ho-Young Bae 1 , Woo-Song Lee 2, Sung-Hyun Han 3
Poster 3	**A Study on Control of Robot Based on Ultrasonic Sensors for FA** Sang-Hyun Kim 1 , Jeong-Seok Kang 2 , Jong-Dae Won 3 ,Sung-Hyun Han 4 ,Han-Sung Kim 4
Poster 4	**A Study on Accurate Motion Control of Mobile Robot with with Two Wheel Driving** Yang-Geun Jeong 1 , Gi-Su Shin 2 , Min-Seong Kim 2 , In-Man Park 3, Sung-Hyun Han 4

Postor Session V [17:30 ~ 18:20] : Room

□ Session II — Chair : Hyun-Suk Sim

Poster 1	**A Real-Time Control for Stable Walking of System Robot** Jea-Ik Paeng 1 , Hee-Jin Kim 2 ,Du-Beum Kim 3
Poster 2	**A Robust Neural Network Control of Robot System for Process Automation** Ki-Won Jang1, Jong-Hoon Kim1, Woo-Song Lee2, Kyung-Wha Yoon3, Uhn-Joo Na4 Sung-Hyun Han4
Poster 3	**A Study on the Trajectory Control and Control of Robot Arm with Seven Joint** Du-Beum Kim ,Keun-Hwan Dong ,Geo-Seung Choi2, Byung-Seuk Yoon3, Sung-Hyun Han4
Poster 4	**A Robust Control of Mobile Robot by Voice Command for FA** Yang-Keun Jeong 1 , Hee-Jin Kim 3 , Woo-Song Lee 4 , Yeon-Guk Noh 5 , Geo-Seung Choi 6 , In-Man Park 7 ,Sung-Hyun Han 9
Poster 5	**A Robust Motion Control of Bipped Robot with 28 Joints** Hyun-Min Kim1, Min-Seong Kim2, Hyun-Woo Song3, Yang-Keun Jung4

An Intelligent Control of Bipped Robot with 27 Joints for Cooperative walking for Smart FA

Hee-jin Kim1,Hyeon-wo Song1, Du-Beum Kim2 , Yang-Keun Jeong3, Sung-Hyun Han4

[1] Department of Advanced Engineering, Graduate School Kyungnam University, MS course, Changwon, Korea
[2] Consolidated maintenance depot., Republic of Korea Army Logistics Command, Korea
[3] Shinla Information Technology Co., Ltd., Changwon, Korea
[4] Department of Mechanical Engineering, Kyungnam University, Changwon, Korea

Abstract: In this study, we propose an voice recognition based on continuous speaking for intelligent robot with dual arm which can robustly recognize voice by adults and children in noisy environments. We evaluate the performance of robot control system in a communication robot placed in a real noisy environment. Voice is captured using a wireless microphone. To suppress interference and noise and to attenuate reverberation, we implemented a multi-channel system consisting of an outlier-robust generalized side-lobe canceller technique and a feature-space noise suppression using criteria. Voice activity periods are detected based end-point detection

Key words: Real-Time, voice recognition, Mobile Robot with Two Arm

1. INTRODUCTION

The proposed robot system has three wheels; two driven wheels fixed at both sides of the mobile robot and one castor attached at the front and rear side of the robot. The ultrasonic sensors are mounted around of the mobile robot in middle layer for the detection of obstacles with various heights. In this study, a sonar array composed of 16 ultrasonic sensors cannot be fired simultaneously due to cross talk.

These methods can utilize pre-recorded noises as described later. Since each of these techniques has advantages and disadvantages, whether it is effective depends on the types of motion and gesture. Thus, just combining these three techniques would not be effective for voice recognition under noises of all types of motion and gestures. The result of an experiment of isolated word recognition under a variety of motion and gesture noises suggested the effectiveness of this approach.[1]

2. CONTROLLER DESIGN

The primitive behaviors may be divided as follows: goal-seeking behavior, ball-following behavior, keep-away behavior, free space explorer and emergency stop, etc. The output of a primitive behavior is defined by the vector.

$$u(t) = (v(t), \Delta\theta(t))^T = (v(t), w(t), Tms)^T \qquad (1)$$

where t and T_{ms} denote the time step and the sampling time, respectively. Here, T denotes the transpose and $\omega(t)$ denotes the angular velocity of the robot.
We will divide the primitive behaviors into two basic: avoidance behavior and goal-seeking behavior.
The avoidance behavior is used to avoid the obstacles irrespective of the goal position, while the goal-seeking behavior is used to seek the goal position irrespective of obstacle location. Design of each behavior proceeds in following sequences.[2]

3. TEST AUEL RESULTS

The proposed robot has the maximum travel speed of 0.6 m/s and the maximum steering rate of 3.0rad/sec. Experiments are performed in an indoor with the first experiment for voice recognition without objects and second experiment for both of them: voice recognition and obstacles avoidance. The first experimental space is approximately 18.0m by 3.0m wide, and the second experimental space is approximately 28m by 4.8m wide. Since this environment is too simple to test the performance of the overall system, several polygon obstacles were randomly placed in the path of the mobile robot navigation.[3]

Through a series of the navigation experiments, it was observed that the heading angle error is a serious problem to the proposed robot depend on dead reckoning The large heading angle error almost resulted from the uncertain parameters when the mobile robot changes its direction Even if the wheel slippage occurs, the true position and heading angle of the mobile robot could be updated by two beacon pairs and consequently the mobile robot could arrive at the given goal position while avoiding the obstacles.[4]

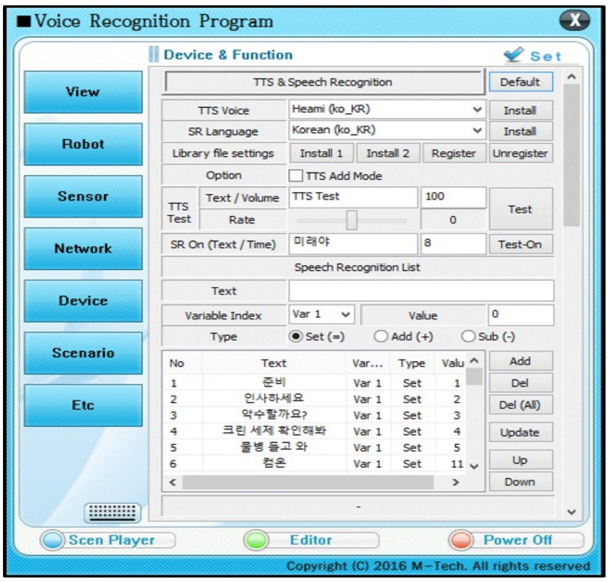

Fig. 1. The voice recognition program

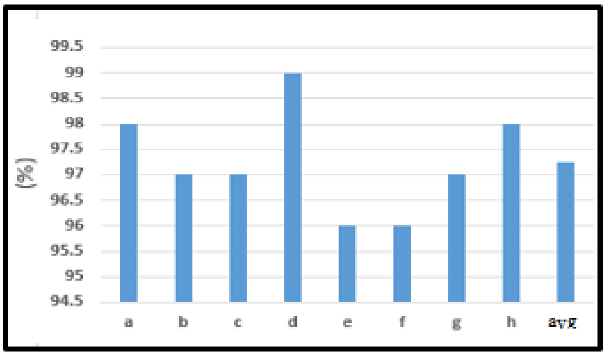

Fig. 2. The results of voice recognition

4. CONCLUSIONS

We proposed the integration of robust voice recognition and navigation system capable of performing autonomous navigation in unknown environments. In order to evaluate the performance of the overall system, a number of experiments have been undertaken in various environments.

To make mobile robot communication natural, it is necessary for the robot to recognize voice even while it is moving and performing gestures. For example, a robot's gesture is considered to play a crucial role in natural mobile robot communication [1-3]. In addition, robots are expected to perform tasks by physical actions to make a presentation. If the robot can recognize human interruption voice while it is executing physical actions or making a presentation with gestures, it would make the robot more useful.

REFERENCES

[1] M. Blanchet, J. Boudy, and P. Lockwood, “Environment adaptation for speech recognition in noise,” in Proc. of EUSIPCO-92, vol. VI,1992, pp. 391–394.

[2] R. P. Lippmann, E. A. Martin, and D. B. Paul, “Multi-style training for robust isolated-word speech recognition,” in Proc. of ICASSP-87. IEEE, 1987, pp. 705–708

[3] J. Barker, M. Cooke, and P. Green, “Robust asr based on clean speech models: An evaluation of missing data techniques for connected digit recognition in noise,” in Proc. of Eurospeech-2001. ESCA, 2001, pp. 213–216.

[4] P. Renevey, R. Vetter, and J. Kraus, “Robust speech recognition using missing feature theory and vector quantization,” in Proc. Of Eurospeech-2001. ESCA, 2001, pp. 1107–1110. S. Yamamoto, K. Nakadai, H. Tsujino, and H. Okuno, “Assessment of general applicability of robot audition system by recognizing three simultaneous speeches.” in Proc. of IEEE/RSJ International Conference on Intelligent Robots and Systems (IROS-2004). IEEE and RSJ, 2001, p. to appear..

A Study on A Robust Control of Mobile Robot for Physical Distribution Automation

Hee-jin Kim[1], Ho-Young Bae[2], O-Deuk Im[3], Hyun-Seok Sim[4]
Eun-Tae Ha[5], Sung-Hyun Han[6]

[1] Department of Advanced Engineering, Graduate School Kyungnam University, MS course, Changwon, Korea
[2] V-Mac Co., Ltd., Changwon, , Korea
[3] Consolidated maintenance depot., Republic of Korea Naval Logistics Command, Korea
[4] Co., Ltd., Hamahn, , Korea
[5] Future Technology Institute Co., Ltd, Changwon, Korea
[6] Department of Mechanical Engineering, Kyungnam University, Changwon, Korea

Abstract: This study proposes the stable autonomous travelling control based on iterative learning for a mobile robot, on uneven terrain. In this paper, a stabilization algorithm is proposed using the ground reaction forces, which are measured using sensors during moving, and the ground conditions are estimated from these data. From this information the robot selects the proper motion pattern and overcomes ground irregularities effectively. In order to generate the proper orientation angles of driving wheel. The performance of the proposed algorithm is verified by simulation and walking experiments for mobile with 18 axes.

Keywords: Intelligent control algorithm, Mobile robot, Stable moving, physical distribution automation

1. INTRODUCTION

In this study, a real-time walking stabilization method utilizing a Intelligent algorithm under uneven terrain is proposed. We focused most of our interest on landing phase. The ground reaction forces, measured by FSR sensors on the sole, are used to assess the ground condition and the robot posture. Simulation and experiment results for the proposed method are given in Section 3, followed by conclusions in the final section.

2. COUTROLLER SCHEME

Basically, a robot walks with the trajectory generated previously assuming even terrain. If different values from the expected sensor are measured during walking, the robot should be deployed using the stabilization algorithm.

When the robot is walking, it measures the ground reaction forces in real-time and utilizes them as inputs to the controller. When the control of the robot is interrupted by an unexpected situation or a unit step has ended, the new trajectory should be generated according to the changed situation.[1]

3. EXPERIMENTS

The robot walks according to a basic trajectory. In basic walking, a stride is 0.12m, velocity is 0.04m/s, and the ground is regarded as being flat. The robot steps on projected ground of 11mm in height with the tie if the swing leg. When the control algorithm is not applied, The robot pushes the ground continuously, and the heel does not contact until the end of the stride.

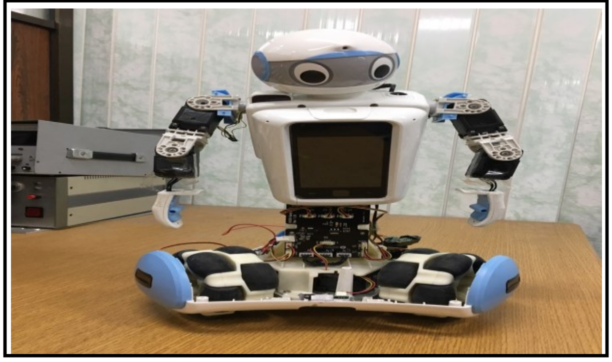

4. CONCLUSION

This paper described a real-time control technology to implement the autonomous travelling of a mobile robot on uneven terrain for unmanned Fig. It was assumed that the ground condition on the basis of ground reaction forces measured sensors on the soles of the feet during moving. The robot maintain balanced moving through control of the driving wheel.

REFERENCES

[1] M. Vukobratovic and D. Juricic, "Contribution to the synthesis of biped gait," IEEE Trans. on Bio-Medical Engineering, vol. 16,pp. 1-6, 1969

A Study on Robust Control of Intelligent Hand Gripper for Unmanned FA

Ho-young Bea[1], Jae-ik Paeng[1], Woo-Song Lee[2],Sung-Hyun Han[3]

[1] Department of Advanced Engineering, Graduate School Kyungnam University, MS course, Changwon, Korea
[2] Sunjin Technology Co., Ltd., Changwon, Korea
[3] Department of Mechanical Engineering, Kyungnam University, Changwon, Korea

Abstract: We propose a new approach to the design and real-time implementation of an controller for robotic hand based on digital signal processors in this paper. The Texas Instruments DSPs(TMS320C80) chips are used in implementing real-time intelligent control algorithms to provide enhanced motion control performance for vertical type robotic manipulators. In the proposed scheme, adaptation laws are derived from model following intelligent control principle.

Keywords: : intelligent Control, Real Time Control, Robust controller

1. INTRODUCTION

This study proposes referring specifically to the case of space applications, a scenario could be considered in which operations have to be performed in a no-gravity environment, where objects cannot be constrained and are therefore free to float in space.

The development of robotic hand finger to implement flexible operations in working cell space is foreseen to grow and cover a relevant part of the activities.[1]

At the moment, this hand finger is installed on a six degree of freedom arm, see Fig. 1. In order to emulate the capabilities of the arm and to develop suitable coordinating strategies taking into account the kinematics capabilities of the whole arm/hand finger system.

2. System Design

The hand finger has been designed considering its installation on the articulated robot arm proposed. This system aims to substitute the astronauts in periodical operations with a semiautonomous robotic device.

The end-effectors for the robot manipulator needs therefore compactness, simplicity and reduced weight as well as capability of operation even on irregular floating objects.

The hand finger has three 8 axes fingers. In each finger, the finger tip and 1 finger link can move on a linear trajectory by the linear motor but the other finger links and wrist part can move on an anger rotation trajectory by the Coreless DC Motors.[2]

In this manner, it is possible to control the motion of each finger, its distance from the object and the forces applied on it during the grasp

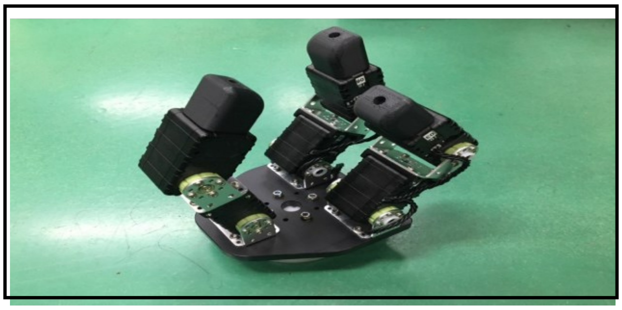

Fig. 1: The structure of hand finger

3. CONCLUSION

In this study, we proposed intelligent controllers of robot hand with several advantages for smart factory.

REFERENCES

[1] P.C.V. Parks, July 1966, "Lyapunov Redesign of Model Reference Adaptive Control System," IEEE Trans. Auto. Contr., Vol. AC-11, No. 3, pp. 362-267.

[2] Y.K. Choi, M.J. Chang, and Z. Bien, 1986, "An Adaptive Control Scheme for Robot Manipulators." IEEE Trans. Auto. Contr., Vol. 44, No. 4, pp. 1185-1191

A Study on Intelligent Control of Bipped Robot Based on voice Recoguition for Smart Factory

Jae-ik Paeng[1], Gyeong-Hwa Yoon[2], Du-Beum Kim[3], Geun-Han Dong[1], Sung-Hyun Han[5]

[1] Department of Advanced Engineering, Graduate School Kyungnam University, MS course, Changwon, Korea
[2] Kunhwa Co., Ltd., Changwon, , Korea
[3] Consolidated maintenance depot., Republic of Korea Army Logistics Command, Korea
[4] Department of Mechanical Engineering, Kyungnam University, Changwon, Korea

Abstract: This study proposes a new approach for real-time walking of a humanoid robot. In this paper, a learning control algorithm for stable handling is proposed based the backpropagation algorithm in neural network, which are measured using force sensors during moving, and the environmental conditions are estimated from these situation. From this information the robot selects the proper motion and overcomes ground irregularities effectively. In order to illustrate stable grasping and pouring into a cup. The performance of the proposed algorithm is illustrated by simulation and experiments for a dual-arm robot with twenty axes.

Keywords: Voice Recognition, Bipped Robot, Real-Time walking, Smart Factory

1. INTRODUCTION

This paper proposes an obstacle avoidance architecture allowing walking humanoid robots to walk safely around in factory and home environment.

A main technological target of the proposed robot is to autonomously explore and wander around in home environments as well as to communicate with humans.

2. DYNAMIC CONTROL

The main board of the CPU receives the resulting disparity image as a digital video signal. The stereo control parameters can be set between the main CPU and the 8bit CPU on board through a special serial communication link.

The vision system receives image from the two cameras. These parameters are useful for computing 3D range data. The disparity is calculated for each pixel in the left image by searching for the corresponding pixel in the right image. An additional reliability image is calculated following criteria to reject results on above conditions.

3. SIMULATION AND EXPERIMENT

Firstly, the disparity is converted into 3D range data using the parameters from camera calibration and then a Hough transformation is applied to all data points. Apply the *randomized Hough transformation* selects sets of data points from which the surface parameters can be directly computed and records the result in a table. If many data sets yield the same parameters, a high score for these parameters is obtained.[1]

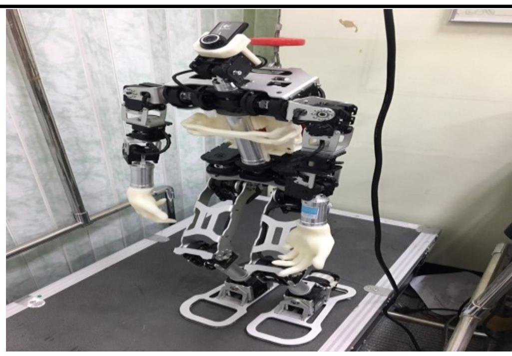

Fig. 1 The humanoid robot

4. CONCLUSION

The mobility for the dual-arm robot in the home environment is realized base on the development of a small vision system, the recognition of floor and obstacles using plane extraction for FA.

REFERENCES

[1] D. Pagac, E. Nebot and H. Durrant-Whyte, “An evidential approach to map-building for autonomous vehicles,” IEEE Transactions on Robotics and Automation, 14(4), 623-629, 1998.

A Study on Intelligent Control of Robot with Four Wheel for Smart Factory

Sang-hyun Kim[1], Geun-Han Dong[1], Hee-Jin Kim[2], Du-Beum Kim[3], Sung-Hyun Han[4]

[1] Department of Advanced Engineering, Graduate School Kyungnam University, MS course, Changwon, Korea
[2] Department of Mechanical Engineering, Industrial Graduate School Kyungnam University, Changwon, Korea
[3] Consolidated maintenance depot., Republic of Korea Army Logistics Command, Korea
[4] Department of Mechanical Engineering, Kyungnam University, Changwon, Korea

Abstract: This study proposes a new technology to control the grasping force and required position based on the mobile robot's own orientation. In this research, It was described iterative emulation control technology for mobile robot system which can robustly recognize voice by adults and children in noisy environments. We prove the performance of robot control system in a communication robot placed in limited environment.

Keywords: Robust control, Imitation learning control, Autonomous Travelling control, Cooperative Working

1. INTRODUCTION

We introduce a new method under robot motor noise. These methods can utilize pre-recorded noises as described later. Since each of these techniques has advantages and disadvantages, whether it is effective depends on the types of motion and gesture. The result of an experiment of isolated word recognition under a variety of motion and gesture noises suggested the effectiveness of this approach.

Each kind of robot motion or gesture produces almost the same noises every time it is performed. By recording the motion and gesture noises in advance, the noises are easily estimated.[1]

2. SYSTEM MODELLING

In this study, a sonar array composed of 16 ultrasonic sensors cannot be fired simultaneously due to cross talk. Instead, we adopt a scheduled firing method where sensors are activated in sequence of $\{s_1, s_{12}, s_2, s_{11} \ldots\}$. The arrangement of the ultrasonic sensors in upper layer and the sensors are marked as dots in the figure. The distances from the origin of the robot frame {Q} to obstacles detected by the sensor s_j, can be defined as Q_r is the radius of the robot and the ε_j, is the range value measured by the sensor s_j .

$$Z(t) = (X(t), \Delta q(t))^T = (X(t), Y(t), Wms)^T \tag{1}$$

3. SIMULATION AND EXPERIMENT

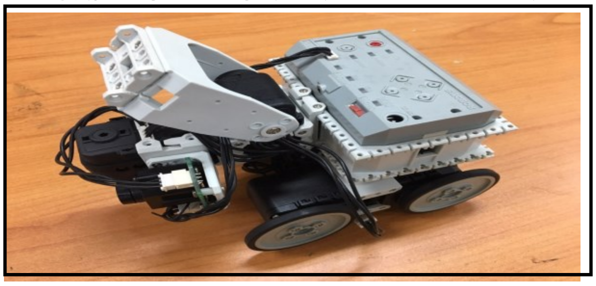

Fig. 1 Hybrid structure robot.

The proposed robot has the maximum travel speed of 0.35 m/s and the maximum steering rate of 2.0rad/sec. Experiments are performed in an indoor with the first experiment for voice recognition without objects and second experiment for both of them: voice recognition and obstacles avoidance.

4. CONCLUSION AND REMARK

In this study, we proposed a new approach to robust control of mobile robot system capable of performing autonomous travelling in uncertain environments. In order to evaluate the performance of the overall system, a number of experiments have been performed in limited environments for grasping and moving of objects.

REFERENCES

[1] M. Blanchet, J. Boudy, and P. Lockwood, "Environment adaptation for speech recognition in noise," in Proc. of EUSIPCO-92, vol. VI,1992, pp. 391–394.

A Orientation Control of Robot Arm Based on Image Feedback

Hee-Jin Kim[1], Woo-Song Lee[2], Sang-Hyun Kim3 ,Sung-Hyun Han4

[1]M.S Course, Manigement & Industry Graduate School
Kyungnam University, 51767, Korea
(E-mail : jizhen79@nate.com)
[2] SUNJIN Technology Co., Ltd., Changwon, 82331, Korea
(E-mail: elflws@nate.com)
[3] Department of Advanced Engineering., Kyungnam University, Changwon, 51767, Korea
(E-mail : kms21018@naver.com)

[4] School of Mechanical Engineering, Kyungnam University, Changwon, 51767, Korea
(E-mail: shhan@kyungnam.ac.kr)

Abstract: This study presents how it is effective to use many features for improving the accuracy of the position control for vertical type articulated robot. Some rank conditions, which relate the image Jacobian, and the control performance are derived. It is also proven that the accuracy is improved by increasing the number of features. Effectiveness of the redundant features is verified by the real time experiments on a Robot manipulator with seven joint.

Keywords: Visual Feedback Control, Redundant Feature, Feature-Based Path Planning, Real-Time Control

1. INTRODUCTION

This paper presents a method to solve this problem by using a binocular stereo vision. The use of stereo vision can lead to an exact image Jacobian not only at around a desired location but also at the other locations. The suggested technique places a robot manipulator to the desired location without giving such prior knowledge as the relative distance to the desired location or the model of an object even if the initial positioning error is large. This paper deals with modeling of stereo vision and how to generate feedback commands. The performance of the proposed visual feedback system was evaluated by the simulations and experiments and obtained results were compared with the conventional methods.

There are mainly two ways to put the visual feedback into practice. One is called look-and-move and the other is visual feedback. Visual feedback is the fusion of results from many elemental areas including high-speed image processing, kinematics, dynamics, control theory, and real-time computing.

2. PATH PLANNING

The origin of the world frame is located at a certain point in the world.

Now let ${}^l p=({}^l x, {}^l y)$ and ${}^r p=({}^r x, {}^r y)$ be the projections onto the left and right images of a point p in the environment, which is expressed as ${}^c p=({}^c x\ {}^c y\ {}^c z)^T$ in the camera frame. Then the following equation is obtained (see Fig. 1).

$$ {}^l x\ {}^c z = f\,({}^c x + 0.5\,d) \qquad (1\text{-a})$$

$$ {}^r x\ {}^c z = f\,({}^c x - 0.5 d) \qquad (1\text{-b})$$

$$ {}^l y\ {}^c z = f\ {}^c y \qquad (1\text{-c})$$

$$ {}^r y\ {}^c z = f\ {}^c y \qquad (1\text{-d})$$

Suppose that the stereo correspondence of feature points between the left and right images is found. In the visual feedback, we need to know the precise relation between the moving velocity of camera and the velocity of feature points in the image, because we generate a feedback command of the manipulator based on the velocity of feature points in the image.

This relation can be expressed in a matrix form which is called the image Jacobian. Let us consider n feature points $p_k\,(k=1,\cdots,n)$ on the object and the coordinates in the left and right images are ${}^l p_k({}^l x_k, {}^l y_k)$ and ${}^r p_k({}^r x_k, {}^r y_k)$, respectively. Also define the current location of the feature points in the image ${}^I p$ as

$$ {}^I p = ({}^l x_1\ {}^r x_1\ {}^l y_1\ {}^r y_1\ \cdots\ {}^l x_n\ {}^r x_n\ {}^l y_n\ {}^r y_n)^T \qquad (2)$$

where each element is expressed with respect to the virtual image frame $\sum_p$.

First, to make it simple, let us consider a case when the number of the feature points is one. The relation between the velocity of feature point in image ${}^I \dot{p}$ and the velocity of camera frame ${}^c \dot{p}$ is given as

$$ {}^I\dot{p} = {}^IJ_c\,{}^c\dot{p} \tag{3} $$

where J_c^I is the Jacobian matrix which relates the two frames. Now let the translational velocity components of camera be σ_x, σ_y and σ_z and the rotational velocity components be w_x, w_y, w_z then we can express the camera velocity V as

$$ \begin{aligned} V &= [\sigma_x\ \sigma_y\ \sigma_z\ w_x\ w_y\ w_z]^T \\ &= [{}^cv\ {}^cw_c]^T \end{aligned} \tag{4} $$

Then the velocity of the feature point seen from the camera frame ${}^c\dot{p}$ can be written

$$ \begin{aligned} {}^c\dot{p} &= \frac{d\,{}^cp}{dt} \\ &= \frac{d}{dt}\,{}^cR_w({}^wp - {}^wp_c) \\ &= {}^cR_w\{-{}^ww_c \times ({}^Wp - {}^wp_c)\} + {}^cR_w({}^W\dot{p} - {}^w\dot{p}_c) \end{aligned} \tag{5} $$

where ${}^cR_w$ is the rotation matrix from the camera frame to the world frame and ${}^wp_c$ is the location of the origin of the camera frame written in the world frame. As the object is assumed to be fixed into the world frame, ${}^w\dot{p}=0$. The relation between ${}^c\dot{p}$ and V is

$$ \begin{aligned} {}^c\dot{p} &= {}^cR_w\{-{}^ww_c \times ({}^wp - {}^wp_c)\} - {}^cR_w\,{}^w\dot{p}_c \\ &= -{}^cw_c \times {}^cp - {}^c\dot{p}_c \\ &= \begin{bmatrix} -w_y\,{}^cz + w_z\,{}^cy - v_x \\ -w_z\,{}^cx + w_x\,{}^cz - v_y \\ -w_x\,{}^cy + w_y\,{}^cx - v_z \end{bmatrix} \end{aligned} \tag{6} $$

Therefore, substituting Eq. (6) into Eq. (3), we have the following equation.

$$ \begin{aligned} {}^I\dot{p} &= {}^IJ_c\,{}^c\dot{p} \\ &= J\,V \end{aligned} \tag{7} $$

In Eq. (7) matrix J which expresses the relation between velocity ${}^I\dot{p}$ of the feature point in the image and moving velocity V of the camera is called the image jacobian.

From the model of the stereo vision Eq. (1), the following equation can be obtained.

$$ 2\,{}^cx\,({}^lx - {}^rx) = d\,({}^lx + {}^rx) \tag{8} $$

$$ {}^cy\,({}^lx - {}^rx) = {}^ly\,d = {}^ryd \tag{9} $$

$$ {}^cz\,({}^lx - {}^rx) = f\,d \tag{10} $$

Above discussion is based on the case of one feature point. In practical situation, however, the visual feedback is realized by using plural feature points. When we use n feature points, image Jacobian $J_1, \cdots, J_n$ are given from the coordinates of feature points in the image. By combining them, we express the image Jacobian (J_{im}) as

$$ J_{im} = [\,J_1 \cdots\cdots J_n\,]^T \tag{11} $$

Then, it is possible to express the relation of the moving velocity of the camera and the velocity of the feature points even in the case of plural feature points, that is,

$$ {}^I\dot{p} = J_{im}V \tag{12} $$

where we suppose that the stereo and temporal correspondence of the feature points are found.

In the case of the monocular, the image Jacobian J has the following form.

$$ J = f\begin{bmatrix} -\frac{1}{{}^cx} & 0 & \frac{{}^cx}{{}^cx^2} & \frac{{}^cx\,{}^cy}{{}^cz^2} & -\left(1+\frac{{}^cx^2}{{}^cz^2}\right) & \frac{{}^cy}{{}^cz} \\ 0 & -\frac{1}{{}^cx} & \frac{{}^cy}{{}^cx^2} & 1+\frac{{}^cy^2}{{}^cz^2} & -\frac{{}^cx\,{}^cy}{{}^cx^2} & -\frac{{}^cx}{{}^cz} \end{bmatrix} \tag{13} $$

3. EXPERIMENTS

We have compared the visual feedback using the monocular vision with that using the stereo vision by the experiment.

The error between the desired location and the current location of the feature points in cases of the monocular and stereo visions are shown in Fig. 2.

Two stereo images were taken and transformed to the binary images in the real time and in parallel by two image input devices and the coordinate of the gravitational center of each feature point was calculated in parallel by two transporters. We gave the stereo correspondence of the feature point in the first sampling. However, the stereo and temporal correspondence of the feature points in the succeeding sampling was found automatically by searching a nearby area where there were the feature points in the previous sampling frame. The coordinates of the feature points were sent to a transporter for motion control and it calculated a feedback command for the robot. The result was sent to the robot controller by using RS-232C, and the robot was controlled by a velocity servo system in the controller.

4. CONCLUSION

We have proposed a new technical of visual feedback with the stereo vision to control the position and orientation of an assembling robot with respect to an object. The method overcomes the several problems associated with the visual feedback with the monocular vision. By using the stereo vision, the image Jacobian can be calculated at any position. So neither shape information nor desired distance of the target object is required. Also the stability of visual feedback is illustrated even when the initial error is very large.

REFERENCES

[1] Chaumette, F., Rives, P., and Espiau, B., "Positioning of a robot with respoect to an object, tracking it and estimating its velocity by visual servoing," In *Proceedings of the IEEE International Conference on Robotics and Automation*, pp. 2248-2253, 1991.

[2] Bernard, E., Francois, C., and Patrick, R., "A new approach to visual servoing in robotics," *IEEE Transactions on Robotics and Automation*, pp. 313-326, 1992.

[3] Weiss, L. E., Sanderson, A. C., and Neuman, C. P., "Dynamic sensor-based control of robots with visual feedback," *IEEE Journal of Robotics and Automation*, pp. 404-417, 1987.

[4] Hashimoto, K., Kimoto, T. Edbine, T., and Kimura, H., "Manipulator control with image-based visual servo," In *Proceedings of IEEE International Conference on Robotics and Automation*, pp. 2267-2272, 1991.

[5] Hashimoto, K., Edbine, T., and Kimura, H., "Dynamic visual feedback control for a hand-eye manipulator," In *Proceedings of the IEEE/RSJ International Conference on Intelligent Robots and Systems*, pp. 1863-1868, 1992.

A Precise Position and Velocity Control of Horizontal Type Robot Arm with Five D.O.F

Jae-Ik Paeng1, Hee-Jin Kim2, Jeong-Suk Kang3, Nam-Il Yoon3, Jong-Bum Won3, Sung-Hyun Han4

[1] Department of Advanced Engineering, Graduate School Kyungnam University, Changwon, 51767, Korea (kms21018@naver.com) * Corresponding author
[2] School of Mechanical Engineering, Kyungnam University, Changwon, 631-701, Korea (shhan@kyungnam.ac.kr)
[3] SMEC Co., Ltd., Gimhae, 50969, Korea(jskang@esmec.com/yni@esmec.com/won@esmec.com)
[4] School of Mechanical Engineering, Kyungnam University, Changwon, 631-701, Korea (shhan@kyungnam.ac.kr)

Abstract: We describe a new approach to the design and real-time implementation of an adaptive controller for robotic manipulator based on digital signal processors in this paper. The Texas Instruments DSPs(TMS320C80) chips are used in implementing real-time adaptive control algorithms to provide enhanced motion control performance for dual-arm robotic manipulators. In the proposed scheme, adaptation laws are derived from model reference adaptive control principle based on the improved direct Lyapunov method.

Keywords: Adaptive Control, Dual-Arm Robot, Real Time Control, Real-Time Implementation

1. INTRODUCTION

This paper describes a new approach to the design of adaptive control system and real-time implementation using digital signal processors for robotic manipulators to achieve the improvement of speedness, repeating precision, and tracking performance at the joint and cartesian space.

2. MODELING

The dynamic model of a manipulator-plus-payload is derived and the tracking control problem is stated in this section.

Let us now consider payload in the manipulator dynamics. Suppose that the manipulator end-effector is firmly grasping a payload represented by the point mass ΔM_p. For the payload to move with acceleration $\ddot{X}(t)$ in the gravity field, the end-effector must apply the n×1 force vector $T(t)$ given by

$$T(t) = \Delta M_p \,[\, \ddot{X}(t) + g \,] \qquad (1)$$

where g is the n×1 gravitational acceleration vector.

The end-effector requires the additional joint torque

$$\tau_f(t) = J(q)^T\, T(t) \qquad (2)$$

where superscript T denotes transposition. Hence, the total joint torque vector can be obtained by combining equations (1) and (4) as

$$J(q)^T\, T(t) + D(q)\,\ddot{q} + N(q,\dot{q}) + G(q) = \tau(t) \qquad (3)$$

Substituting equations (2) and (3) into equation (4) yields

$$\Delta M_p\, J(q)^T [\, J(q)\,\ddot{q} + \dot{J}(q,\dot{q})\,\dot{q} + g \,] + D(q)\ddot{q} + N(q,\dot{q}) + G(q) = \tau(t) \qquad (4)$$

3. SIMULATION AND EXPERIMENT

This section represents the simulation results of the position and velocity control of a four-link robotic manipulator by the proposed adaptive control algorithm, as shown in Fig.1, and discusses the advantages of using joint controller based-on DSPs for motion control of a dual-arm robot. The adaptive scheme developed in this paper will be applied to the control of a dual-arm robot with eighth axes. Fig.1 represents link coordinates of the dual-arm robot.

Fig.1. Link coordinates of dual-arm robot

4. CONCLUSION

The proposed DSP-based adaptive controllers have several advantages over the analog control and the micro-computer based control. This allows instructions and data to be simultaneously fetched for processing. Moreover, most of the DSP instructions, including multiplications, are performed in one instruction cycle.

REFERENCES

[1] M. Vukobratovic and D. Juricic, "Contribution to the synthesis of biped gait," IEEE Trans. on Bio-Medical Engineering, vol. 16,pp. 1-6, 1969

$$ds = vdt; \quad d\phi = \dot{\phi}dt; \quad d\theta = \dot{\theta}dt \tag{2}$$

The speed v, the angular speeds $\dot{\phi}$ and $\dot{\theta}$ are used as control variables of the robot and generated by the fuzzy controller.

Perception of each ultrasonic sensor i of the mobile robot is assigned a vector ki. Its direction equals the orientation of the sensor´s axis and its length is a function of the distance di measured by this sensor:

$$k_i = \frac{d_{\max} - d_i}{d_{\max} - d_{\min}} \tag{3}$$

where dmin and dmax designate the shortest and longest distance respectively at which an object may be positioned to be reliably detected. ki is limited to 0 and 1 respectively

Since a vehicle with nonholonomic constraints cannot move itself in any direction at every time instant, it is interesting to weight the different perceptions according with the direction where the obstacle was detected. In other words, an obstacle is less important if it is placed at a location that cannot be reached by the mobile robot, but it is more dangerous if it is on a reachable position. This task can be accomplished by considering the perception angle (θi) in the computation of the perception function

$$k_i = f(d_s, \theta_i) = sat_{0,1}\left(\frac{d_{\max}(\theta_i) - d_s}{d_{\max}(\theta_i) - d_{\min}(\theta_i)}\right) \tag{4}$$

where sat0,1(x) states for the saturation of x in the range [0, 1]. In this way, it is possible to assign different perceptions, i.e. different weights, to objects detected at the same distance relative to the mobile robot but at different directions. For example, perception function ki is obtained by using the nonlinear function

$d_{\min}(\theta_i) = d_m(1-\varepsilon) \big/ (1-\varepsilon\cos\theta_i)$, and $d_{\max} = nd_{\min}(\theta_i)$ (with n>1), in Eq. (4).

$$k_i = f(d_s, \theta_i) = sat_{0,1}\left(\frac{nd_m(1-\varepsilon) - d_s(1-\varepsilon\cos\theta_i)}{(n-1)d_m(1-\varepsilon)}\right) \tag{5}$$

Furthermore, it is interesting to stress that the perception vector implies a fuzzy high level description of the environment, being independent of the type of range sensor used. So, it is possible to use different perception functions from Eq. 4 for each kind of sensor (laser, ultrasonic, infrared). Thus, sensor data fusion can be reduced to compute different vectors from the sensor measurements and to combine them to obtain the perception vector.

The previous perception can be updated as follows: consider a robot of arbitrary shape equipped with proximity sensors. Any such sensor may be located at a position U, with its axis pointing to the direction s

A frame r represents the robots position and orientation, x and θ, respectively, with respect to the world reference system w. The velocity υ of the reference point and the angular velocity $\omega_{r/w} = \dot{\varphi}$ of the robot with respect to the fixed frame w, give the state of motion. Furthermore, the virtual perception coordinate system is assumed to be located at E, pointing to the direction of attention a1. Then, an object detected by a proximity sensor at a distance ds could be detected by a virtual sensor placed at E a distance d, and with an orientation θ with respect to the vehicle's direction of attention a1.

Now the virtual perception will be updated taking into account the robots motion as follows: considering a perception function k = f(d, θ) and the corresponding inverse perception function, d = g(k, θ), and carrying out some calculations, it can be shown that the derivatives of angle and length of the perception vector are given by (assuming g ≠ 0 and $\partial g/\partial k \neq 0$).

$$\dot{\theta} = \frac{1}{g}\{(\dot{x} + \omega_{r/w} \times e)[r_1\cos(\alpha+\theta) - r_2\cos(\alpha+\theta)]\} - \omega_{r/w} - \omega_{a/r} \tag{6}$$

$$\dot{k} = -\frac{1}{\partial g/\partial k}\left\{(\dot{x} + \omega_{r/w} \times e)[r_1\cos(\alpha+\theta) - r_2\cos(\alpha+\theta)] + \frac{\partial g}{\partial k}\dot{\theta}\right\} \tag{7}$$

where $\omega_{r/w} = \dot{\alpha}$ is the angular velocity of the virtual perception coordinate system relative to the robot.

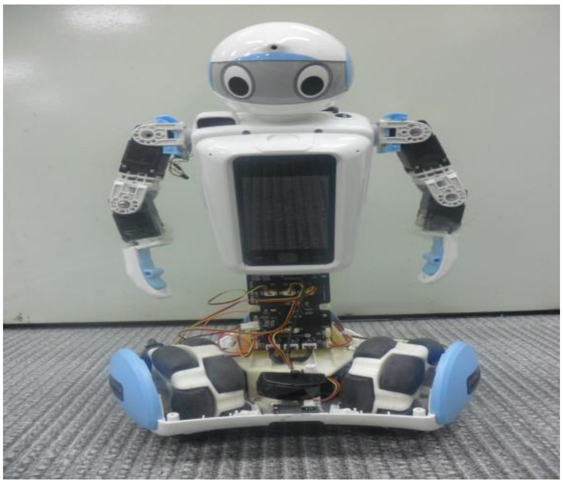

Fig. 1. The mobile robot with dual-arm

3. EXPERIMENTS

We have performed experimental results of the proposed methods to the mobile robot ROBO-N. The vehicle carries on-board a heterogeneous configuration of ultrasonic sensors. It is presented two kinds of experiment including general perception and application of fuzzy perception. All the experiments have been implemented in the ROBO-N embed.

In this, instead of a typical ring of identical sonars, there are 12 sonars of three different types, placed at different locations. Six of them are large-range sensors (0.5–2.5m), four are mid-range (0.3–1.0m), and the other two are of short-range (0.06–0.5m). Furthermore, these ultrasonic sensors use a higher frequency and have a narrower sonar beam than the commonly used sonars in these kinds of applications. The sensors are arranged in a way that six of them cover the front part of the vehicle and the other four cover its lateral sides.

Experiments result is shown in where the robot has to navigate through a corridor which is partially obstructed by an obstacle. The robot starts at point A with corridor tracking behavior, since it has equal perception at both sides. As the robot moves on it detects free space to its left and changes its behavior smoothly to follow right wall. When entering the corridor it tries again to center itself in the corridor B.

4. CONCLUSIONS

We propose a new approach to control of mobile robot of trajectory following and fuzzy perception concept with a nonholonomic mobile robot.

Experimental results, of an application to control the autonomous vehicle, demonstrate the robustness of the proposed method.

REFERENCES

[1] R. Braunstingl, "Improving reactive navigation using perception tracking", *Robotics and Manufacturing, Recent Trends in Research and Applications*, Vol. 6, pp 25-30, New York, 1996.

[2] J.J. Leonard, H.F. Durrant-Whyte, "Directed Sonar Sensing For Mobile Robot Navigation", Kluwer Academic Publishers, pp 147-155, 1992.

[3] A. Ollero, A. Garcia-Cerezo, J.L. Martinez, A. Mandow, "Fuzzy tracking methods for mobile robots", Prentice-Hall, pp 347-364, 1997.

[4] Ollero, G. Ulivi, F. Cuesta, "Fuzzy logic applications in mobile robotics", Kluwer Academic Publishers, pp. 301–324, 1999.

A Study on Learning Control of Mobile Robot

Woo-Song Lee[1] Ki-Young Ko[2], Ho-Young Bae[3], Mun-Keun Cho[4],
Ki-Hyun Kim[5], and Sung-Hyun Han[6]

[1] SUNJIN Technology Co., Ltd., Changwon, 82331, Korea
(E-mail: elflws@nate.com)
[2] Doosan Heavy Industries & Construction Co., Ltd., Changwon, 51711, Korea
(kiyoung.ko@doosan.com)
[3] V-Mac Company Co., Ltd. Changwon, 50850, Korea
(E-mail: sswq1r@hanmail.net)
[4] Doosan Heavy Industries & Construction Co., Ltd., Changwon, 51711, Korea
(E-mail: kihyeon.kim@doosan.com)
[5] ATM Korea Co., Ltd, Gumi, 642-820 Korea
(E-mail: pjm8927@naver.com)
[6] School of Mechanical Engineering, Kyungnam University,
Changwon, 631-701, Korea (E-mail: shhan@kyungnam.ac.kr)

Abstract: The main focus of this paper is obtaining a fuzzy perception of the environment in the design of each reactive behavior and solving the problem of behavior combination to implement a fuzzy behavior based control architecture. It should be remarked that, the proposed technique of the nonholonomic constraints are considered in the design of each behavior. Furthermore, in order to improve the capabilities of the intelligent control system and its practical applicability, teleoperation and planned behaviors, together with their combination with reactive ones, have been considered.

Keywords: Real-Time control, Sensor, Fuzzy Controller, Non-holonomic

1. INTRODUCTION

The real-time trajectory control is the process of determining and maintaining a path or trajectory to a goal destination. Autonomous mobile robots are required to navigate in more complex domains, where the environment is uncertain and dynamic. Autonomous navigation in these environments demands adaptation and perception capabilities. This paper describes improvements in the perception functions used in these kinds of robots. It should be noted that this is a nonholonomic vehicle with significant limitations in the reactive capabilities due to kinematic and dynamic constraints, and a few number of sensors and large blind sectors in between them, making autonomous navigation a nontrivial task. The methods presented in this paper have been conceived to deal with these limitations of conventional vehicles.

In addition, fuzzy perception can be used straightforward to perform the control of the mobile robot by means of fuzzy behavior-based scheme already presented in literature. The main differences of the proposed approach with respect to other behavior based methods are: 1 - The nonholonomic constraints are directly taken into account in the behaviors. 2 - The fuzzy perception itself can be used both in the design of each reactive behavior and to solve the problem of blending behaviors.

Hence, the fuzzy behavior-based control scheme presented in this research allows not only implement reactive behaviors but also teleoperation and planned behaviors, improving system capabilities and its practical application. Furthermore, in these behaviors, soft computing techniques play an important role to solve different problems.

2. CONTROL SCHEME

The following considerations are based on a mobile robot with the three degrees of freedom of planar movement, x, y and θ. It is equipped with a ring of 12 ultrasonic sensors which are able to perceive vertical or nearly vertical planes. The number of sensors is irrelevant as long as there are no blind sectors between them. θ refers to the orientation of this ring of sensors and not to the orientation of the robot itself, which is of no importance for the wall following algorithm. With $\dot{\phi}$ indicating the direction of movement the kinematics model of such a robot is described as follows:

$$dx = v\cos\phi dt; \quad dy = -v\sin\phi dt; \quad d\theta = \dot{\theta}dt \tag{1}$$

Since there is no modeling of the environment the absolute position of the robot does not matter. So there is no world frame used here and the kinematics model can be expressed instead as:

A Study on Motion Control of Humanoid Robot by Voice Command for Stable Walking

Yang-Geun Jeong1, Jae-Ik Paeng2, Yeon-Guk Noh3, and Sung-Hyun Han4
[1] Shinla Information Technology CO., Ltd., Changwon City, 51390, Korea (E-mail : shintech@hanmail.net)
[2] Department of Advanced Engineering., Kyungnam University, Changwon, 51767, Korea (E-mail : kms21018@naver.com)
[3] SFNT Co., Ltd., Changwon, 631-821, Korea (ykno1339@naver.com)
[4] Department of Mechanical Engineering, Kyungnam University, Changwon, 51767, Korea (shhan@kyungnam.ac.kr)

Abstract: Generally, it is possible to control the walking information based on the biped robot's own postures, because a type of motion and gesture produces almost the same pattern of noise every time. In this paper, we describe an voice recognition control technology for biped robot system which can robustly recognize voice by adults and children in noisy environments. We prove the performance of robot control system in a communication robot placed in a real noisy environment. Voice is captured using a wireless communication.

Keywords: Robust voice recognition, Side-lobe canceller, navigation system

1. INTRODUCTION

Each kind of robot motion or gesture produces almost the same noises every time it is performed. By recording the motion and gesture noises in advance, the noises are easily estimated. By using this, we introduce a new method for VRCS under robot motor noise. Our method is based on three techniques, namely, multi-condition training, maximum-likelihood linear regression, and missing feature theory. These methods can utilize pre-recorded noises as described later. Thus, just combining these three techniques would not be effective for voice recognition under noises of all types of motion and gestures. The result of an experiment of isolated word recognition under a variety of motion and gesture noises suggested the effectiveness of this approach.

2. CONTROL SCHEME

The proposed robot system has three wheels; two driven wheels fixed at both sides of the mobile robot and one castor attached at the front and rear side of the robot. The ultrasonic sensors are mounted around of the mobile robot in middle layer for the detection of obstacles with various heights. In this study, a sonar array composed of 16 ultrasonic sensors cannot be fired simultaneously due to cross talk. Instead, we adopt a scheduled firing method where sensors are activated in sequence of $\{s_1, s_{12}, s_2, s_{11} \ldots\}$. The arrangement of the ultrasonic sensors in upper layer and the sensors are marked as dots in the figure. The distances e_j $(j = 1, 2, \ldots 12)$ from the origin of the robot frame {R} to obstacles detected by the sensor s_j, can be defined as $e_j = \delta_j + R_r$. Here, R_r is the radius of the robot and the δ_j, is the range value measured by the sensor s_j .

The primitive behaviors may be divided as follows: goal-seeking behavior, ball-following behavior, keep-away behavior, free space explorer and emergency stop, etc. The output of a primitive behavior is defined by the vector.

3. EXPERIMENTS

The proposed robot has the maximum travel speed of 0.55 m/s and the maximum steering rate of 3.0rad/sec. Experiments are performed in an indoor with the first experiment for voice recognition without objects and second experiment for both of them: voice recognition and obstacles avoidance.

Through a series of the navigation experiments, it was observed that the heading angle error is a serious problem to the proposed robot depend on dead reckoning The large heading angle error almost resulted from the uncertain parameters when the mobile robot changes its direction Even if the wheel slippage occurs, the true position and heading angle of the mobile robot could be updated by two beacon pairs and consequently the mobile robot could arrive at the given goal position while avoiding the obstacles.

4. CONCLUSION

This paper proposed the integration of robust voice recognition and navigation system capable of performing autonomous navigation in unknown environments. In order to evaluate the performance of the overall system, a number of experiments have been undertaken in various environments.

REFERENCES

[1] M. Blanchet, J. Boudy, and P. Lockwood, “Environment adaptation for speech recognition in noise,” in Proc. of EUSIPCO-92, vol. VI,1992, pp. 391–394.

[2] R. P. Lippmann, E. A. Martin, and D. B. Paul, “Multi-style training for robust isolated-word speech recognition,” in Proc. of ICASSP-87. IEEE, 1987, pp. 705–708.

Growth Performance of chinese cabbage in different cultivation substrate

Wonsik Choi[1*], Jinkyu Park[2], Ji-Hee Woo[1],Eunsuk Lee[1],Jaeyoung Byun[1], Keefe Dimas Harris Sean[1],
Departement of Bio Industry Machinery engineering, Pusan National University[1], JEONG-IL GLOCHEM Co., Ltd.[2]

Abstract

Growing plant in potting media without soil is known as Soilless cultivation. This method is used mostly in greenhouse cultivation to increase horticultural commodities production. Peat moss is commonly utilized as potting media substrate because of its characteristic. However, peat moss price is high because of the quantity of peat moss in nature has been decreased. Recently, most of the research is conducted to find the alternative growing medium to cultivate horticulture plant in potting media. Perlite and rice husk ash were mentioned that had a potent as alternative growing media for seasonal plants to increase agriculture production due to the lack of production area. This research aims to determine the growth of in rice husk ash, perlite and peat moss as growing substrates. The method used was the soilless cultivation. The chinese cabbage was planted in the pot with perlite media, rice husk ash media, and peat moss media. The chinese cabbage was measured after 35 days after planting. The result showed that peatmoss was more potentials in chinese cabbage growth performance than rice husk ash and perlite. Peat moss had the significant result of every research parameters such as plant height, plant weight, number of leaves, plant diameter, root length, and root weight. The best alternative for cultivation chinese cabbage without substrate based on this research was peat moss then rice husk ash and perlite.

1. Introduction

The need for land as agricultural land will continue to increase along with the increasing human population. Today the human population has exceeded 7 billion worldwide. In addition to land requirements, the challenge in agricultural production is low water availability and land degradation [1][2]. Therefore, an appropriate crop production system must be used to achieve maximum production results. For example, efficient use of land, soil and water. So, this system can be used both in urban and rural areas. This new planting medium is expected to be used in pot media in greenhouses. Finding planting media that can replace peat moss can reduce environmental problems and reduce peat moss price increases in the market. This research aims to determine the growth of in rice husk ash, perlite and peat moss as growing substrates.

2. Material and Method

The research was conducted at the Bio Institute of Materials Manufacturing System Laboratory, Pusan National University, Miryang Campus, South Korea. This study used a completely randomized design with a single factor with three treatments that were repeated three times. The material used in this study was cabbage, rice husk, perlite, peat moss, and water. The tools used in this study were water tank, hose, bed, ruler, paper, scale, bucket and camera. Seedlings of cabbage were obtained from agricultural shops in Miryang City. Then, the cabbage seeds were transplanted to the planting media. Cabbage plants were grown in three different types of planting media, namely rice husk, perlite and peat moss. Each planting medium consists of 5 cabbages. Plants were watered twice a day at 9am and 5pm. Plants were observed after 35 days after planting. Variables observed were plant height, plant weight, number of leaves, plant diameter, root length, and root weight. Ruler was used to measure plant height, leaf width, plant diameter and root length. Then, analytical scale was used to measure plant weight and root weight. Data that has been collected will be analyzed using a spss program with a 5% error rate. Calculation data showing significant results, will then be tested using the duncan test.

3. Result and Discussion

The results showed that the application of several potting media substrates media affects the growth of (table 1). The growth variables of Chinese cabbage that are significantly influenced each research parameter. Peat moss growing substrate showed a greater result to plant height, plant weight, number of leaves, leaf width, plant diameter, root length, and root weight compared to another planting medium. While the perlite media showed a greater result to the root weight compared to rice husk ash growing substrate. In other hand, rice husk ash showed a greater result to the plant weight compared to perlite growing medium. Overall, the growing substrates that used in this research showed greatest results for four plant growth variables. Greenhouse cultivation is most widely method to increase agricultural production that can control the growth aspect [3].

Table 1 Cabbage growth under different medium

Treatment	Root length (cm)	Length of leaf (cm)	Number of leaf
Rice husk ash	23.26a	8.82b	11.20b
Perlite	9.62b	4.02c	4.20c
Peat moss	22.46a	22.46a	20.00a
Treatment	Diameter of cabbage (cm)	Root weight (mg)	Plant weight (mg)
Rice husk ash	4.16b	617.90b	6102.80b
Perlite	2.00c	1009.90b	653.99b
Peat moss	28.84a	5463.90a	9400.00a

Fig. 1. Chinese cabbage after harvested

4. Conclusions

In this research, Peat moss had more potential for than rice husk ash and perlite growing substrate according to its performance to growth. Peat moss growing substrate exposed the greatest performance for each research parameter. The differences between the result of this research and other research may be due to the substrate condition and environmental condition. Further studies also should be made to identify and evaluate the effect of using the alternative substrate as potting media in physical and chemical properties.

Acknowledgements

This work was supported by korea Institute of planning and evaluation for technology in food, Agriculture, forestry (IPET) through agriculture and Livestock machinery / equipment industry technology development program, funded by ministry of agriculture, food and rural affairs. (MAFRA)(118074-03)

[References]

1) H. Lehman, E.A. Clark, S.F. Weise, 1993, Clarifying the definition of sustainable agriculture Agric. Environ. Ethics, 6, pp. 127-143.
2) R. Lal, 2013, Beyond Intensification, Paper Presentation at the ASA, CSSA, & SSSA International Annual Meetings, Tampa, Florida, USA.
3) S. Ondono, M.-S. J.J and J. Moreno, "The inorganic component of green roof substrates impacts the growth of Mediterranean plant species as well as the C and N sequestration potential," Ecological indicator, vol. 61, pp. 739-752, 2015.

The adverse effects of clover grass and large crabgrass overtime of exposure in 1, 2, 3, and 4 days in saline water.

Okechukwu Nnaemeka Nicholas[1], Ji-Hee Woo[1], Jae -Young Byun[1], Eunsuk Lee[1],Choi Won Sik[1*]
Department of Bio Industrial Machinery Engineering , Pusan University[1]

Abstract

A comparative study was conducted on both large crabgrass and clover grass to test for adverse effects when exposed to various concentrations of yellow sea saltwater (25%, 50%, and 100%) for 1 through 4 days. A comparison was performed within each group of grass samples (A, B, C) and also between both grass groups. Our results showed a more adverse effect on both 100% and 50% of saline water concentration exposure over 25% on clover grass. Large crabgrass showed a less detrimental impact on 100% saline water concentration than both 50% and 25% concentrations. Despite day 4 showed increased adverse effects overtime on both clover grass and large crabgrass, large crabgrass exhibit less adverse effect at 100% saline water when compared to clover grass.

1. Introduction

For most of the salt-sensitive or moderately salt-tolerant species, there is no ‘safe limit’ of salinity. Certain varieties of grasses are more sensitive to salt than others. The effect varies with species. Large crabgrass is a yearly, summer-sprouting plant, having a prostrate habit with stems that root at the nodes. Its fibrous root system is similar to Poaceae family. It is believed to be a belligerent weed in certain crops particularly subtropical crops such as soya (Jehlik, 1998). It is known as a troublesome weed in corn within Europe (Mikulka et al., 2005). Shamrocks are part of the clover plant family. It refers to species Trifolium dubium, Trifolium repen, and Oxalis acetosella. In an uncontrolled environment, they are weeds. Because of their creeping design, they can cover grounds quickly. Mowing does not have an adverse effect because it can quickly recover. Lastly, their need for moisture and nutrients can be a threat to the desired plants from developing (weed extinguishers, 2018).

2. Materials and Method

2.1 Material components: 100% yellow sea water
Form: liquid water

Main component: 5% or more sodium chloride (NaCl)

Mineral: 100% highly concentrated natural minerals.

2. 2 Clover grass (sham rock)

Figure 1: Showed day 4 treatments of sample A, B, C with saline water (100%, 50%, 25% concentration) respectively.

A B C

Figure 1. Day 4 treatment

2. 3 Large crabgrass

Figure 2: Showed day 4 treatments of sample A, B, C with saline water (100%, 50%, 25% concentration) respectively.

A B C

Figure 2. Day 4 treatment

3. RESULTS

In the exposure of shamrock grass to saline water over time, sample A and B showed a higher adverse effect at both concentration of 100% and 50% respectively with changes in leaves coloration (brown) and dead leaves on the day 4. For the large crabgrass, although sample A was toxic at 100% concentration saline water when compared with sample B and C at 50% and 25% concentration, they showed more adverse effect than sample A.

4. CONCLUSION

In conclusion, this paper has centered on overtime adverse effects of two groups of grasses when exposed to saline water at various concentrations. The outcome from the investigation deduced that shamrock could be removed entirely with four days of exposure to 100% saline water in an uncontrolled environment than in large crabgrass.

[REFERENCE]

(1)https://www.nobugsnoweeds.com/is-the-shamrock-plant-a-weed.

(2) Jehlík V., 1998, Cizí a expanzivní plevele České republiky a Slovenské republiky [Alien and expansive weeds of the CR and SR], Praha, Academia.

(3) Mikulka J. & Kneifelova M. (eds.), 2005, Plevelne rostliny [Weed plants], Praha, Profi Press.

CHARACTERISTIC CONDITIONS OF CHINESE BUSH-CLOVER (*Sericea lespedeza*) FERMENTATION BY YINKIN FERMENTED POWDER

Maynanda Brigita Chrysta, Eun Suk Lee, Ji Hee Woo, Destiani Supeno, Mi Kyung Nam, Won Sik Choi
Department of Bio-Industrial Machinery Engineering, Pusan National University

ABSTRACT

Sericea lespedeza is a plant that has many benefits. This study aims to show the characteristics of changes in conditions that occur during the fermentation process of these plants. The observed conditions were sugar content, pH value, and alcohol content. The variation of fermentation was given by giving sugar at 10°Brix and 20°Brix. The fermentation process was carried out in fermentation room at 35 1.7°C for 30 days. The results of this study indicate that the characteristics of changes occur during the process for both conditions have a little common. However, the initial sugar content has an effect on the product condition. The best condition for *Sericea lespedeza* fermentation based on this research was using an initial sugar at 20°Brix.

1. Introduction

Chinese bush-clover, known as Sericea lespedeza, is a species flowering plant in the legume family. This plant is widely distributed in China, Taiwan, Japan, and Korea [1]. This plant is also known as a traditional herb that has been associated with multiple biological activities, including in Korea. From previous research also many uses have been studied from this plant, such as for ingredients that can be used in the treatment of testicular tuberculosis, enuresis, toothache, dental caries, hernias, skin ulcers, enteritis, and dysentery [2]. Not only that, the extract from this plant is also known to be used as a cosmetic ingredient, especially in terms of anti-melanogenesis, antioxidants, and anti-aging/anti-wrinkle [3]. But even so, there is still no research that tries to examine the results of the fermentation process of this plant, even though as is well known that the level of beverage consumption in Korea is also quite high. Therefore, in this study will look at the characteristic conditions of fermented Sericea lespedeza, especially in the sugar, pH, and alcohol contents during the process.

2. Material and Method

2.1 Fermentation process

The fermentation sample contains of 1 Kg of Chinese bush-clover, 10 L of water, 5 grams of salt, 5 grams of fermented powder (Yinkin, Korea), and some amount of sugar. This Chinese bush-clover was fermented using two different sugar contents, 10°Brix (Sample A) and 20°Brix (Sample B). The fermented powder used in this experiment served to increase the efficiency of the fermentation process [4]. After the fermentation samples completed, the samples stored in the fermentation room at 35 1.7°C for 30 days.

2.2 Observation of fermentation condition

The observed conditions of fermented product in this study were sugar content, pH, and alcohol content. The sugar content observation was measured using pocket refractometer (Pocket Refractometer Cat No. 3810, ATAGO, Japan) by following ISO 2173 (2003) method. The pH of the sample was measured using pH meter (NeoMet pH 250L, iSTEK, Korea). Whereas the alcohol content was determined with digital alcohol-meter PET-109 (ATAGO, Japan). The examination of each condition was done in triplicate.

3. Results and Discussion

The sugar content and pH condition of Sericea lespedeza fermented product in this study generally were decreasing during the fermentation process (Fig.1 and 2). The decreased sugar content occurs because of the conversion of sugar into alcohol and carbon dioxide [5]. While for Sericea lespedeza fermented pH condition is decreased because the organic acids are also produced during fermentation process as a result of the ethanol conversion produced from the synthesis of sugar [6].

Based on the data obtained (Fig. 3) it can be seen that the alcohol content in the sample also depends on the sugar content of the sample. While changes in alcohol levels during the process between the two variations are not much different.

4. Conclusion

From the two variations made on Sericea lespedeza fermentation, it can be seen that changes in sugar contents and pH values in sample B tended to be higher than sample A, although it was appeared that there were slight similarities in the characteristics of the changes. The alcohol content in sample B was also higher than sample A. This proves that the best condition for producing fermented products from Sericea lespedeza is the initial sugar content of 20°Brix at 35°C.

[References]

[1] Han, J.E., Chung, K.H., Nemoto, T., & Choi, B.H. 2010. Phylogenetic analysis of eastern Asian and eastern North American disjunct Lespedeza (Fabaceae) inferred from nuclear ribosomal ITS and plastid region sequences. Botanical Journal of the Linnean Society, 164(3): 221235.

[2] Marvin, E.W. & John, R.G. 1977. A Barefoot Doctor's Manual: A Guide to Traditional Chinese and Modern Medicine. Cloudburst Press. Philadelphica.

[3] Seong, J.S., Xuan, S.H., Park, S.H., Lee, K.S., Park, Y.M., & Park, S.N. 2017. Antioxidative and antiaging activities and component analysis of Lespedeza cuneata G. Don extracts fermented with Lactobacillus pentosus. J. Microbiol. Biotechnol., 27(11): 1961-1970.

[4] Hwang, S.R., Destiani, S., Kwon, S.H., Chung, S.W., Kwon, S.G., Park, J,M., Kim, J.S., and Choi, W.S. 2017. A Study on the Vinegar Fermentation Processes of Fresh Korean Ginseng Extract Using Mix Microbial Yinkin. Journal of The Korean Society of Industry Convergence, 20(4): 345-350.

[5] Gonzales-Saiz, J.M., Pizarro, C., Esteban-Diez, I., Ramirez, O., Gonzales-Navarro, C.J., Saiz-Abajo, M.J., and Itoiz, R. 2007. Monitoring of Alcoholic Fermentation of Onion Juice by NIR Spectroscopy: Valorization of Worthless Onions. J. Agricultural and Food Chem., 55: 2930-2936.

[6] Sreeramulu, G., Knol, W., and Zhu, Y. 2000. Kombucha Fermentation and Its Antimicrobial Activity. J. Agricultural and *Food Chem.,* 48(6): 2589-2594.

Characteristics of Yellow Onion (*Allium cepa)* Fermentation with Uinkin for Fermentation Starter

Destiani Supeno[1], Ji-Hee Woo[1], Eunsuk Lee[1], Won Sik Choi[1]
Department of Bio Industrial Machinery Engineering, Pusan National University[1]

Abstract

This study evaluates the effects of temperature, mother of vinegar, and amount of sugar on the fermentation of yellow onion (Alium cepa). To investigate the fermentation characteristics, samples were fermented in incubator at temperature 28C. Uinkin was added as yield. The initial brix were varied such as 0%, 12% and 24%. The fermentation is divided into periods of alcoholic fermentation and vinegar fermentation. Evaluations were done by analyzing the pH value, brix development, acidity level and microbial visual observation. The development of pH and sugar content in the vinegar influence the general bacteria and acetic acid bacteria in the early fermentation stage, while they influence the yeast in the second period of fermentation.

1. Introduction

Onions are the world's third most produced vegetable after tomatoes and watermelons owing to its excellent climate adaptability. In Korea, approximately 1,500,000 tons of onions are produced per year. However, about 15% of harvested onions are usually disposed of as agricultural waste because they fail to meet quality standard. Therefore, it is necessary to increase the value of onions by processing. Onions are rich in flavonoids, such as quercetin, sulfur compounds, and alcohol propyldisulfide, which confer health benefits in humans. Quercetin, the main flavonoid in onions, can prevent cancer and heart disease and alleviate phenomena associated with aging. In addition, onion consumption seems to have a beneficial effect in improving the diabetic state. Despite the many advantageous properties of onions, they do not have favorable organoleptic properties, owing to their unique bitter taste; this can be improved by fermentation.

2. Materials and methods

2.1 Materials

The main material for this research is yellow onion, *Allium cepa* variety purchased on local market in Miryang-si, Gyeongsangnam-do area. Supplemented materials such as granulated sugar, uinkin, mineral water, salt are needed.

2.2 Method

Blending the whole onion with mineral water, sterilize at 121°C for 15min. After first stage of fermentation done (+/- 3days) filter to remove the solids. The pH was measured by a pH-meter (ISTEK, Inc. Type: pH-250L, Korea), acidity measured by titration methods, Brix or sugar contant measured by Refractometer (ATAGO, Japan), and percentage of alcohol measured by alcohol meter (ATAGO, Japan). The fermentation was done for 8 days, and the datas was collected once a day.

3. Result and discussion

Fig. 1 shows the pH development during fermentation. In the first 24 hour the pH is significantly decreased from 6.5 to 5 and during the next day the pH is decreased slowly. Fig. 2 shows acidity development during fermentation. It shows that the final acidity for 0% brix is 1.2%, 12% brix is 1%, and 24% brix is 0.8%. Fig. 3 shows the sugar content during fermentation. It shows that the sugar level decreased during fermentation. Fig. 4 shows the percentage alcohol at final day. It shows that the alcohol level of 24% brix is higher than other sugar level.

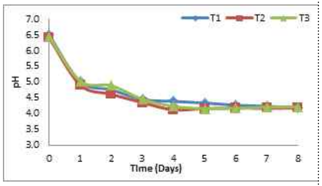

Fig. 1. pH development during fermentation

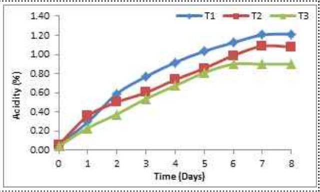

Fig. 2. Acidity development during fermentation

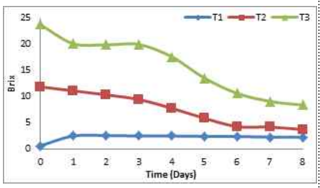

Fig. 3. Sugar content development during fermentation

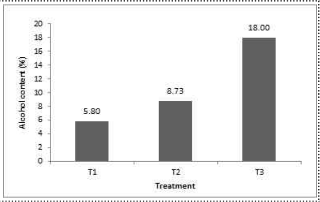

Fig. 4. Percentage of alcohol at final day

4. Conclusion

Uinkin has good properties for the fermentation of vinegar using onion, such as high acid production, good growth rate in onion juice, and high acid- and alcohol-tolerance. Onion vinegar fermented in this study showed higher functional properties, including antioxidant activities and higher organoleptic acceptability than commercial onion vinegar. In an aspect of agricultural economics, this study presented a way to utilize surplus onion which otherwise would be disposed of as agricultural waste.

Reference

1) El-Demerdash, F.M., Yousef, M.I., Abou El-Naga, N.I. "Biochemical study on the hypoglycemic effects of onion and garlic in alloxan-induced diabetic rats". Food Chem. Toxicol. Vol.43, pp. 57 - 63, 2005.
2) Griffiths, G., Trueman, L., Crowther, T., Thomas, B. "Onions—A global benefit to health". Phytother. Res. Vol. 17, pp. 603 - 615, 2002.
3) Shin, J.S., Lee, O.S., Jeong, Y.J. "Changes in the components of onion vinegars by two stages fermentation". Korean J. Food Sci. Technol. Vol. 34, pp. 1079 - 1084, 2002.

Performance Comparison of Cutter Head Shapes in Soybean Crusher Machine

Pandu Sandi Pratama[1],,Jaeyoung Byun[1],Ji-Hee Woo[1],Eunsuk Lee[1],Mi Kyung Nam, Okechukwu Nnaemeka Nicholas[1], Ji-Ung Yang[1], Joon Young Ko[1], Won Sik Choi[2]
Life Industry Convergence Research, Pusan National University[1], Department of Bio Industrial Machinery Engineering, Pusan National University[2]

Abstract

In this study, the shape of cutter head in soybean crusher machine was investigated to improve the quality of soybean powder. Two types of cutter heads was investigated such as cutter with 3 cutter head namely cutter 1 and cutter with 6 cutter head namely cutter 2. Experiment was done to clarify the effectiveness of the cutter head. The results showed that the cutter 1 particle size is mainly consist of 70mesh and cutter 2 is 100 and 150mesh. It can be concluded that cutter 2 is superior than cutter 1 in term of particle size result.

1. Introduction

In recent years, the impact of soy foods and supplements upon human health has become consideration among the general public. Soybean product has many benefits for human body such as relief of menopausal symptoms and prevention of heart disease, breast cancer, prostate cancer, and osteoporosis. To obtained high quality soybean powder the good quality of crusher machine was required. Different shape of cutter head gave different performance during crushing. In this research, performance of two cutter heads were compared to grind the soybean powder.

2. Material and Method

2.1 System Description

The developed bean crusher machine is shown in Fig. 1. The dimension of the machine was calculated optimally to maximize the capacity and the material strength. The nominal angular velocity of the crusher machine is 3000 rpm. The fine soybean powder is escape through the mesh and grain powder outlet. The pulverizer consists of side tooth, cutter and the mesh.

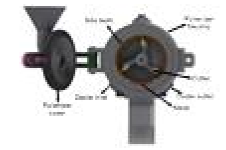

Fig. 1. Developed crusher machine

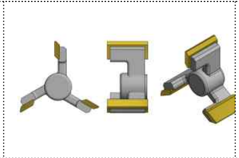

Fig. 2. Cutter head 1

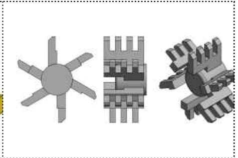

Fig. 3. Cutter head 2

2.2 Method

Two different types of cutter was developed as shown in Fig. 2 and Fig. 3. Cutter head 1 consist of 3 heads and flat shape on each head. Cutter 2 consist of 6 heads and each head are divided into 3 and 4 cutter. To understand the characteristics of each cutter head, one kilogram of soybean was feed into the crusher machine. The crusher machine was operated during 5 minutes. The soybean powder was separated using powder strainer with multiple mesh size such as 50 mesh, 70 mesh, 100 mesh, 150 mesh, and 200 mesh. The weight of soybean powder obtained from each stainer then measured using digital scale. The results then been compared and analyzed.

3. Result and Discussion

Fig. 4 shows the powder weight distribution obtained from cutter head 1. It shown that the particle size obtained from this head shape is mainly 70mesh. Fig. 5 shows the powder weight distribution obtained from cutter head 2. It shown that the particle size obtained from this head shape is mainly 100mesh and 150mesh. It can be concluded that using cutter 2 is better than cutter 1 since the particle size obtained from cutter 2 is smaller then cutter 1.

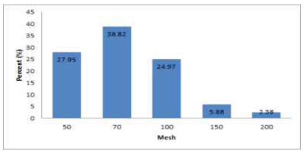

Fig. 4. Powder weight distribution of cutter 1

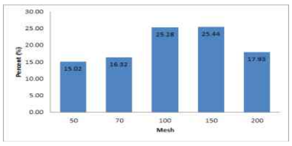

Fig. 5. Powder weight distribution of cutter 2

4. Conclusion

There are many factors that determine the overall capacity of crusher. These critical aspects include characteristics of materials to be crushed, nature or type of the crushing cutter, number of rows of crushing cutter, and Feed size. By knowing the working principle of hammer mills and various aspects that determine production, your equipment will definitely operate optimally.

Acknowledgement

This work was supported by Korea Institute of Planning and Evaluation for Technology in Food, Agriculture, Forestry and Fisheries (IPET).

References

1) Rhode M.J., "Introduction to Particle Technology". John Wiley and Sons Ltd, Chichester, West Sussex, England, 2008.
2) Niazi S. K., "Handbook of Pharmaceutical Manufacturing Formulations: Semisolid Products". Informa Healthcare USA, Inc., New York, 2009.
3) Sushant S., and K. Archana, "Methods of Size Reduction and Factors Affecting Size Reduction in Pharmaceutics". International Research Journal of Pharmacy. Vo;. 4(8), pp. 57-64, 2013.
4) Swain A.K, P. Hemlata and G.K. Roy, "Mechanical Operations". Tata McGraw Hill Education Private Limited, New Delhi, 2011.

An Image Anaysis for Classification of Alzheimer with Deep Learning

Marshall Wiranegara, Sanghup Lee, Baris Bardargil, Jangsik Park, Do-Young Kang
Dept. of Electronic Engineering, Kyungsung University
Dept. of nuclear medicine Dong-A university college of medicine, Dong-A university hospital,

Abstract: Analysis and diagnosis has always been part of the basic medical practice and also part of the initial step in recognizing the presence of any possible medical issue. Using technique of image analysis and deep learning, this paper explores the posibility of using a 3 dimensional brain model reconstructed from 110 Positron Emission Topography axial plane images and then extracting the sliced sagittal plane images of the brain model to run them through 3 different deep leraning models: AlexNet, GoogLeNet, and VGG-16 for image classification to help detecting Alzheimer's disease. The number of sagittal plane images used for this research is distributed as 685 images for Alzhaimer disease, 505 images for mild cognitive jmpairment and 330 images for normal control, VGG-16 resulted with the highest network accuracy of 78.20%, followed with GoogLeNet 73.73%, and AlexNet 64.73%. Each model detects the NC class with 100% accuracy with substantially lower MCI classification accuracy. The AD classification accuracy of VGG-16, GoogLeNet and AlexNet is 79.9%, 95.7%, and 94.2% respectively. From the inference results of the trained network, it is possible to use 3D generated model of PET images to classify Alzhaimer's disease with the help of deep learning.

Keywords: Image analysis, deep learning, CNN, Alzheimer, Positron Emission Topography.

1. INTRODUCTION

Alzheimer's Disease (AD) is the most common type of dementia. Dementia refers to diseases that are characterized by a loss of memory or other cognitive impairments, and is caused by damage to nerve cells in the brain. In the United States, an estimated 5.2 million people of all ages have AD in 2014. Mild cognitive impairment (MCI) is a condition in which an individual has mild but noticeable changes in thinking abilities. Individuals with MCI are more likely to develop AD than individuals without [1].

Early detection of the disease can be achieved by magnetic resonance imaging (MRI), a technique that uses a magnetic field and radio waves to create a detailed 3D image of the brain. A multitude of machine learning methods have been tried for this task in recent years, including support vector machines, independent component analysis and penalized regression. Some of these methods have been shown to be very effective in diagnosing AD from neuroimages, sometimes even more effective than human radiologists. For instance, recent studies have shown that machine learning algorithms were able to predict AD more accurately than experienced clinicians [2]. It is therefore of great interest to develop and improve such prediction methods[3].

Recently, a study on brain imaging using deep learning has been underway to detect Alzheimer's and brain tumors. One of them is a U-Net Based Deep Convolutional Networks which is a network that employes the skip-architecture, to solve the cell tracking problem.[4] U-net consists of a down-sampling (encoding) path and an up-sampling (decoding) path; using this method achieves 0.81 DSC for the enhancing tumor segmentation in the HGG cohort.

Early detection of Alzheimer's disease will help a lot in the treatment process. Yet, it might not be so apparent to the human eyes. Hence we rely on image analysis techniques and by using a dedicated network for recognizing Alzheimer's disease, this paper hope to provide a method of early detection for Alzheimer's disease. In this paper, we propose a method to generate 3D brain model from axial images of PET and get sagittal images. It is performed to train deep learning and compare the performance of deep learning models using axial and sagittal images as training dataset. As results of simulations, it is shown that the proposed image analysis can be utilized as classification for Alzheimer's disease.

2. IMAGES OF ALZHEIMER'S DISEASE

Diagnosis of Alzheimer's disease is commonly done with cognitive testing, medical imaging (PET, CT, or MRI), and with blood tests.

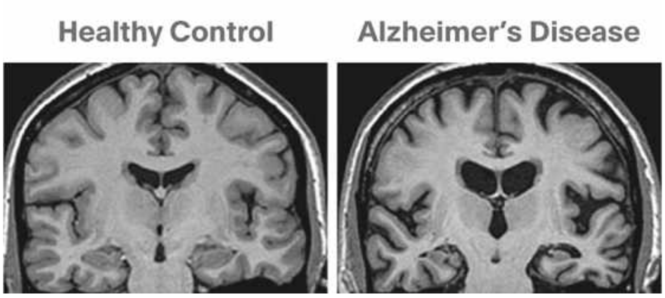

Fig. 1 Normal brain vs Alzheimer's disease on MRI. Source: Lundbeck Institute

Most of the imaging techniques involve injecting the patient a specific radioactive ink that activates when it comes to contact with calcification of amyloid-β peptide so that the affected area is visible in the resulting image as shown in Fig. 1.

3. PROPOSED BRAIN IMAGE PROCESSING

This study proposes the usage of convolutional neural network(CNN) to compare the diagnostic performance of Alzheimer's disease by various thresholds. Traditionally, axial plane images the brain have been used for giving diagnosis on brain scan. This study tries to use the other planes images of the brain in recognizing the Alzheimer's disease to analyze and selecting the result with the highest probability. Fig. 2 illustrates the orientation of the different planes.

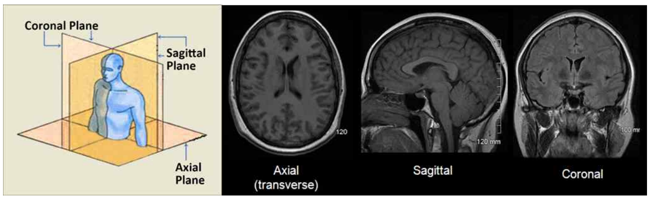

Fig. 2 Illustration of axial, sagittal, and coronal plane images

Our proposed idea is to use different planes of the brain scan result to help identifying Alzheimer's disease as shown in Fig. 3.

And to do that, first we needed to procure different plane's images as well from axial plane images only, hence the usage of 3D model generator. After that the newly generated sagittal and coronal plane images can be put through the trainer and inference engine as well.Using the more commonly available PET axial plane images, a 3D image model of the brain is reconstructed using spline interpolation. The reconstructed 3D brain model is then sliced along the sagittal and coronal planes to produce the dataset images. The 3D model and sagittal plane images are obtained by a program which is implemented by analyzing DICOM format images using implementation on C#.

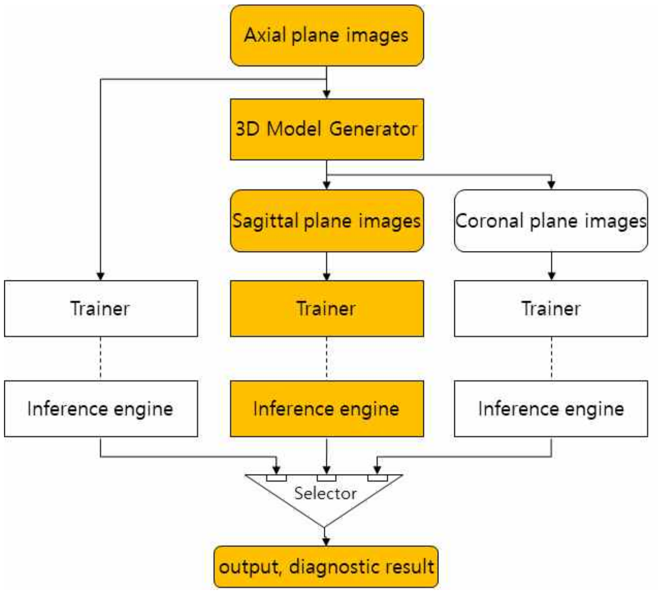

Fig. 3 Block diagram of the proposed PET image analysis

4. EXPERIMENTAL RESULTS AND CONSIDERATIONS

The sagittal images shown in Fig. 4 are used to train some deep learning.

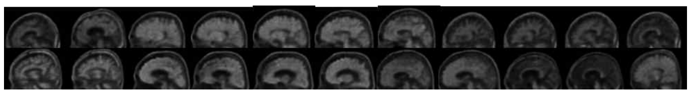

Fig. 4 Examples of triaining dataset.

The following are the training graph process of the networks using the cropped sagittal plane images. The accuracy of AlexNet is 64.73%, While the accuracy of GoogLeNet is 73.73%, 1. And the accuracy of VGG-16 is 78.20%

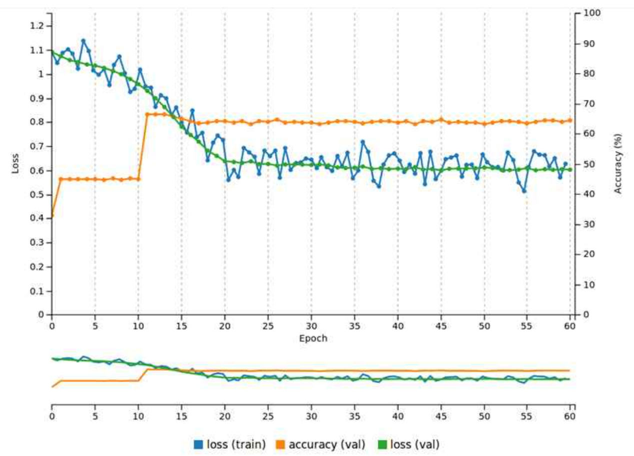

(a)

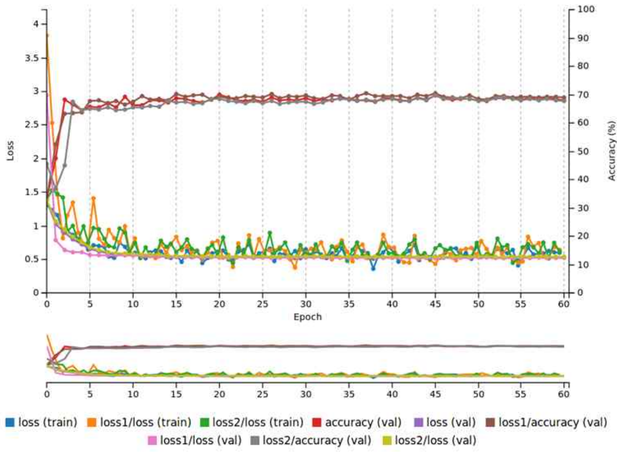

(b)

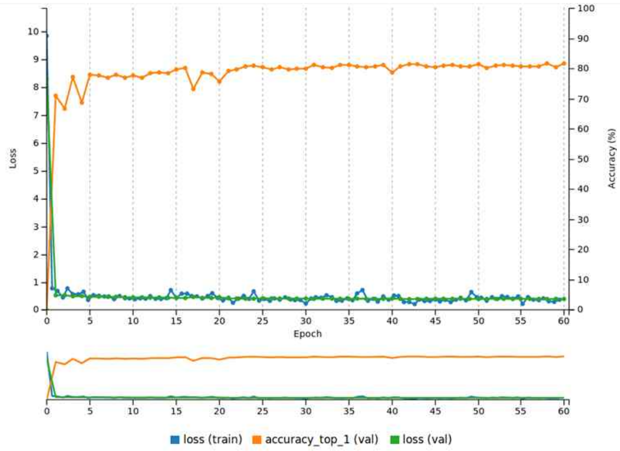

(c)

Fig. 4 Learning curvers of deep learning models, (a) AlexNet, (b) GoogLeNet, (c) VGG-16

The training result from original results in AlexNet having the highest accuracy among them, while using the cropped images resulted in VGG with the best accuracy, albeit distributed among the three subsets.

Table 1. Performance comparison results

DL Model	AD	MCI	NC
AlexNet	94.2%	0.0%	100.0%
GoogLeNet	95.7%	25.5%	100.0%
VGG16	79.7%	54.9%	100.0%

5. CONCLUSION

The main purpose of this experiment is to improve Alzheimer's disease detection from PET images through the use of 3D modelling and sagittal plane images analysis with CNN. AlexNet, GoogLeNet, and VGG-16 were chosen as the networks. Accuracies are 64.73%, 73.73% and 78.20% respectively. For each model, NC classification accuracy was 100%, but MCI classification accuracy was significantly lower. AD accuracy of AlexNet, GoogLeNet and VGG-16 model is 94.2%, 95.7% and 79.9%. Future works are improving the quantity and quality of the datasets. Using the two three planes together to get a better threshold.

ACKNOWLEDGEMENTS

This work has supported by the National Research Foundation of Korea(NRF) grant funded by the Korea government(MSIT)(No. A Study of PET Image Analysis Based on Deep Learning for Alzheimer Disease Diagnosis and Estimation) and Brain Busan 21+ 2018.

REFERENCES

[1] Alzheimer's Association. "2014 Alzheimer's Disease Facts and Figures," *Alzheimer's and Dementia*, vol. no. 2, 2014.

[2] Stefan Kloppel, Cynthia M Stonnington, Josephine Barnes, Frederick Chen, Carlton Chu, Catriona D Good, Irina Mader, L Anne Mitchell, Ameet C Patel, Catherine C Roberts, et al. "Accuracy of dementia diagnosis - a direct comparison between radiologists and a computerized method," *Brain,* vol. 131 no. 11, pp. 2969–2974, 2008.

[3] Adrien Payan and Giovanni Montana, "Predicting Alzheimer's Disease : a Neuroimaging Study with 3D Convolutional Neural Networks," *proc. of int. conf. on Pattern Recognition Applications and Methods*, ICPRAM 2015, Lisbon, Portugal, vol. 2, pp. 355-362, Jan. 2015.

[4] Hao Dongm, Guang Yang, Fangde Liu, Yuanhan Mo, Yike Guo, "Automatic Brain Tumor Detection and Segmentation Using U-Net Based Fully Convolutional Networks", MIUA2017, 069, vol. 3, 2017.

A Feature of Biometry for Human Activity Recognition

Serkan Serdaroglu, Faruk Ince, Jangsik Park

Department of Electronic Engineering, Kyungsung University

Abstract: Human behavior recognition has gaining an important role for computer vision in order to support medical purposed and video surveillance systems. It is proposed for an approach for a biometric method to understand human behavior or activity. The proposed method with the help of machine learning leads to determine a pattern on various behavior using angles between inter-joints of human. Fundamentally, behavior correlated joint angles are gathered from Kinect V2. Human activity recognition with a time interval, angle of joint is stored in every 20 frames. Collected information builds the feature set with includes activities, are essential for human behavior recogntion. For training and testing support vector machine is used. As results of simulations, the accuracy of the proposed method is 99.99% with 6 different human activities.

Keywords: Human activity recognition, support vector machine, inter-joint angles.

1. INTRODUCTION

Human behavior recognition (HBR) intends to recognize human behavior which are relying on activities, using adopting model. Utilitarian solutions can be applied for numerous human centered life issues such as video medical systems, surveillance systems and eldercares. Behavior recognition can be completed successfully. As an example, by utilizing the information gathered from Kinect v2 device that has benefits for making a classification on human activities such as standing, walking, laying, walking upstairs and walking downstairs etc. [1]. It can also be accomplished by using RGB and RGB-depth cameras by means of body parts' signals though a supervised machine learning algorithms.

Human activity understanding includes activity recognition and activity pattern discovery. Human behavior recognition (HBR) aims to detect human behavior with high accuracy by implementing a predefined behavior model. To do this, the recognition of human behavior, at first creation of a high level conceptual model is needed and then run the model by creating a common system. Meanwhile, the discovery of the behavior patterns that are associated more directly with finding the unknown pattern from the low level sensor data without pre-defined models or assumptions. Therefore, a common system should be established before analyzing the sensor data to find patterns of activity. Despite differences in the approaches of each technique, the target is the same technology to the development of human behavior. [1].

In this study, we did a biometric system that uses the angle between the skeletal joints to recognize human behavior using the Microsoft Kinect v2 devices. After obtaining angles, it is temporarily stored in a queue and is used as a feature set. Support Vector Machine algorithm through, activity patterns are resolved. In the test process, the system controls the activity patterns of people and decides what action is for every 20 frames.

This paper is organized as follows: In section 2, the previous approaches to the recognition of human behavior recognition, and human activity Kinect v2 Using the RGB-Depth camera is described in detail. Dataset definition of the proposed method is specified and real-time performance of experimental environment with the results of recognition of human behavior. In the last chapter, conclusions and thoughts about the proposed method is discussed.

2. HUMAN ACTIVITY RECOGNITION

Up to now, it has published numerous approaches to the analysis of human activity recognition. In the first example, Gaglio, Lo Re and Morana [2], using 3-D position data held for human behavior recognition. Hidden Markov Model and K-means clustering and Support Vector Machines as they performed three different algorithms. Absolute / recall as performance results are 77.3% and 76.7 respectively.

Sung, Ponce, and Saxena [3], the hierarchical maximum entropy Markov Models (Memmi) uses the idea emerged. First, the RGB-Depth camera (Kinect) received the information from the skeleton and they thought that human activity consists of a series of sub-activities.

Twelve different methods were tested on human activity and the mean accuracy was 84.3%. between the joints, to obtain information of the skeleton is quite necessary. So Microsoft Kinect v2 provides great convenience to obtain the skeleton data using its own software development kit. Microsoft Kinect v2 sensor can detect 25 different skeletal joints and can be seen in figure (1). Kinect not only recognize people, it can also watch them. Infrared (IR) sensor, it is possible to detect up to six people on stage, but two of them traceable.

Range of the sensor can be determined by adjusting the IR sensor. In the default setting, standing between 0.8 meters and 4.0 meters a person can recognize, but Microsoft recommendation is from 1.2 to 3.5 meters.

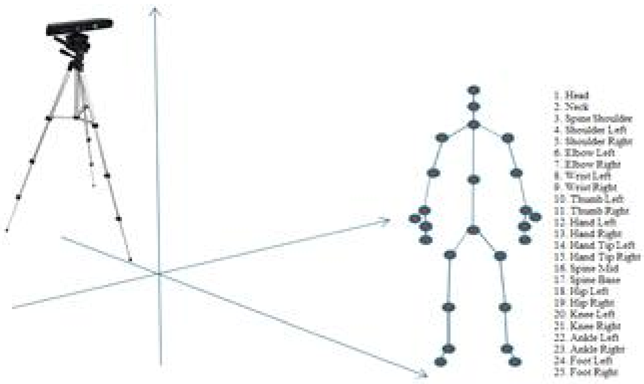

Fig.1 Microsoft Kinect v2 skeleton joint map in the scene.

After obtaining; frame data is switched by applying mathematical equations can be obtained. The joint angles make periodic fluctuations in the time domain. These fluctuations make the recognition of human behavior oscillations is different every possible activity.

A Support Vector Machine (SVM) is a machine learning algorithm which learns by instance to appoint labels to objects [4]. SVM offers a statistical learning theory that declines the structural risk training error which eventually expresses an upper bound for the general minimization error [5].

A penalty term for misclassification determining a tradeoff between resolution and generalization performance [5,6] is the only parameter that needs to be set. The aforementioned algorithm continuously looks into a unique decision surface in order to support cluster vectors, and defines classification output relative to fractional data points added for support vectors with inputs obtained from samples extracted from training data

3. PROPOSED HUMAN ACTIVITY RECOGNITION

The method employed in this study estimates joint angles' sequences information to recognize human behavior by codifying into Support Vector Machine classifier. Compared with the other methods, suggested method uses lower cost calculations because of robust, and effective feature set. A skeletal representation of a person consists of 25 joints and angle representation is offered by Microsoft Kinect framework, namely Vitruvius. Features are selected in accordance with the relevance of the human activities. As RGB-depth sensor is employed, the angle becomes scale and rotation invariant. It is because skeletal joint information is detected and tracked by depth sensor. Thus, location or direction of the person in the scene cannot have an effect on the performance result of the proposed study. More detailed information regarding the structure of proposed approach is suggested in Fig. 2.

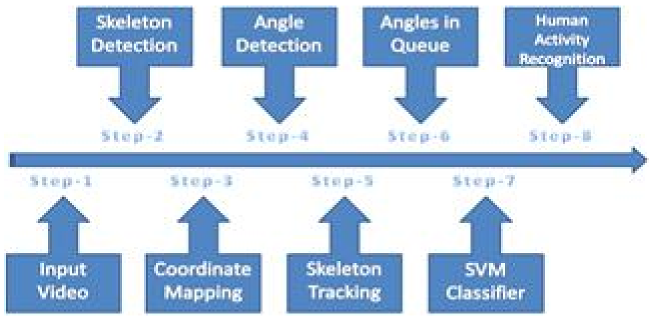

Fig. 2 Chattering in output of SMC whereas PDSMC is smooth

First of all, when a person appears in front of the sensor, the 2D color image needs to be projected onto the body. This is required for skeleton detection and monitoring. In particular, since the Kinect combines several sensors in a single device such as an RGB color camera (1920 × 1080), a depth sensor (512 × 424), and an infrared sensor (512 × 424), the resolutions are different and not perfectly aligned. As a result, the field of view will be different.

The projection of the human body joints in the RGB image requires a depth sensor, which is because Kinect uses the dept sensor to monitor the body. However, in 3D space, the coordinates of the human body (x, y, z) will not be aligned in the 2D color image. I mean, the skeleton is completely out of place. Because Microsoft is aware of the situation, the software development kit has a proper utility called Coordinate Mapper. Basically, it reflects the points in the corresponding 3D space in the 2D color image.

As noted in Chapter 2, Kinect, infrared (IR) camera can detect up to six people. Two of these from 6 people can be followed specifically. In terms of the Kinect v2 detects the 25 joints and skeleton tracks however early Kinect v1 can detect up to 20 skeletal joints.

To select the feature set is the most important part for identification. Selected activities are walking, standing, jumping, lifting, sitting and hand clapping. It is need to select the angle between the inter-joints of behavior. Consequently angles of, both shoulders, elbows and knee was chosen as sequestering properties.

After angle is obtained, the next step is to store it in a queue for this array. In this case, each frame is obtained wherein the number is 6 × n, where n represents the queue capacity. 20 is assigned to queue capacity, which forms a frame 120 for each feature. This first-in, first worked as a concept is the object collection. For example, the data will be considered as a bridge and cars. The first cars will appear at the entrance of the bridge. Probably, properties are ignored in the first frame and the frame is dequeued 21. In each frame, multi-label SVM classifier will classify the feature vectors stored in the queue data structure. For example, if the queue capacity is set to 20, then starting from the 21stframewillbedecidedbythenumberofthefeaturetohumanactivities.Basic flowchart of queue concept can be seen in Fig. 3.

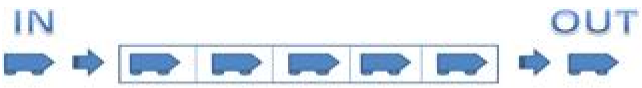

Fig. 3: Working concept of queue object collection. First data in, leaves first (FIFO).

In this study, multiple labeled SVM algorithms with Gaussian kernel have been used to identify the human activity. Multi-label classification is assigned a set of goals to label each sample. In other words, mutually acceptable non-shared data point qualities. Basically, in this method, not only it gives an output which is the data of the assigned class. Therefore, the threshold value is applied to get the expected tag. In this case, the threshold value is the probability of 85%. Assigned does not pass the threshold, the system "unknown events" will return a label called. Moreover, the SVM algorithm so labeled, Gaussian kernel is executed. The reason for this is that it can draw non-linear models of some event. I.e., it can get better accuracy by using nonlinear kernels. However, core parabolic, cubic core and so on. Using does not comply with the nature of human activity. Therefore Gaussian kernel is executed.

4. EXPERIMENTAL RESULTS AND CONSIDERATIONS

This chapter discusses the results from experiments carried out. Video recordings for this experiment are all done by Kyungsung University, Department of Electronic Engineering taken at Kyungsung University campus, Busan, Republic of Korea. Implementation of Microsoft Kinect SDK 2.0 and Vitruvius were done using Microsoft Visual Studio 2013. The Microsoft Kinect v2 stands 1.7 meters above the ground with the experiment subject located straight in front of it. 5 uniquely classified human behaviors were taken independently. The sequence of each behavior last for about 10 seconds, which translates roughly to 900 to 1,220 frames. Each behavior is repeated a number of times within the allocated 10 seconds, while the variance occured due to the differing speed of each subjects at completing the routine for each sequence. Each behavior of each subjects were recorded 10 times. Fig.4 shows the demonstration of the behavior involved in the experiment.

Fig. 4 Six unique human behaviors that were uniquely classified. From left to right, top to bottom: walking, jumping, sitting, lifting, hand-clapping, and standing.

The program for evaluating the human behavior shows the angular values calculated at the top part of the window. There are 4 main buttons for this application: system training, system testing, performance validation, and show all joint angles when more than one subject exist inside the image. Furthermore, there exists the start and stop buttons which can interrupt whatever process currently running (i.e. training, testing, etc.). They can be attributed as the switch for the whole system. From the experimental results, the proposed approach produced 99.999482% accuracy for six different human behaviors, as shown in Fig. 4.

5. CONCLUSION

This paper proposes a new method to recognize human behaviors by using RGB-Depth camera. Nowadays, video surveillance systems are expected to do more than providing security recordings. Having the ability to identify the human behavior happening will help surveillance camera in preventing possible crimes and possibly help on the medical field. To ensure correct identification of each behavior, it is necessary to classify human behavior with distinct and easily identified features. In this direction, this paper takes general human behavior as its main focus. By scaling the trained behavior at different sizes, the system is expected to be able to identify differing behavior at differing distance from the camera. Performance of the system is measured by calculating the testing data which yield a satisfactory result of 99.999482 % accuracy for six uniquely classified human behaviors. Through this method, it is possible to expand the classified human behaviors and build a more robust and intelligent system

ACKNOWLEDGEMENT

This work was supported by KEIT grant funded by the Korea Government(No. 20001497, ATC program, Development of IoT basic Bio Lab system for people and animal welfare, safety) and Brain Busan 21+ 2018.

REFERENCES

[1] Gaglio, Salvatore et al. “Human Activity Recognition Process Using 3-D Posture Data.” IEEE Trans. Human-Machine Systems 45, pp. 586-597, 2015

[2] Gaglio, Salvatore, Giuseppe Lo Re, Marco Morana, “Human Activity Recognition Process Using 3-D Posture Data,” IEEE Trans. Human-Machine Systems 45, pp. 586-597, 2015

[3] Jaeyong Sung, Colin Ponce, Bart Selman, and Ashutosh Saxena. “Human activity detection from RGBD images”. In Proceedings of the 16th AAAI Conference on Plan, Activity, and Intent Recognition (AAAIWS'11-16). AAAI Press 47-55. 2011

[4] Cortes, C and Vapnik V "Support-vector networks", Machine Learning. 20 (3): pp. 273–29 , 1995

[5] Genov, R., Gert, C.: Kerneltron: Support Vector “Machine” in Silicon. IEEE Transactions on Neural Networks 14(5), 2003

[6] Girosi, F., Jones, M., and Poggio, T., “Regularization Theory And Neural Networks Architectures”, Neural Comput. 7, pp. 219–269, 1995

A Study on Motion Control of Bipped Robot for Human-Robot Interaction

Sang-Hyun Kim[1], Byeong-Gap Moon[2], Kyu-Hyun Jung[3],
Myeong-Hwan Park[4], Ju-Jang Lee[5], Sung-Hyun Han[6]
[1] Department of Advanced Engineering, Graduate School Kyungnam University, Changwon, 51767, Korea (kms21018@naver.com)
[2] KWANGJIN PRECISION Co., Ltd., Changwon, 51220, Korea (kkj362@naver.com)
[3] SEYOUNG INDUSTRY Co., Ltd., Changwon, 51211, Korea (sysky25@naver.com)
[4] ROBOT VALLEY Co., Ltd., Changwon, 51572, Korea (mhpark01@korea.com)
[5] KAIST, Daejun, 34141, Korea(jjlee@ee.kaist.ac.kr)
[6] Department of Mechanical Engineering, Kyungnam University, Changwon, 51767, Korea (shhan@kyungnam.ac.kr)

Abstract: This paper deals with the stable walking for a biped robot, on uneven terrain, A biped robot necessitates achieving posture stabilization since it has basic problems such as structural instability. In this paper, a stabilization algorithm is proposed using the ground reaction forces, which are measured using FSR (Force Sensing Resistor) sensors during walking, and the ground conditions are estimated from these data. From this information the robot selects the proper motion pattern and overcomes ground irregularities effectively. In order to generate the proper angel of the joint. The performance of the proposed algorithm is verified by simulation and walking experiments on a 24-DOFs biped robot.

Keywords: Force sensing resistor, Fuzzy algorithm, Biped robot, Stabilization

1. INTRODUCTION

In this paper, a real-time walking stabilization method utilizing a fuzzy algorithm under uneven terrain is proposed. We focused most of our interest on landing phase. The ground reaction forces, measured by FSR sensors on the sole, are used to assess the ground condition and the robot posture. Simulation and experiment results for the proposed method are given in Section 3, followed by conclusions in the final section.

2. WALKING PATTEN

Basically, a robot walks with the trajectory generated previously assuming even terrain. If different values from the expected sensor are measured during walking, the robot should be deployed using the stabilization algorithm. Fig.1 presents the walking algorithm.

When the robot is walking, it measures the ground reaction forces in real-time and utilizes them as inputs to the controller. When the control of the robot is interrupted by an unexpected situation or a unit step has ended, the new trajectory should be generated according to the changed situation.

3. BIPED ROBOT AND SYSTEM

The robot walks according to a basic trajectory. In basic walking, a stride is 0.12m, velocity is 0.04m/s, and the ground is regarded as being flat. The robot steps on projected ground of 11mm in height with the tie if the swing leg. When the control algorithm is not applied, the sensor data is presented as given in Fig.2, The robot pushes the ground continuously, and the heel does not contact until the end of the stride.

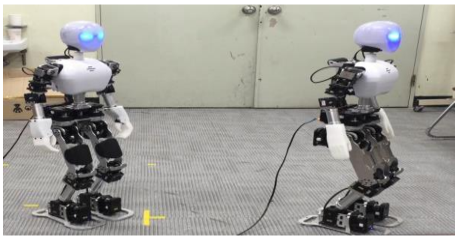

Fig. 1 The biped robot for cooperative working.

4. CONCLUSION

This paper described a real-time control technology to implement the walking of a biped robot on uneven terrain. It was assumed that the ground condition on the basis of ground reaction forces measured sensors on the soles of the feet during walking. The robot could maintain balanced walking through control of the ankle joints using a fuzzy algorithm.

REFERENCES

[1] M. Vukobratovic and D. Juricic, "Contribution to the synthesis of biped gait," IEEE Trans. on Bio-Medical Engineering, vol. 16,pp. 1-6, 1969

2018 Changwon International Conference on Intelligent Robot and Convergence Industry (CICIRO 2018)
Dec 13(Thusday) ~ Dec 14(Friday), 2018 Changwon International Hotel, Changwon, Korea

A Study on Motion Control of Three Wheel Driving Mobile Robot for Smart Factory

Ki-Won Jang1, Ho-Young Bae 2, Woo-Song Lee 3and Sung-Hyun Han4

[1] Doosan Heavy Industries & Construction Co., Ltd., Changwon, 51711, Korea
(E-mail: kihyeon.kim@doosan.com)
[2] V-Mac Company Co., Ltd. Changwon, 50850, Korea (E-mail: sswq1r@hanmail.net)
[3] SUNJIN Technology Co., Ltd., Changwon, 82331, Korea
(E-mail: elflws@nate.com)
[4] School of Mechanical Engineering, Kyungnam University,
Changwon, 631-701, Korea (E-mail: shhan@kyungnam.ac.kr)

Abstract: In this paper, we describe an voice recognition control technology for Mobile robot system which can robustly recognize voice by adults and children in noisy environments. We evaluate the performance of robot control system in a communication robot placed in a real noisy environment. Voice is captured using a wireless microphone. To suppress interference and noise and to attenuate reverberation, we implemented a multi-channel system consisting of an outlier-robust generalized side-lobe canceller technique and a feature-space noise suppression using criteria. Voice activity periods are detected based end-point detection

Key words: Robust voice recognition, Side-lobe canceller, navigation system

1. INTRODUCTION

To make mobile robot communication natural, it is necessary for the robot to recognize voice even while it is moving and performing gestures. For example, a robot's gesture is considered to play a crucial role in natural mobile robot communication [1-3]. In addition, robots are expected to perform tasks by physical actions to make a presentation. If the robot can recognize human interruption voice while it is executing physical actions or making a presentation with gestures, it would make the robot more useful.

Each kind of robot motion or gesture produces almost the same noises every time it is performed. By recording the motion and gesture noises in advance, the noises are easily estimated. By using this, we introduce a new method for VRCS under robot motor noise. Our method is based on three techniques, namely, multi-condition training, maximum-likelihood linear regression[5], and missing feature theory. These methods can utilize pre-recorded noises as described later. Since each of these techniques has advantages and disadvantages, whether it is effective depends on the types of motion and gesture. Thus, just combining these three techniques would not be effective for voice recognition under noises of all types of motion and gestures. The result of an experiment of isolated word recognition under a variety of motion and gesture noises suggested the effectiveness of this approach.

2. CONTROL SCHEME

The proposed robot system has three wheels; two driven wheels fixed at both sides of the mobile robot and one castor attached at the front and rear side of the robot. The ultrasonic sensors are mounted around of the mobile robot in middle layer for the detection of obstacles with various heights. In this study, a sonar array composed of 16 ultrasonic sensors cannot be fired simultaneously due to cross talk. Instead, we adopt a scheduled firing method where sensors are activated in sequence of $\{s_1, s_{12}, s_2, s_{11} \ldots\}$. The arrangement of the ultrasonic sensors in upper layer and the sensors are marked as dots in the figure. The distances e_j $(j = 1, 2, \ldots 12)$ from the origin of the robot frame {R} to obstacles detected by the sensor s_j, can be defined as $e_j = \delta_j + R_r$. Here, R_r is the radius of the robot and the δ_j, is the range value measured by the sensor s_j .

A local map is introduced to record the sensory information provided by the 16 sonar sensors with respect to the mobile robot frame $\{R\}$. Sector map defined locally at the current mobile robot frame is introduced. Then, the obstacle position vector se'_j with respect to the frame $\{R\}'$ can be calculated by

$$Se_j' = \begin{bmatrix} \cos\delta\theta & \sin\delta\theta & 0 & -\sin\delta\theta/\rho_p \\ -\sin\delta\theta & \cos\delta\theta & 0 & (1-\cos\delta\theta)/\rho_p \\ 0 & 0 & 1 & 0 \\ 0 & 0 & 0 & 1 \end{bmatrix} \quad (1)$$

where se_j denotes the obstacle position vector defined at the frame $\{ R \}$. When the mobile robot is located at a point $0'$. the distance value $se'_j = \| se'_j \|$ from the origin of the frame $\{R\}'$ to the obstacle and angle $s\varphi'$ can be calculated by Eq.(1) . Here, $\|.\|$ denotes Euclidean norm.

The local map defined at the frame $\{R\}'$ is newly constructed by using the previous local map defined at the frame (R) as follows:

$$Se_n \leftarrow Se'_j, n = INT(\frac{s\varphi'_j}{\bar{\varphi}}) + \frac{N}{2}; \; j = 1,2,\ldots,N \qquad (2)$$

Where ← and *INT* denote the updating operation and integer operation, respectively. Here, se_n, denotes the distance value of n sector and N represents the number of the sector. If the range values obtained by sensors when the mobile robot is located at a point o' are e_j = (j = 1,2 ,... 12) , the new local map is partially updated as follows : $se_j \leftarrow e_j$, j = 1,2 .... 12. The maximum range of the sonar sensor is set to be $\delta_{max} = \delta_{max} - R_r$. Any return range which is larger than is ignored.

The primitive behaviors may be divided as follows: goal-seeking behavior, ball-following behavior, keep-away behavior, free space explorer and emergency stop, etc. The output of a primitive behavior is defined by the vector.

$$u(t) = (v(t), \Delta\theta(t))^T = (v(t), w(t), Tms)^T \qquad (3)$$

where t and T_{ms} denote the time step and the sampling time, respectively. Here, T denotes the transpose and $\omega(t)$ denotes the angular velocity of the robot.

We will divide the primitive behaviors into two basic: avoidance behavior and goal-seeking behavior.

The avoidance behavior is used to avoid the obstacles irrespective of the goal position, while the goal-seeking behavior is used to seek the goal position irrespective of obstacle location. Design of each behavior proceeds in following sequences; (A) fuzzification of the input/output variables, (B) rule base construction through reinforcement learning, (C) reasoning process, (D) defuzzification of output variables.

In order for the mobile robot to arrive at the goal position without colliding with obstacles, we must control the mobile robot motion in consideration of the obstacle position X_{oi}, = (x_{oi}, y_{oi}) , the mobile robot position X = (x , y) and its heading angle θ with respect to the world coordinate frame $\{W\}$ shown in Fig. 1.

In order to avoid the increase in the dimension of input space, the distance values d_i , (i = 1.2,3,4) are defined by

$$\begin{aligned} d_1 &= \min(se_1, se_2, se_3) \\ d_2 &= \min(se_4, se_5, se_6) \quad 4a \\ d_3 &= \min(se_7, se_8, se_9) \quad 4b \\ d_4 &= \min(se_{10}, se_{11}, se_{12}) \end{aligned} \qquad (4)$$

$\phi_m (-\pi \le \phi_m \le \pi)$ denotes the orientation of a sector with the shortest range. We choose the input variables for avoidance behavior as ϕ_m and $d_i = \|X_{0i} - X\|, (i = 1,2,3,4)$ for goal-seeking behavior as heading angle difference ψ and distance to goal $z = \|X_g - X\|$. The input linguistic variables d_i, ψ, ϕ_m and z are expressed by linguistic values (VN, NR, FR), (NB, NM, ZZ, PS, PM, PB), (LT, CT, RT) and (VN, NR, FR, VF), respectively Their membership functions are expressed as shown in fig. 1.

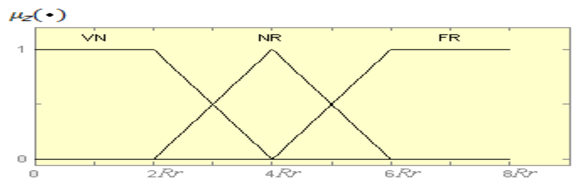

(a) The distance value

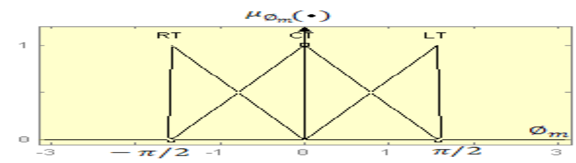

(b) The orientation of the sector with the shortest range value

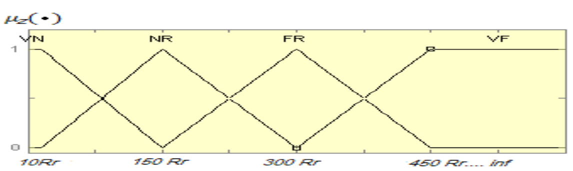

(c) The distance to goal position

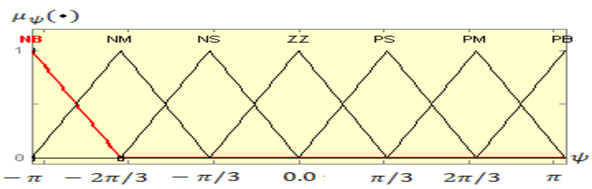

(d) The heading difference

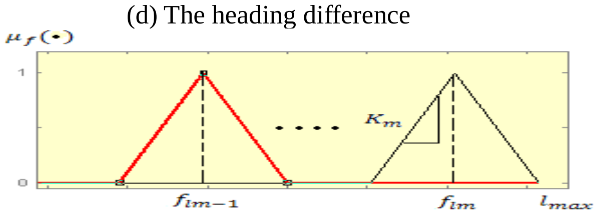

(e) The linear velocity of mobile robot for the k-th behavior

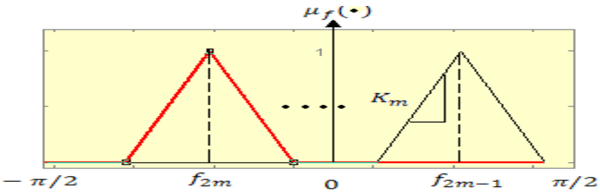

(f) The incremental steering angle for k-th behavior
Fig. 1 The membership functions of the input-output variables

3. EXPERIMENTS

The proposed robot has the maximum travel speed of 0.6 m/s and the maximum steering rate of 3.0rad/sec. Experiments are performed in an indoor with the first experiment for voice recognition without objects and second experiment for both of them: voice recognition and obstacles avoidance. The first experimental space is approximately 9.0m by 1,5m wide, and the second experimental space is approximately 14m by 2.4m wide. Since this environment is too simple to test the performance of the overall system, several polygon obstacles were randomly placed in the path of the mobile robot navigation.

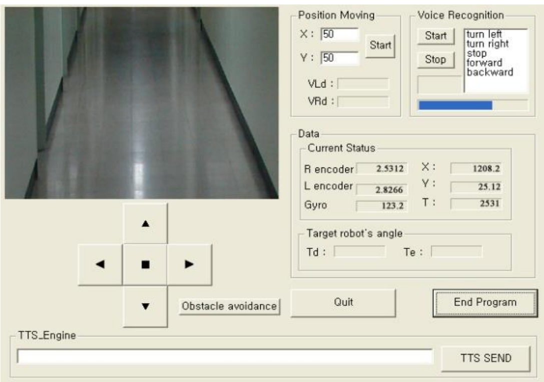

Fig. 4. Voice recognition interface

Through a series of the navigation experiments, it was observed that the heading angle error is a serious problem to the proposed robot depend on dead reckoning The large heading angle error almost resulted from the uncertain parameters when the mobile robot changes its direction Even if the wheel slippage occurs, the true position and heading angle of the mobile robot could be updated by two beacon pairs and consequently the mobile robot could arrive at the given goal position while avoiding the obstacles.

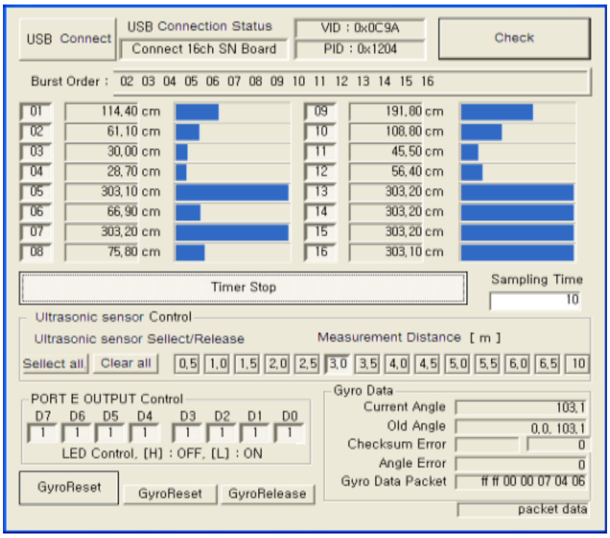

Fig. 3. Obstacle detection using ultraasonic sensors

4. CONCLUSIONS

This paper proposed the integration of robust voice recognition and navigation system capable of performing autonomous navigation in unknown environments. In order to evaluate the performance of the overall system, a number of experiments have been undertaken in various environments.

REFERENCES

[1] M. Blanchet, J. Boudy, and P. Lockwood, “Environment adaptation for speech recognition in noise,” in Proc. of EUSIPCO-92, vol. VI,1992, pp. 391–394.

[2] R. P. Lippmann, E. A. Martin, and D. B. Paul, “Multi-style training for robust isolated-word speech recognition,” in Proc. of ICASSP-87. IEEE, 1987, pp. 705–708.

[3] J. Barker, M. Cooke, and P. Green, “Robust asr based on clean speech models: An evaluation of missing data techniques for connected digit recognition in noise,” in Proc. of Eurospeech-2001. ESCA, 2001, pp. 213–216.

[4] P. Renevey, R. Vetter, and J. Kraus, “Robust speech recognition using missing feature theory and vector quantization,” in Proc. Of Eurospeech-2001. ESCA, 2001, pp. 1107–1110.

A Robust Control of Robot System with 7 Joints for Casting Trimming Automation

Jae-Ik Paeng1, Jong-Hun Kim1, Sung-Hun Noh2, Jeong-Suk Kang4,
Jong-Bum Won4and Sung-Hyun Han5

[1] Department of Advanced Engineering, Graduate School Kyungnam University,
Changwon, 51767, Korea (kms21018@naver.com/ kimjh4750@naver.com) * Corresponding author
[2] YoungChang Robotech Co., Ltd., Gimhae, 50969, Korea(giosugo@naver.com)
[3] ANY TOY CO. Ltd., Kyungnam University, Changwon, 51767, Korea
(E-mail : Shings@naver.com)
[4] SMEC Co., Ltd., Gimhae, 50969, Korea(jskang@esmec.com/won@esmec.com)
[5] Department of Mechanical Engineering, Kyungnam University,
Changwon, 51767, Korea (shhan@kyungnam.ac.kr)

Abstract: We describe a new approach to the design and real-time implementation of an adaptive controller for robotic manipulator based on digital signal processors in this paper. The Texas Instruments DSPs(TMS320C80) chips are used in implementing real-time adaptive control algorithms to provide enhanced motion control performance for vertical type robotic manipulators. In the proposed scheme, adaptation laws are derived from model reference adaptive control principle based on the improved direct Lyapunov method

Keywords: : Adaptive Control, Dual-Arm Robot, Real Time Control, Real-Time Implementation

1. ROBOT MODELING DYNAMICS

The dynamic model of a manipulator-plus-payload is derived and the tracking control problem is stated in this section.

Let us now consider payload in the manipulator dynamics. Suppose that the manipulator end-effector is firmly grasping a payload represented by the point mass ΔM_p. For the payload to move with acceleration $\ddot{X}(t)$ in the gravity field, the end-effector must apply the n×1 force vector $T(t)$ given by

$$T(t) = \Delta M_p [\ \ddot{X}(t) + g\ ] \qquad (1)$$

where g is the n×1 gravitational acceleration vector.

The end-effector requires the additional joint torque

$$\tau_f(t) = J(q)^T\, T(t) \qquad (2)$$

2. SIMULATION AND EXPERIMENT

This section represents the simulation results of the position and velocity control of a four-link robotic manipulator by the proposed adaptive control algorithm, as shown in Fig.1, and discusses the advantages of using joint controller based-on DSPs for motion control of a dual-arm robot. The adaptive scheme developed in this paper will be applied to the control of a vertical type robot with seven axes. Fig.1 represents link coordinates of the vertical type robot.

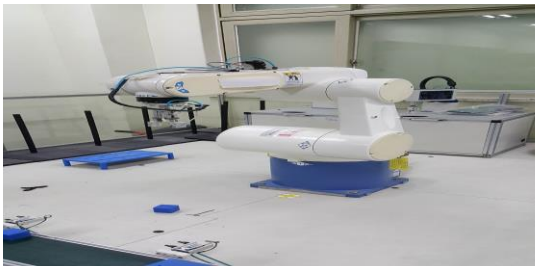

Fig. 1 link coordinates of the vertical type robot.

3. CONCLUSION

The proposed DSP-based adaptive controllers have several advantages over the analog control and the micro-computer based control. This allows instructions and data to be simultaneously fetched for processing. Moreover, most of the DSP instructions, including multiplications, are performed in one instruction cycle.

4. ACKNOWLEDGEMENT

This study was performed by project of the robot business belt construction enterprise. And supported by the Ministry of Trade, Industry and Energy. (R0004565)

REFERENCES

[1] P.C.V. Parks, July 1966, "Lyapunov Redesign of Model Reference Adaptive Control System," IEEE Trans. Auto. Contr., Vol. AC-11, No. 3, pp. 362-267.

[2] Y.K. Choi, M.J. Chang, and Z. Bien, 1986, "An Adaptive Control Scheme for Robot Manipulators." IEEE Trans. Auto. Contr., Vol. 44, No. 4, pp. 1185-1191.

2018 Changwon International Conference on Intelligent Robot and Convergence Industry (CICIRO 2018)
Dec 13(Thusday) ~ Dec 14(Friday), 2018 Changwon International Hotel, Changwon, Korea

Analysis of Traffic Sign Classification using Multiple Image Preprocessing Methods

Qing Tang[1] and Kang-Hyun Jo[2*]

The Graduate School of Electrical Engineering, University of Ulsan[1]

The School of Electrical Engineering, University of Ulsan, Ulsan 44610, Korea[2*]

Abstract: This paper presents a method for traffic sign classification using a 2-stage ConvNet. In this method, we compare different input which are RGB, grayscale, YUV images. Also we use histogram equalization to enhance contrast of input images. We also normalize every input image in the range (-1,1) as the preprocessing step. To increase robustness of classification model, we apply a dataset augmentation algorithm. Experimental results show that the method is effective in classifying traffic signs. Also the appropriate input images can improve classification model's performance well.

1. Introduction

Traffic sign plays a significant role in the regulating traffic behavior, ensuring the safety of the traffic and guiding the vehicles and pedestrians.

Generally, the traffic-sign recognition system includes two steps, which are detection and classification [7]. A number of research solve the detection and classification simultaneously [1]-[3]. Traffic sign recognition technology is regarded as a challenging task due to diversified backgrounds and various complexities, such as view point variations, lighting conditions, various types of sign and different resolution of the traffic sign input images [2, 3].

The model can classify 43 categories of traffic signs. The model can classify 43 categories of traffic signs. To train and evaluate the proposed system, the GTSRB dataset [4] is utilized.

2. Image Preprocessing and Model Architecture

2.1 Color Space

The size of each image of GTSRB dataset is not the same, we resize all the image into 32x32x3, represented as [0, 255] integer values in RGB space. For choosing the better color space, we also transfer image from RGB to YUV color space. Classes of dataset are 43, such as, Speed limit, No entry and Keep left, etc.

2.2 Histogram Equalization and Normalization

In the real world, in order to be easily recognized and distinguished by the drivers, traffic sign are always designed in specific shapes and high saturated colors. We try to adapt histogram equalization to imput image to improve saturation, so the model can capture the high saturation region of traffic sign well.

And the second step is normalize image from (0, 255) to (-1, 1). Normalization can reduce the effect of illumination on image.

2.3 Dataset Augmentation

Dataset augmentation helps us generate additional training examples, also reduce the effect of dataset imbalance, which will lead bias toward the classes which have more samples and lead to misclassification. We use dataset augmentation algorithm [5] and we just change the brightness of input image.

2.4 Model Architecture

The architecture of neural network in this paper is a 2-stage ConvNet [5] which been proposed by Pierre Sermanet and Y. LeCun [6], and we change a little in S4 layer [5]. Also we add a Dropout module before the last layer of fully connection. The dropout probability is 0.5. Using the dropout unit can avoid over-fitting to improve validation accuracy.

3. Experiments

We focus on the German Traffic Sign Benchmarks (GTSRB) data set to evaluate the method in the paper, the GTSRB dataset consists of 43 classes of traffic sign. To evaluate the effectiveness of the different preprocessing method, we report the result of the experiment.

In Fig.1, 'Gray400_0.9367' means that the input are grayscale image, also if there are less than 400 samples in one class of GTSRB dataset, we will generate samples using dataset augmentation algorithm for that class until the number of sample reach 400, and the test accuracy of the Gary400 model is 0.9367. 'HE' means that the input are RGB image with histogram equalization step. 'RGB' means that the input are RGB image without histogram equalization step. 'YUV' means that the input are YUV image.

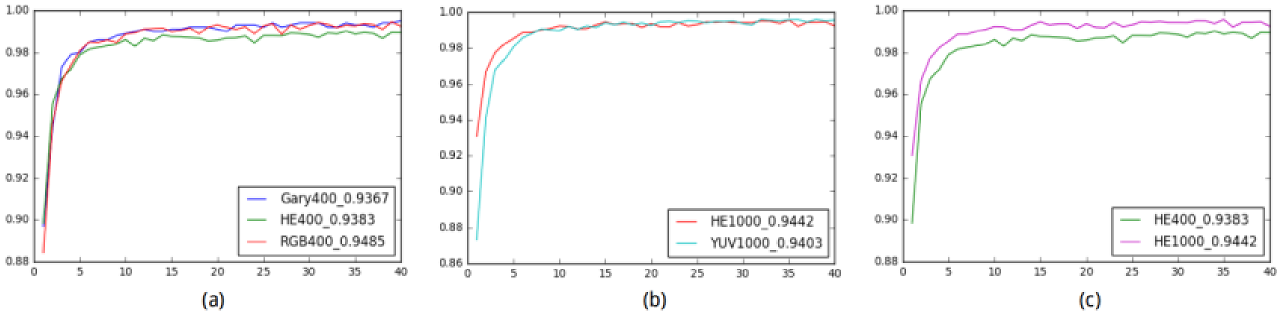

Fig.1 Accuracy of training and test step. The abscissa is epoch, the ordinate is validation accuracy. The number which behind the model name are the test accuracy of the model.

From Fig.1(a) we can see that using grayscale image to train the model can achieve better accuracy rather than test accuracy, also histogram equalization could not improve model performance in both validation and test step. In Fig.1(b), we compare these two methods which are using RGB image with histogram equalization and using YUV image as input. The experimental result shows that using RGB color channel can achieve better accuracy of the validation and test step. Compare with the model 'HE400', 'HE1000' generate more image for training using dataset augmentation algorithm. And the result show that dataset augmentation has a great help to performance.

4. Conclusion

We presented a traffic sign classification method based on Convolutional Neural Network architecture. We compare different preprocessing method for traffic sign classification model. In the future work, we will use RGB image to train the model. Also, we will try to use other neural networks to classify and compare with 2-stage ConvNet which we use in this paper.

REFERENCES

[1] C. Fang, C. Fuh, S. Chen, and P. Yen, "A road sign recognition system based on dynamic visual model," in The 2003 IEEE Computer Society Conf. Computer Vision and Pattern Recognition, Madison, Wisconsin, pp. 750-755 (2003).

[2] Miura, T. Kanda,mand Y.nShirai, "An active vision system for real-time traffic sign recognition," in 2000 IEEE Intelligent Transportation Systems, Dearborn, MI, USA, pp. 52-57 (2000).

[3] S. Vitabile, G. Pollaccia, G. Pilato, and F. Sorbello, "Road sign Recognition using a dynamic pixel aggregation technique in the HSV color space," in 11th Inter. Conf. Image Analysis and Processing, Palermo, Italy, pp. 572-577 (2011).

[4] Stallkamp, J, Schlipsing, M, Salmen, J, and Igel, C. "The German Traffic Sign Recognition Benchmark: A multi-class classification competition." In International Joint Conference on Neural Networks, (2011)

[5] Q. Tang, L. Kurnianggoro, K.H. Jo. "Traffic Sign Classification with Dataset Augmentation and Convolutional Neural Network." In 9thInternationalConferenceonGraphicandImage Processing,(2017).

[6] Pierre Sermanet and Yann LeCun. "Traffic Sign Recognition with Multi-Scale Convolutional Networks." In 2011 International Joint Conference on Neural Networks, IJCNN 2011 - Final Program, pp. 2809-2813 (2011)

[7] A. de la Escalera, J.M Armingol, M. Mata. "Traffic sign recognition and analysis for intelligent vehicles." Image and Vision Computing, vol. 11, n. 3, p. 247-258 (2003)

2018 Changwon International Conference on Intelligent Robot and Convergence Industry (CICIRO 2018)
Dec 13(Thusday) ~ Dec 14(Friday), 2018 Changwon International Hotel, Changwon, Korea

Exploiting Different Shape Features for Fall Action Classification

Sowmya Kasturi[1] Kang-Hyun Jo[2*]

The Graduate School of Electrical Engineering, University of Ulsan[1]

The School of Electrical Engineering, University of Ulsan, Ulsan 44610, Korea[2*]

Abstract: The number of older people living alone has been increased over the past years. It is observed that fall and resulting injuries have become a major health problem among those older people. A vision based system for fall action classification from other actions would be of a great help in this case. But the inherent problem is the choice of features, which can distinguish a fall from non-fall action accurately. So, the proposed method exploits the bounding box and elliptical features over the human silhouette, separated from background. All the experiments are performed on top viewed Kinect depth images of UR fall detection dataset. Results showed that ellipse based features are superior to classic bounding box based features.

1. Introduction

Falls are one of the major cause for injuries and hospitalization of many older people. According to a study [1], 13% of 828 older Korean adults living in a community experienced falls during a period of one year. As the older people living alone are rapidly increasing in the society, in the absence of care taker, a fall event unattended could lead to a serious injury and hospitalization. Many automatic sensor based fall detection systems were developed to detect and alarm the caretaker in the occurrence of fall event. However, these systems often cause discomfort to wear all day around and easily prone to vibrations from surrounding environment causing false alarms. So the concentration has been shifted to develop RGB vision based systems to exploit the rich information offered by surveillance systems, but these are privacy intrusive and easily subjected to occlusion. In the proposed method, top viewed depth images has been considered to deal with the problems in the former one.

2. Theory

2.1 Shape features

Vision based systems uses a variety of features namely shape based, posture based, spatio- temporal, 3D head change and motion inactivity features [2]. The shape of the human varies drastically during a fall when compared to other non-fall actions like walking or standing. In [3], height, width, depth of a 3D bounding box features are used for fall classification. In the current method different bounding box and ellipse based shape features are exploited to choose features which are more helpful to classify a fall from a non-fall action. Seven bounding box features namely bounding box height and width, area, centroid, orientation, extent and eccentricity are extracted. The ellipse fitting based features considered are major and minor axis of the ellipse, area, centroid, orientation, extent and eccentricity. The area represents the number of pixels and eccentricity is the measure of aspect ratio and the extent is given by the ratio of number of pixels in the silhouette to the bounding box or ellipse.

$$Extent = \frac{N_s}{N_{be}}$$

The centroid, orientation of the ellipse changes greatly for fall and non-fall action and is calculated from the moments [4]

3. Results and Discussion

The experiments are conducted over 760 image frames from 5 videos of UR fall detection dataset [5]. Two classes are defined, fall and all the other negative samples as non-fall. The non-fall events considered are walking, standing and no human in the frame. A fixed background Fig. 1. (a) is manually selected and foreground is extracted from it by performing frame differencing with any current input frame (b). After the foreground extraction (c), the largest connected component is extracted which is the human silhouette (d). The bounding box and ellipse features are extracted from the silhouette and given as input to a binary SVM classifier. Two classes namely fall and no-fall are manually labelled for the training purpose and the classifier, classifies the action as one of these classes. One half of the dataset is used for training and the other for testing. Sample bounding box and ellipse fit results are shown in Fig.2 and Fig.3. The experimental results shows the supremacy of ellipse fit features over traditional bounding box features with an improved accuracy of almost 5% as shown in the Table 1. It is observed that the accuracy of the system is affected in the case where human body touches the nearby chair as shown in Fig.4

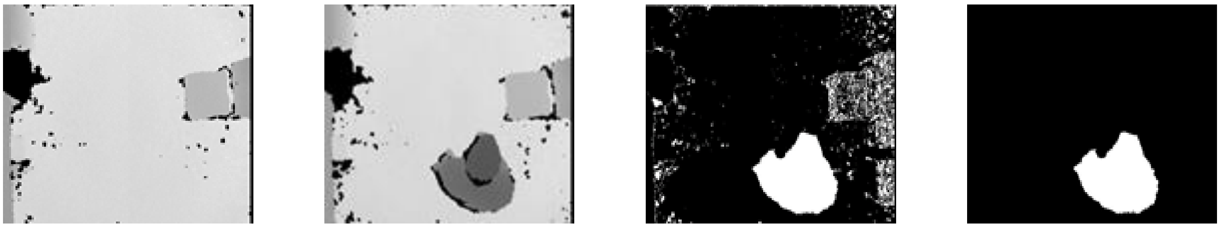

(a) (b) (c) (d)

Fig. 1. Human silhouette extraction

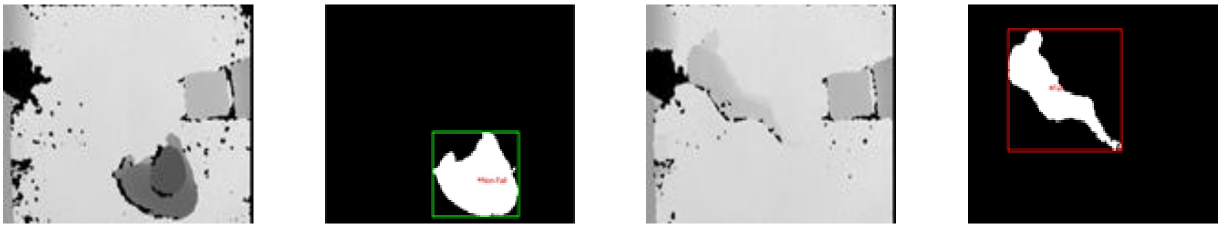

Fig. 2. Examples of bounding box results for a non-fall and fall action

Fig.3. Examples of ellipse fit results for a non-fall and fall action

Features	Classification accuracy (%)	Sensitivity(%)
Bounding box	85.64	79.81
Ellipse fit	90.93	91.11

Table 1. Performance evaluation of different shape based features

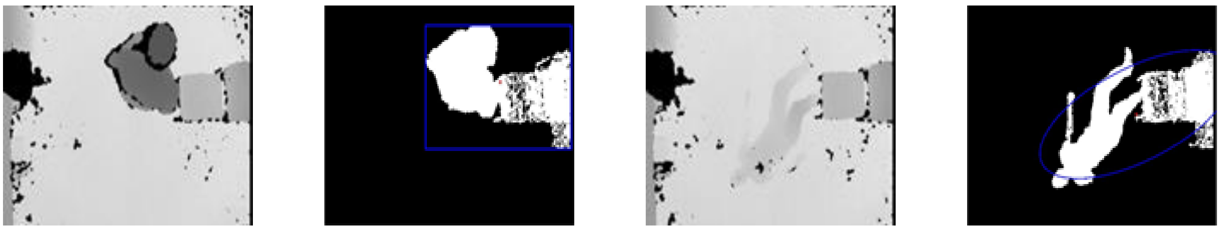

Fig.3. Examples of ellipse fit results for a non-fall and fall action

4. Conclusion

The paper exploits different bounding box and ellipse based shape features for the human fall action classification. The shaped based features are extracted from the separated human silhouette. A binary SVM classifier is fed with these features and classifies the event as fall or non-fall. The experimental results shows the robustness of ellipse fit features over traditional bounding box methods. In addition, both the features are observed to be insufficient for the action classification when the human silhouette is in touch with other objects in the environment.

REFERENCES

[1] Kim, Kwang-Il, "Evidence-based guideline for fall prevention in Korea," Journal of the Korean Geriatrics Society, Vol. 20, No. 1, pp. 1-28, 2016.

[2] Chung, Man Cheung, "A survey on fall detection: Principles and approaches," Neurocomputing , Vol.100, No. 100, pp.

144-152, 2013.
[3] Bevilacqua, Vitoantonio, "Fall detection in indoor environment with kinect sensor," Innovations in Intelligent Systems and Applications (INISTA) Proceedings2014 IEEE International Symposium on, pp. 319-324, 2014.
[4] J. Dongyao, V. Groza, L. XiaoHui, L. Xu, Z. Huaihua, and Q. Zeng, "A method of detecting human body falling action in a complex background," in Intelligent Engineering Systems (INES), 2016 IEEE 20th Jubilee International Conference on. IEEE, 2016, pp. 51-56.
[5] B. Kwolek and M. Kepski, "Human fall detection on embedded platform using depth maps and wireless accelerometer," Computer methods and programs in biomedicine, vol. 117, no. 3, pp. 489-501, 2014.

A Study on Stable Control of Hymanoid Robot for Smart Factory

Un-Tae Ha1, Min-Seong Kim2, Byung-Suk Yoon3, Jung-Eup Gye4, Jong-Gyo Jung5
and Sung-Hyun Han6

[1] PhD. Course, Graduate School Kyungnam University,
Changwon, 51767, Korea (euntha@hanmail.net) * Corresponding author
[2] Department of Advanced Engineering, Graduate School Kyungnam University,
Changwon, 51767, Korea (kms21018@naver.com)
[3] Doosan Heavy Industries & Construction Co., Ltd., Changwon, 51711, Korea (rtrshbaek@hanmail.net)
[4] Ministry of Trade, Industry & Energy Office of Strategic R&D Planning, Sejong, 30118, Korea(jekeh66@naver.com)
[5] KAVAS Co., Ltd., Changwon, 630-812, Korea (jongkyo@kavas.co.kr)
[6] Department of Mechanical Engineering, Kyungnam University,
Changwon, 51767, Korea (shhan@kyungnam.ac.kr)

Abstract: We present a new technology for real-time walking of a humanoid robot. A humanoid robot necessitates achieving stabilization for real time walking since it has basic problems such as structural stability. In this paper, a robust control algorithm for stable walking is proposed based the ground reaction forces, which are measured using force sensors during walking, and the environmental conditions are estimated from these situation. From this information the robot selects the proper motion and overcomes ground irregularities effectively. In order to generate the proper angel of the joint. The performance of the proposed algorithm is verified by simulation and experiments for a 20-DOFs humanoid robot.

Keywords: Stable walking, Control algorithm, Humanoid robot, Robust walking

1. INTRODUCTION

This paper proposes an obstacle avoidance architecture allowing walking humanoid robots to walk safely around in factory and home environment.

A main technological target of the proposed robot (Model:V-HUR) is to autonomously explore and wander around in home environments as well as to communicate with humans.

2. ROBOT CONTROL SYSTEM

The main board of the CPU receives the resulting disparity image as a digital video signal. The stereo control parameters can be set between the main CPU and the 8bit CPU on board through a special serial communication link.

The vision system (mentioned above) receives image from the two CCD cameras. These parameters are useful for computing 3D range data. The disparity is calculated for each pixel in the left image by searching for the corresponding pixel in the right image. An additional reliability image is calculated following criteria to reject results on above conditions.

3. EXPERIMENT

Firstly, the disparity is converted into 3D range data using the parameters from camera calibration and then a Hough transformation is applied to all data points. Apply the *randomized Hough transformation* selects sets of data points from which the surface parameters can be directly computed and records the result in a table. If many data sets yield the same parameters, a high score for these parameters is obtained.

Fig. 1 The humanoid robot

4. CONCLUSION

The autonomous mobility for the humanoid robot V-HUR in the home environment is realized base on the development of a small stereo vision system, the recognition of floor and obstacles using plane extraction.

REFERENCES

[1] D. Pagac, E. Nebot and H. Durrant-Whyte, "An evidential approach to map-building for autonomous vehicles," IEEE Transactions on Robotics and Automation, 14(4), 623-629, 1998.

2018 Changwon International Conference on Intelligent Robot and Convergence Industry (CICIRO 2018)
Dec 13(Thusday) ~ Dec 14(Friday), 2018 Changwon International Hotel, Changwon, Korea

A Study on Optimal Trajectory Control of Robot System for FA

Du-Beum Kim1, Young-Hwa Jeong2, Sung-Hyun Han3

[1] Department of Advanced Engineering., Kyungnam University, Changwon, 51767, Korea (E-mail : kms21018@naver.com)
[2] Daeho Technology Korea Co., Ltd., 513983, Korea (yhjung@daehoteck.co.kr)
[3] Department of Mechanical Engineering, Kyungnam University, Changwon, 51767, Korea (shhan@kyungnam.ac.kr)

Abstract: We present a new technology for real-time walking of a humanoid robot. A humanoid robot necessitates achieving stabilization for real time walking since it has basic problems such as structural stability. In this paper, a robust control algorithm for stable walking is proposed based the ground reaction forces, which are measured using force sensors during walking, and the environmental conditions are estimated from these situation. From this information the robot selects the proper motion and overcomes ground irregularities effectively. In order to generate the proper angel of the joint. The performance of the proposed algorithm is verified by simulation and experiments for a 20-DOFs humanoid robot
Keywords: Stable Walking, Control Algorithm, Humanoid Robot, Robust Walking

1. INTRODUCTION

This paper proposes an obstacle avoidance architecture allowing walking humanoid robots to walk safely around in factory and home environment.

A main technological target of the proposed robot (Model:V-HUR) is to autonomously explore and wander around in home environments as well as to communicate with humans.

2. SYSTEM MODELING

The main board of the CPU receives the resulting disparity image as a digital video signal. The stereo control parameters can be set between the main CPU and the 8bit CPU on board through a special serial communication link.

The vision system (mentioned above) receives image from the two CCD cameras. These parameters are useful for computing 3D range data. The disparity is calculated for each pixel in the left image by searching for the corresponding pixel in the right image. An additional reliability image is calculated following criteria to reject results on above conditions. After block matching has been carried out, the matching score is calculated by interpolating scores near the highest peak.

The sharpness of this peak corresponds to the available texture around this pixel and thus can be used as a reliability value for the disparity calculation. If there are other peaks with similar matching scores then the disparity computation is ambiguous and the reliability is set to a low value. (The matching score is compared with neighboring scores).

3. EXPERIMENT

Firstly, the disparity is converted into 3D range data using the parameters from camera calibration and then a Hough transformation is applied to all data points. Apply the *randomized Hough transformation* selects sets of data points from which the surface parameters can be directly computed and records the result in a table. If many data sets yield the same parameters, a high score for these parameters is obtained.

Although applying floor detection methods, obstacles and regions the robot can walk on can be found. However, in general it is difficult to decide from a single observation with a limited field of view, the action the robot should carry out next. We follow this notion and introduce a terrain map where all observations and motions are integrated.

4. CONCLUSION

The autonomous mobility for the humanoid robot V-HUR in the home environment is realized base on the development of a small stereo vision system, the recognition of floor and obstacles using plane extraction.

The terrain is represented in a robot centric coordinate system without making any structural assumptions about the surrounding world. And the representation of a terrain map based on these observations, robot motion, and the generation of a walking path on the terrain map

REFERENCES

[1] D. Pagac, E. Nebot and H. Durrant-Whyte, “An evidential approach to map-building for autonomous vehicles,” IEEE Transactions on Robotics and Automation, 14(4), 623-629, 1998.

A Study on Robust Control of Hand with 10 Joints

Jae-Jong Kim[1], In-Man Park[2], Hyun-Suk Sim[3]
and Sung-Hyun Han[4]

[1] Navy munitions situation,Changwon, Korea (1975kjj@hanmail.net)
[2] Intem Co., Ltd., Changwon, 642-370, Korea
(intem237@hanmail.net)
\[3] DongSan Tech Co., Ltd., Haman, 637-821, Korea
(hs8388@dscast.co.kr)
[4] School of Mechanical Engineering, Kyungnam University,
Changwon, 51767, Korea (shhan@kyungnam.ac.kr)

Abstract: Recently it is very important to control robot hands more compact and integrated sensors in order to increase compensate the grasping capability and to reduce cabling through the finger in the manipulator. As a matter of fact, the miniaturization and cabling harness represents a significant limitation to the design of small sized precise sensor. The main focus of this research is on a flexible grasping control of hand fingers, which consists of a flexible multi-fingered hand-arm system.

Keywords: Grasping Control, Hand Finger, Precise Sensing, Hand Design

1. INTRODUCTION

Recently Manipulation capability is important for a robot. Interaction between a robot hand and objects can be properly controlled only is suitable sensors are available. In particular, information about the forces applied at the contact, the contact location, other indirect measurements, e.g. estimate of mass object, its inertia ellipsoid, or even non mechanical measurements, may play a crucial role to implement secure grasp and safe manipulation tasks. In the past two decades several robot hands and dexterous grippers have been developed. The major goals have been on one hand that of studying and implement newer mechanical solutions in order to increase miniaturization and dexterity, and, on the other, to investigate manipulation models and control techniques. At mechanical level study on dextrous grippers has mainly focused on the actuation and kinematics aspects.

Actuation of tendon based robot grippers poses various technical problems. Tendons coupling on one hand, friction and elasticity on the other, pose important problems for the control of tendon actuated mechanisms. However, the mechanical accuracy required to design a miniature (e.g. human sized) dexterous gripper, is by far less than an equivalent design based on gears or other stiff transmission mechanism. Recently the tendency is to create robot hands more compact and high integrated sensors system, in order to increase the grasping capability and in order to reduce cabling through the finger, the palm and the arm. As a matter of fact, miniaturization and cabling harness represents a significant limitation to the design of small sized embedded sensor.

2. SYSTEM DESIGN

The mechanism of a flexible hand gripper requires the mass of the hand should be as low as possible. It is highly desirable that the hand weigh less than 1kg. Furthermore the low mass of the finger mechanism is desirable not only to achieve flexible motion but also for stable control.

Our philosophy about dynamic manipulation is maximization of the power and minimization of the mechanism. In particular four factors are important: (1)light weight, (2) high speed and high acceleration, (3) accuracy, (4) possibilities of flexible grasping.

The finger has strain gauges at the joint 1 and joint 2 for force control. In addition a 6-axis force/torque sensor and a tactile sensor are mounted on each fingertip.

The flexible motion imposes a heavy load on the finger mechanism. For this reason a simple mechanism should be used for reduction gear, transmission, etc. In most traditional hand systems a wire-driven mechanism is used. But this is not suitable for a lightweight mechanism, because it is large and complicated.

In our hand a newly developed small harmonic drive gear and a high-power mini actuator are fitted in each finger link and all of these parts are hidden in the plastic case. A harmonic drive gear has desirable properties for control such as no backlash and a high reduction rate.

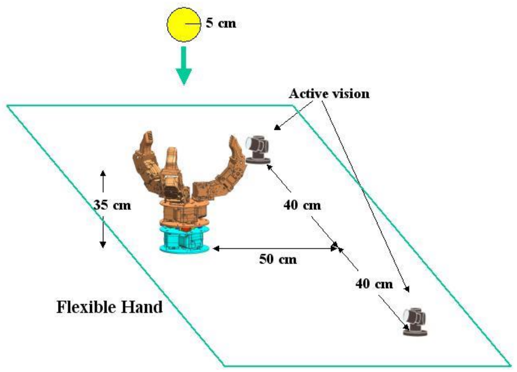

Fig. 1. Visual feedback control system

Following the purpose of this paper; we discus about the system set up in Fig. 1. Vision is with a massive parallel vision system called column-parallel high-speed vision system.

Early image processing is performed in order to achieve segmentation of the image, extraction of the target area, and computation of the image moments. From these data, the position of the target is computed; each vision sensor is mounted on an active vision.

The tactile transducer is a matrix of 64 electrodes covered by a layer of pressure sensitive conductive rubber (PCR Co. Ltd.). The electrodes are etched on a flexible PCB substrate in order to conform to a cylindrical surface. A thin elastic sheet covers the whole sensor and provides a mild preload useful to reduce noise. Pressure due to contacts produces changes of resistance among the electrodes. The geometry of the electrodes Fig. 1, has been defined with the goal of limiting the spurious currents that may occur across the various electrodes, and interfere with measurement, as discussed in.

Tactile data are sampled by the on-board MCU, with 10 bit resolution. Preliminary tests show an actual sensor resolution of 8 bit/taxel. Each tactile image consists of 64 taxels.

During contact, a number of adjacent taxels are subject to pressure. The analog output of the tactile sensor allows to measure the distribution of pressure over all the transducer. Therefore, we propose to compute the contact centroid , as

$$\hat{C} = \frac{\sum_{i=1}^{N}\sum_{j=1}^{N} x_{ij}.p(x_{ij})}{\sum_{i=1}^{N}\sum_{j=1}^{N} p(x_{ij})} \quad (1)$$

where **ˆC** is the computed contact centroid, **x***ij* is the coordinate of the taxel and *p*(**x***ij*) the weight of this. As a matter of fact further geometric information about the distribution of the pressure during contact could be useful, although not directly relevant to point contact model solution. To this aim the pressure distribution is approximated as an ellipsoid, as follows:

$$E = \frac{\sum_{i=1}^{N}\sum_{j=1}^{N} (x_{ij}-\hat{C})(x_{ij}-\hat{C})^{T}.p(x_{ij})}{\sum_{i=1}^{N}\sum_{j=1}^{N} p(x_{ij})} \quad (2)$$

Where **E** is a symmetric matrix who represent the ellipsoid. The approach used to compute and the associated approximate ellipsoid, is strongly based on the availability of an analog tactile sensor.

3. EXPERIMENT

Catching is one of the most important tasks for dynamic manipulation. In this section catching is shown using our flexible hand with a visual feedback controller. We used a rubber ball with radius of 5cm as a target, and we dropped it from about 1.2m in height. The speed of the falling ball is about 5.9m/s just before it hits the ground.

Table. 1. The specification of robot hand.

Total D.O.F	12
Weight [g]	700
Max. Speed at a finger tip [m/s]	3.5
Max. force at a finger tip [N]	30
Joint resolution [deg]	0.4

The catching tasks for the ball are:
- Approaching (0÷40ms)
- Locking (40÷50ms)
- Rebounding (50÷60ms)
- Holding (60ms÷).

From various experimental trials, we have decided on the catching strategy shown in Fig. 2.

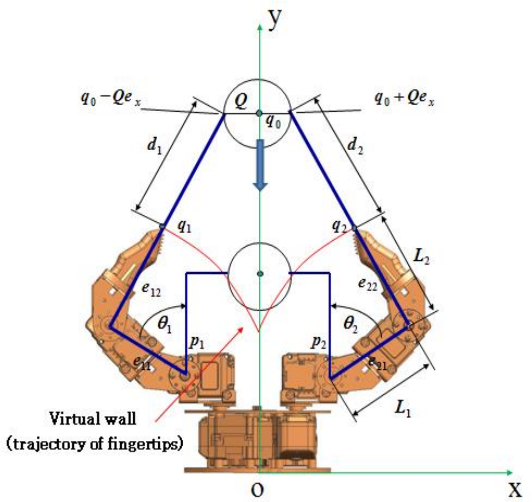

Fig. 2. The coordinates system for catching algorithm of grasping.

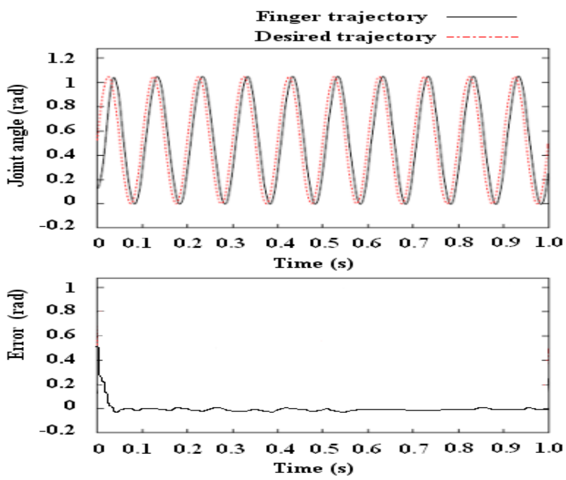

(a) Result for sine wave input trajectory

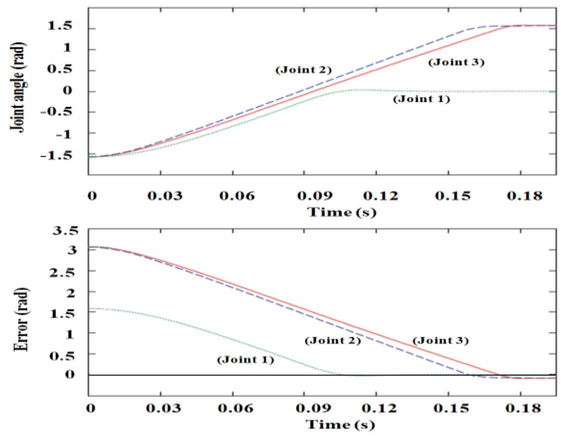

(b) Result for the step input trajectory

Fig. 3. Result of performance test for finger trajectory tracking

Fig. 3 shows the results when we changes the target position q_o and Fig. 8 when we changes the distance d1 and d2, (X-Y axis, q_o, d1 and d2 were defined in fig. 3.)

4. CONCLUSION

An integrated force and tactile sensor with embedded electronics has been presented in a lightweight flexible hand with 12 D.O.F, and the associated visual feedback control. The sensor consists of a three components commercial force sensor and of a custom matrix tactile sensor based pressure sensitive conductive rubber.

The need for a robotic hand that works in the real world is growing. And such a system should be able to adapt to changes in environment. We think that the concept of a flexible hand system with real-time control implementation will become an important issue in robotic research.

REFERENCES

[1] S.C.Jacobsen, E.K. Iversen, D.F. Knutti, R.T. Johnson andK.B. Biggers, "Design of the Utah/MIT dexterous hand", Proc. IEEE Int. Conf. On Robotics and Automation, pp. 1520-1532, 1986

[2] Anotonio Bicchi, J. Kennedy Salisbury, David L. Brock "Contact Sensing from Force Measurements" International Journal of Robotics Research. Vol. 12, No. 3, June 1993.

[3] S. Toyama, S. Hatae and S. Sugitani, "Multi-Degree of spherical ultrasonic motor", Proc. ASME Japan/USA Sympo. Flexible Automation, 169, 1992

[4] Gongliang Guo, William A. Gruver, "A new design for a dexterous robotic hand mechanism" IEEE Control Systems Magazine, v 12, n 4, Aug, 1992, p 35-38.

[5] Hideaki Hashimoto, Hideki Ogawa, Toshiya Umeda, Masao Obama Kyoichi Tatsuno, "An Unilateral Master-Slave Hand System with a Forcecontrolled Slave Hand" IEEE International Conference o Robotics and Automation 1995.

A Study on Stable Control of Walking Robot by Voice Command

Ho-Young Bae 1 , Woo-Song Lee 2, Sung-Hyun Han 3
[1] KyeongWon Industry Co., Ltd.,51402, Korea (ock38317@naver.com)
[2] SUNJIN Technology Co., Ltd., Changwon, 82331, Korea
(elflws@nate.com)
[3] School of Mechanical Engineering, Kyungnam University,
Changwon, 51767, Korea (shhan@kyungnam.ac.kr)

Abstract: Generally, it is possible to control the walking information based on the bipped robot's own postures, because a type of motion and gesture produces almost the same pattern of noise every time. In this paper, we describe an voice recognition control technology for bipped robot system which can robustly recognize voice by adults and children in noisy environments. We evaluate the performance of robot control system in a communication robot placed in a real noisy environment. Voice is captured using a wireless microphone. To suppress interference and noise and to attenuate reverberation, we implemented a multi-channel system consisting of an outlier-robust generalized side-lobe canceller technique and a feature-space noise suppression using criteria. Voice activity periods are detected based end-point detection
Key words: Robust voice recognition, Side-lobe canceller, navigation system

1. INTRODUCTION

To make human-robot communication natural, it is necessary for the robot to recognize voice even while it is moving and performing gestures. For example, a robot's gesture is considered to play a crucial role in natural human-robot communication [1-3]. In addition, robots are expected to perform tasks by physical actions to make a presentation. If the robot can recognize human interruption voice while it is executing physical actions or making a presentation with gestures, it would make the robot more useful.

Each kind of robot motion or gesture produces almost the same noises every time it is performed. By recording the motion and gesture noises in advance, the noises are easily estimated. By using this, we introduce a new method for VRCS under robot motor noise. Our method is based on three techniques, namely, multi-condition training, maximum-likelihood linear regression[5], and missing feature theory. These methods can utilize pre-recorded noises as described later. Since each of these techniques has advantages and disadvantages, whether it is effective depends on the types of motion and gesture. Thus, just combining these three techniques would not be effective for voice recognition under noises of all types of motion and gestures. The result of an experiment of isolated word recognition under a variety of motion and gesture noises suggested the effectiveness of this approach.

2. CONTROL SCHEME

The proposed robot system has three wheels; two driven wheels fixed at both sides of the mobile robot and one castor attached at the front and rear side of the robot. The ultrasonic sensors are mounted around of the mobile robot in middle layer for the detection of obstacles with various heights. In this study, a sonar array composed of 16 ultrasonic sensors cannot be fired simultaneously due to cross talk. Instead, we adopt a scheduled firing method where sensors are activated in sequence of $\{s_1, s_{12}, s_2, s_{11} \ldots\}$. The arrangement of the ultrasonic sensors in upper layer and the sensors are marked as dots in the figure. The distances e_j $(j = 1, 2,\ldots 12)$ from the origin of the robot frame {R} to obstacles detected by the sensor s_j, can be defined as $e_j = \delta_j + R_r$. Here, R_r is the radius of the robot and the δ_j, is the range value measured by the sensor s_j .

A local map is introduced to record the sensory information provided by the 16 sonar sensors with respect to the mobile robot frame $\{R\}$. Sector map defined locally at the current mobile robot frame is introduced. Then, the obstacle position vector se'_j with respect to the frame $\{R\}'$ can be calculated by

$$Se_j' = \begin{bmatrix} \cos\delta\theta & \sin\delta\theta & 0 & -\sin\delta\theta/\rho_p \\ -\sin\delta\theta & \cos\delta\theta & 0 & (1-\cos\delta\theta)/\rho_p \\ 0 & 0 & 1 & 0 \\ 0 & 0 & 0 & 1 \end{bmatrix} \quad (1)$$

where se_j denotes the obstacle position vector defined at the frame $\{R\}$. When the mobile robot is located at a point $0'$. the distance value $se'_j = \| se'_j \|$ from the origin of the frame $\{R\}'$ to the obstacle and angle $s\varphi'$ can be calculated by Eq.(1) . Here, $\|.\|$ denotes Euclidean norm.

The local map defined at the frame $\{R\}'$ is newly constructed by using the previous local map defined at the frame (R) as follows:

$$Se_n \leftarrow Se_j', n = INT(\frac{s\varphi_j'}{\bar{\varphi}}) + \frac{N}{2}; \; j = 1,2,\ldots, N \quad (2)$$

Where ← and INT denote the updating operation and integer operation, respectively. Here, se_n, denotes the distance value of n sector and N represents the number of the sector. If the range values obtained by sensors when the mobile robot is located at a point o' are e_j = (j = 1,2 ,... *12)* , the new local map is partially updated as follows :

$se_j \leftarrow e_j$, j = 1,2 .... *12*. The maximum range of the sonar sensor is set to be $\delta_{max} = \delta_{max} - R_r$. Any return range which is larger than is ignored.

The primitive behaviors may be divided as follows: goal-seeking behavior, ball-following behavior, keep-away behavior, free space explorer and emergency stop, etc. The output of a primitive behavior is defined by the vector.

$$u(t) = (v(t), \Delta\theta(t))^T = (v(t), w(t), Tms)^T \qquad (3)$$

where t and T_{ms} denote the time step and the sampling time, respectively. Here, T denotes the transpose and $\omega(t)$ denotes the angular velocity of the robot.

We will divide the primitive behaviors into two basic: avoidance behavior and goal-seeking behavior.

The avoidance behavior is used to avoid the obstacles irrespective of the goal position, while the goal-seeking behavior is used to seek the goal position irrespective of obstacle location. Design of each behavior proceeds in following sequences;

(A) fuzzification of the input/output variables, (B) rule base construction through reinforcement learning, (C) reasoning process, (D) defuzzification of output variables.

In order for the mobile robot to arrive at the goal position without colliding with obstacles, we must control the mobile robot motion in consideration of the obstacle position X_{oi}, = (x_{oi}, y_{oi}) , the mobile robot position $X = (x , y)$ and its heading angle θ with respect to the world coordinate frame {W} shown in Fig. 1.

In order to avoid the increase in the dimension of input space, the distance values d_i , *(i* = 1.2,3,4) are defined by

$$\begin{aligned} d_1 &= \min(se_1, se_2, se_3) \\ d_2 &= \min(se_4, se_5, se_6) \qquad 4a \\ d_3 &= \min(se_7, se_8, se_9) \qquad 4b \\ d_4 &= \min(se_{10}, se_{11}, se_{12}) \end{aligned}$$

$\phi_m (-\pi \le \phi_m \le \pi)$ denotes the orientation of a sector with the shortest range. We choose the input variables for avoidance behavior as ϕ_m and $d_i = \|X_{0i} - X\|, (i = 1,2,3,4)$ for goal-seeking behavior as heading angle difference ψ and distance to goal $z = \|X_g - X\|$. The input linguistic variables d_i, ψ, ϕ_m and z are expressed by linguistic values (VN, NR, FR), (NB, NM, ZZ, PS, PM, PB), (LT, CT, RT) and (VN, NR, FR, VF), respectively Their membership functions are expressed .

3. EXPERIMENTS

The proposed robot has the maximum travel speed of 0.55 m/s and the maximum steering rate of 3.0rad/sec. Experiments are performed in an indoor with the first experiment for voice recognition without objects and second experiment for both of them: voice recognition and obstacles avoidance.

Through a series of the navigation experiments, it was observed that the heading angle error is a serious problem to the proposed robot depend on dead reckoning The large heading angle error almost resulted from the uncertain parameters when the mobile robot changes its direction Even if the wheel slippage occurs, the true position and heading angle of the mobile robot could be updated by two beacon pairs and consequently the mobile robot could arrive at the given goal position while avoiding the obstacles.

4. CONCLUSIONS

This paper proposed the integration of robust voice recognition and navigation system capable of performing autonomous navigation in unknown environments. In order to evaluate the performance of the overall system, a number of experiments have been undertaken in various environments.

REFERENCES

[1] M. Blanchet, J. Boudy, and P. Lockwood, “Environment adaptation for speech recognition in noise,” in Proc. of EUSIPCO-92, vol. VI,1992, pp. 391–394.

[2] R. P. Lippmann, E. A. Martin, and D. B. Paul, “Multi-style training for robust isolated-word speech recognition,” in Proc. of ICASSP-87. IEEE, 1987, pp. 705–708.

[3] J. Barker, M. Cooke, and P. Green, “Robust asr based on clean speech models: An evaluation of missing data techniques for connected digit recognition in noise,” in Proc. of Eurospeech-2001. ESCA, 2001, pp. 213–216.

[4] P. Renevey, R. Vetter, and J. Kraus, “Robust speech recognition using missing feature theory and vector quantization,” in Proc. Of Eurospeech-2001. ESCA, 2001, pp. 1107–1110. S. Yamamoto, K. Nakadai, H. Tsujino, and H. Okuno, “Assessment of general applicability of robot audition system by recognizing three simultaneous speeches.” in Proc. of IEEE/RSJ International Conference on Intelligent Robots and Systems (IROS-2004). IEEE and RSJ, 2001, p. to appear.

A Study on Control of Robot Based on Ultrasonic Sensors for FA

Sang-Hyun Kim 1 , Jeong-Seok Kang 2 , Jong-Dae Won 3 ,Sung -Hyun Han 4 ,Han-Sung Kim 4

[1] Department of Advanced Engineering., Kyungnam University, Changwon, 51767, Korea
(E-mail : kms21018@naver.com)
[2] SMEC co., Ltd. Gimhae City, 50969, Korea
(E-mail : jskang@esmec.com)
[3] Young Chang Roboteck Co., Ltd., Gimhae City, 50969, Korea
(E-mail : wonjd@hanmail.net])
[4] School of Mechanmical Engineering, Kyungnam University, Changwon, 51767, Korea
(E-mail: shhan@kyungnam.ac.kr)
[4] School of Mechanmical Engineering, Kyungnam University, Changwon, 51767, Korea
(E-mail: hkim@kyungnam.ac.kr)

Abstract: In this study, we propose a new approach to control a robotic gripper based on the pressure sensor for application to the forging process automation. The increasing requirement for robotic grippers applications in limited environments such as forging process is motivating the need for flexible grippers which have the wide variety of objects encountered in 3D environments. The human hand is a very complex grasping tool that can handle objects of different sizes and shapes. Many researches have been carried out to develop artificial robot grippers with capabilities similar to the human hand. This gripper is the wide working space compared with its physical dimensions and the capability to deal with objects in working environment conditions. This tasks is achieved by using pressure sensor and by properly controlling and coordinating the gripper and the carrying arm. After a brief illustration of the gripper for forging process, the experimental activity is proposed and the results achieved are applied to the forging process.

Keywords: Robot Gripper, Flexible control, Wide working space, Force sensor, wide variety, forging process.

1. INTRODUCTION

At mechanical level study on dextrous grippers has mainly focused on the actuation and kinematics aspects. With very few exceptions, tendon actuated mechanisms, and their numerous variants, still represent an effective way to implement compact manipulators. Actuation of tendon based robot grippers poses various technical problems. Tendons coupling on one hand, friction and elasticity on the other, pose important problems for the control of tendon actuated mechanisms. However, the mechanical accuracy required to design a miniature dextrous gripper, is by far less than an equivalent design based on gears or other stiff transmission mechanism. Recently the tendency is to create robot hands more compact and high integrated sensors system, in order to increase the grasping capability and in order to reduce cabling through the finger, the palm and the arm. As a matter of fact, miniaturization and cabling harness represents a significant limitation to the design of small sized embedded sensor. [1]

The major contribution of this paper is to present the design of a fully integrated tactile and 3-axis force sensor, with embedded electronics. The approach adopted has been that of using low cost components available off-the-shelf, and to pursue a highly modular pressure sensor. The system is scalable and designed to be integrated on the supporting two joint.[2]

2. GRIPPER CONTROL

The mechanism of a flexible hand gripper requires the mass of the hand should be as low as possible. It is highly desirable that the hand weigh less than 1kg. Furthermore the low mass of the finger mechanism is desirable not only to achieve flexible motion but also for stable control.

Our philosophy about dynamic manipulation is maximization of the power and minimization of the mechanism. In particular four factors are important: (1) light weight, (2) high speed and high acceleration, (3) accuracy, (4) possibilities of flexible grasping. Fig. 1 shows the mechanical design of the hand, and Fig. 2 shows a scene of the Gripper control. We used three fingers, which is the minimum number to achieve a stable grasp. Each of fingers has 4 degrees of freedom (D.O.F); the hand system has 13 D.O.F included 1 D.O.F on the hand link. Note that the Joint 4 consists of the linear motor so that the finger tip can move as slide but other links just moving as rotate around a horizontal axis. In general a hand needs 9 D.O.F to move a target to any position and orientation. But our hand has 13 D.O.F so that the applications are very wide in the working environments, and the fingers are arranged so as to grasp the objects like circular and prismatic, etc. In order to achieve "lightning" high acceleration, we have developed a new actuator that allows a large current flow for a short time. Table 1 shows the specification for the actuator.

The finger has strain gauges at the joint 1 and joint 2 for force control. In addition a 6-axis force/torque sensor and a tactile sensor are mounted on each fingertip.

The flexible motion imposes a heavy load on the finger mechanism. For this reason a simple mechanism should be used for reduction gear, transmission, etc. In most traditional hand systems a wire-driven mechanism is used. But this is not suitable for a lightweight mechanism, because it is large and complicated.

Early image processing is performed in order to achieve segmentation of the image, extraction of the target area, and computation of the image moments. From these data, the position of the target is computed; each vision sensor is mounted on an active vision.

2.1 Pressure Sensor

Manipulation control requires in general some sort of feedback which could provide information about the interactions occurring during contact between the gripper and the grasped object. Assumptions must be made about the nature of the contact and, on the base of the selected contact models, it is possible to specify the nature of feedback required to properly control the interaction. Detailed contact mechanics models are in general too complex to be taken into account in real-time control applications.

The device consists of three strain sensitive thick-film resistors. A force applied to the interface stick produces a change of resistivity. Proper arrangement of the resistors in three Wheatstone bridges, and a simple decoupling amplifier, allow obtaining three voltages proportional to the applied force components. Digital potentiometers are used for self-calibration of the bridges and three instrument amplifiers provide appropriate signal conditioning before sampling.

3. EXPERIMENTS

The main advantage of a multi-fingered hand is that it can grasp various objects by changing its shape. Several classifications of grasping have been proposed. In this proposal various grasps are classified into three large categories: a power grasp that passively resists arbitrary external forces exerted on the object, a precise grasp to manipulate the object, and an intermediate grasping which some fingers are used for a power grasp and the other fingers are used for a precise grasp.

We achieved these typical grasp types in our developed hand. Table. 1 shows the specification of robot hand and fig. 2 is some examinations of flexible gasping objects.

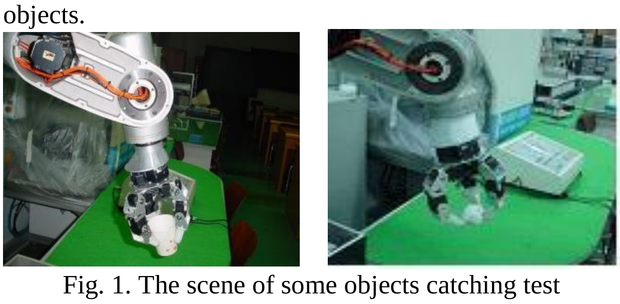

Fig. 1. The scene of some objects catching test

Catching is one of the most important tasks for dynamic manipulation. In this section catching is shown using our flexible hand with a visual feedback controller. We used a rubber ball with radius of 5cm as a target, and we dropped it from about 1.2m in height. The speed of the falling ball is about 5.9m/s just before it hits the ground.

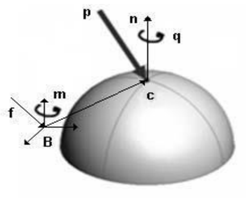

Fig. 2. Point of contact (**q**=0) and soft finger contact model.

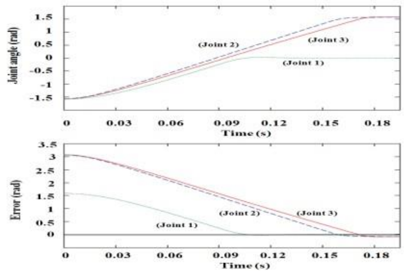

Fig. 3. Result of performance test for of gripper control

The success rate was more than 95% and tolerance of position error of the target was about ±1.5cm from the center of the palm.

Several types of failure modes were observed. The direction of a bounced ball depends on the coefficient of friction and restitution. It is difficult to know the accurate values of these parameters, but the errors in their measurement may be ignored if the speed of the fingertip is fast enough.

4. CONCLUSION

The sensor consists of a three components commercial force sensor and of a custom matrix tactile sensor based pressure sensitive conductive rubber. The joint used of both tactile and force information allows the direct solution of the point contact problem. A technique to compute the contact centroid and a quadratic approximation of the pressure distribution during contact has been proposed.

ACKNOWLEDGEMETN

This study was performed by project of the robot business belt construction enterprise.

REFERENCES

[1]T. Asfour, K. Berns and R. Dillmann, "The Humanoid Robot ARMAR", Proc. of the Second International Symposium on Humanoid Robots (HURO´99), October 8- 9, 1999, Tokyo, Japan

[2] T. Asfour, K. Berns, J. Schelling and R. Dillmann, "Programming of Manipulation Tasks of the Humanoid Robot ARMAR", The 9th International Conference on Advanced Robotics (ICAR'99), 25-27 October, Tokyo, Japan

A Study on Accurate Motion Control of Mobile Robot with with Two Wheel Driving

Yang-Geun Jeong 1 , Gi-Su Shin 2 , Min-Seong Kim 2 , In-Man Park 3, Sung-Hyun Han 4

[1] Shinla Information Technology CO., Ltd., Changwon City, 51390, Korea (E-mail : shintech@hanmail.net)
[2] ANY TOY CO. Ltd., Kyungnam University, Changwon, 51767, Korea (E-mail : Shings@naver.com)
[2] Department of Advanced Engineering., Kyungnam University, Changwon, 51767, Korea (E-mail : kms21018@naver.com)
[3] Intem Co., Ltd., Changwon City, 51565, Korea (E-mail: intem237@hanmail.net)
[4] School of Mechanical Engineering, Kyungnam University, Changwon, 51767, Korea (E-mail: shhan@kyungnam.ac.kr)

Abstract: The main focus of this paper is obtaining a fuzzy perception of the environment in the design of each reactive behavior and solving the problem of behavior combination to implement a fuzzy behavior based control architecture. It should be remarked that, the proposed technique of the nonholonomic constraints are considered in the design of each behavior. Furthermore, in order to improve the capabilities of the intelligent control system and its practical applicability, teleoperation and planned behaviors, together with their combination with reactive ones, have been considered.

Keywords: Real-Time control, Sensor, Intelligent Controller, Non-holonomic

1. INTRODUCTION

The real-time trajectory control is the process of determining and maintaining a path or trajectory to a goal destination. Autonomous mobile robots are required to navigate in more complex domains, where the environment is uncertain and dynamic. Autonomous navigation in these environments demands adaptation and perception capabilities. This paper describes improvements in the perception functions used in these kinds of robots. It should be noted that this is a nonholonomic vehicle with significant limitations in the reactive capabilities due to kinematic and dynamic constraints, and a few number of sensors and large blind sectors in between them, making autonomous navigation a nontrivial task. The methods presented in this paper have been conceived to deal with these limitations of conventional vehicles.

2. CONTROL SCHEME

The following considerations are based on a mobile robot with the three degrees of freedom of planar movement, x, y and θ. It is equipped with a ring of 12 ultrasonic sensors which are able to perceive vertical or nearly vertical planes. The number of sensors is irrelevant as long as there are no blind sectors between them. θ refers to the orientation of this ring of sensors and not to the orientation of the robot itself, which is of no importance for the wall following algorithm. With $\dot{\phi}$ indicating the direction of movement the kinematics model of such a robot is described as follows:

$$dx = v\cos\phi dt;\quad dy = -v\sin\phi dt;\quad d\theta = \dot{\theta}dt \tag{1}$$

Since there is no modeling of the environment the absolute position of the robot does not matter. So there is no world frame used here and the kinematics model can be expressed instead as:

$$ds = vdt;\quad d\phi = \dot{\phi}dt;\quad d\theta = \dot{\theta}dt \tag{2}$$

The speed v, the angular speeds $\dot{\phi}$ and $\dot{\theta}$ are used as control variables of the robot and generated by the fuzzy controller.

Perception of each ultrasonic sensor i of the mobile robot is assigned a vector ki. Its direction equals the orientation of the sensor´s axis and its length is a function of the distance di measured by this sensor:

$$k_i = \frac{d_{\max} - d_i}{d_{\max} - d_{\min}} \tag{3}$$

where dmin and dmax designate the shortest and longest distance respectively at which an object may be positioned to be reliably detected. ki is limited to 0 and 1 respectively

Since a vehicle with nonholonomic constraints cannot move itself in any direction at every time instant, it is interesting to weight the different perceptions according with the direction where the obstacle was detected. In other words, an obstacle is less important if it is placed at a location that cannot be reached by the mobile robot, but it is more dangerous if it is on a reachable position.

where sat0,1(x) states for the saturation of x in the range [0, 1]. In this way, it is possible to assign different perceptions, i.e. different weights, to objects detected at the same distance relative to the mobile robot but at different directions. For example, perception function ki is obtained by using the nonlinear function

$d_{\min}(\theta_i) = \dfrac{d_m(1-\varepsilon)}{(1-\varepsilon\cos\theta_i)}$, and

$d_{\max} = n d_{\min}(\theta_i)$ (with n>1), in Eq. (4)

$$k_i = f(d_s, \theta_i) = sat_{0,1}\left(\frac{nd_m(1-\varepsilon) - d_s(1-\varepsilon\cos\theta_i)}{(n-1)d_m(1-\varepsilon)}\right) \quad (5)$$

Furthermore, it is interesting to stress that the perception vector implies a fuzzy high level description of the environment, being independent of the type of range sensor used. So, it is possible to use different perception functions from Eq. 4 for each kind of sensor (laser, ultrasonic, infrared). Thus, sensor data fusion can be reduced to compute different vectors from the sensor measurements and to combine them to obtain the perception vector.

The previous perception can be updated as follows: consider a robot of arbitrary shape equipped with proximity sensors. Any such sensor may be located at a position U, with its axis pointing to the direction s

A frame r represents the robots position and orientation, x and θ, respectively, with respect to the world reference system w. The velocity υ of the reference point and the angular velocity $\omega_{r/w} = \dot{\varphi}$ of the robot with respect to the fixed frame w, give the state of motion. Furthermore, the virtual perception coordinate system is assumed to be located at E, pointing to the direction of attention a1. Then, an object detected by a proximity sensor at a distance ds could be detected by a virtual sensor placed at E a distance d, and with an orientation θ with respect to the vehicle's direction of attention a1.

3. EXPERIMENTS

We have performed experimental results of the proposed methods to the mobile robot . The vehicle carries on-board a heterogeneous configuration of ultrasonic sensors. It is presented two kinds of experiment including general perception and application of fuzzy perception.

In this, instead of a typical ring of identical sonars, there are 12 sonars of three different types, placed at different locations. Six of them are large-range sensors (1.0–2.6m), four are mid-range (0.5–1.0m), and the other two are of short-range (0.1–0.5m). Furthermore, these ultrasonic sensors use a higher frequency and have a narrower sonar beam than the commonly used sonars in these kinds of applications. The sensors are arranged in a way that six of them cover the front part of the vehicle and the other four cover its lateral sides.

4. CONCLUSIONS

We propose a new approach to control of mobile robot of trajectory following and fuzzy perception concept with a nonholonomic mobile robot.

Experimental results, of an application to control the autonomous vehicle, demonstrate the robustness of the proposed method.

REFERENCES

[1] R. Braunstingl, "Improving reactive navigation using perception tracking", *Robotics and Manufacturing, Recent Trends in Research and Applications*, Vol. 6, pp 25-30, New York, 1996.

[2] J.J. Leonard, H.F. Durrant-Whyte, "Directed Sonar Sensing For Mobile Robot Navigation", Kluwer Academic Publishers, pp 147-155, 1992.

[3] A. Ollero, A. Garcia-Cerezo, J.L. Martinez, A. Mandow, "Fuzzy tracking methods for mobile robots", Prentice-Hall, pp 347-364, 1997.

[4] Ollero, G. Ulivi, F. Cuesta, "Fuzzy logic applications in mobile robotics", Kluwer Academic Publishers, pp. 301–324, 1999.

A Real-Time Control for Stable Walking of System Robot

Jea-Ik Paeng 1 , Hee-Jin Kim 2 ,Du-Beum Kim 3

[1] Navy Shipyard, Changwon, Korea(thanggl@naver.com)
[2] Intem Co., Ltd., Changwon, 642-370, Korea (intem237@hanmail.net)
[3] School of Mechanical Engineering, Kyungnam University, Changwon, 51767, Korea (E-mail: shhan@kyungnam.ac.kr)

Abstract: This paper deals with the stable walking for a biped robot, on uneven terrain, A biped robot necessitates achieving posture stabilization since it has basic problems such as structural instability. In this paper, a stabilization algorithm is proposed using the ground reaction forces, which are measured using FSR (Force Sensing Resistor) sensors during walking, and the ground conditions are estimated from these data. From this information the robot selects the proper motion pattern and overcomes ground irregularities effectively. In order to generate the proper angel of the joint. The performance of the proposed algorithm is verified by simulation and walking experiments on a 24-DOFs biped robot.

Keywords: Force sensing resistor, fuzzy algorithm, biped robot, stabilization

1. INTRODUCTION

In this paper, a real-time walking stabilization method utilizing a fuzzy algorithm under uneven terrain is proposed. We focused most of our interest on landing phase. The ground reaction forces, measured by FSR sensors on the sole, are used to assess the ground condition and the robot posture. Simulation and experiment results for the proposed method are given in Section 3, followed by conclusions in the final section.

2. STABILIZATION

2.1 Walking pattern

Basically, a robot walks with the trajectory generated previously assuming even terrain. If different values from the expected sensor are measured during walking, the robot should be deployed using the stabilization algorithm. Fig.1 presents the walking algorithm.

When the robot is walking, it measures the ground reaction forces in real-time and utilizes them as inputs to the controller. When the control of the robot is interrupted by an unexpected situation or a unit step has ended, the new trajectory should be generated according to the changed situation. The newly verification based on the ZMP criterion. Once the stability of the trajectory is guaranteed, the robot becomes able to resume the walking.

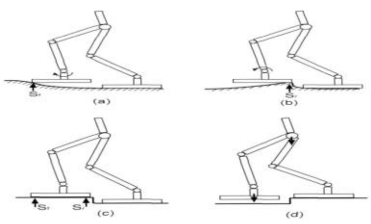

Fig. 1 The walking irregular ground condition.

2.2 Stabilization algorithm

In order to ensure that the robot walks stably, the motion should basically be stable and smooth. In addition, the robot must be able to detect approaching situations, and to control itself accordingly. When this control concept is applied, the robot is able to walk stably coping with unexpected external disturbances.

A robot can face unexpected situations during walking such as projecting ground, depressed ground, and projected ground as described in Fig.1.

3. STABILIZATION

3.1 Biped robot and sensor system

The second part consisting of the paper body must be edited in the double column format, with each column 80mm width and separated by 10mm. The top-level heading, usually called section, numbered in Arabic numerals, shall appear centered on the column with Times New Roman capital bold 11pt. The numbered level-two heading starts from the left in Times New Roman bold 10pt font. The main text uses Times New Roman 10pt font with single spacing. New paragraphs indent 4mm on the first line.

The simulation is based on a biped robot. The robot has a height of about 950mm, a weight of roughly 35kg, and 24 DOFs. The robot determines a walking pattern using the ground reaction forces measured from the sole.

The robot measures these forces using FSR sensors fixed at the sole, and the obtained data is employed as the input of the stabilization algorithm. FSR sensors are generally used for measuring the dynamic force by the variation of resistance in the force or pressure acting on the surface. FSR sensors are economical, thin, light, and easy to use. In addition, Moving-Average Filter is applied to reduced influence of the disturbance by sensor noise. Equation (1) shows the Moving-Average Filter.

$$\mathrm{R(n)}\,\frac{\sum_{i=0}^{k} f(n-i)}{k}$$

The robot measures these forces using FSR sensors fixed at the sole, and the obtained data is employed as the input of the stabilization algorithm. FSR sensors are generally used for measuring the dynamic force by the variation of resistance in the force or pressure acting on the surface. FSR sensors are economical, thin, light, and easy to use. In addition, Moving-Average Filter is applied to reduced influence of the disturbance by sensor noise. Equation (1) shows the Moving-Average Filter.

In (1) k, and R(n) are the raw sensor data at n time, orders of filter, and filtered data, respectively.

Four sensors are equipped at 4 corners of each foot. In order to minimize impact and deformation, and also to distribute repulsive power, the sole is composed of a bakelite plate and a rubber plate. The sensors are fixed between the two plates.

The robot walks according to a basic trajectory. In basic walking, a stride is 0.12m, velocity is 0.04m/s, and the ground is regarded as being flat. The robot steps on projected ground of 11mm in height with the tie if the swing leg. When the control algorithm is not applied, the sensor data is presented as given in Fig.2, The robot pushes the ground continuously, and the heel does not contact until the end of the stride.

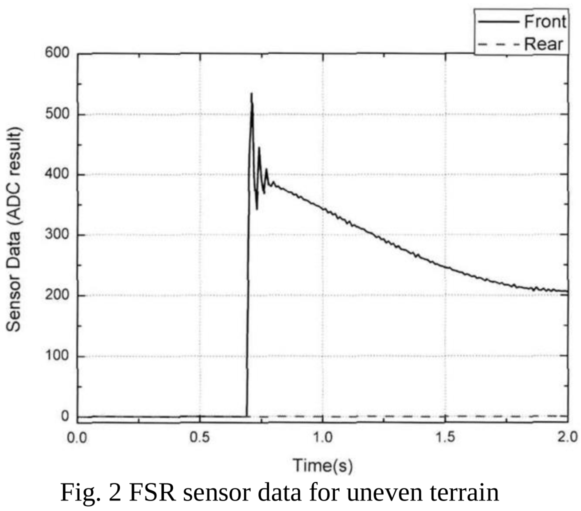

Fig. 2 FSR sensor data for uneven terrain

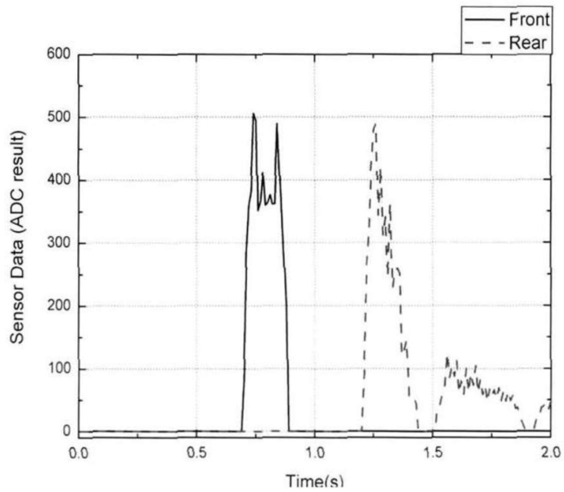

Fig. 3 Controller input for constant control.

4. CONCLUSION

This paper described a real-time control technology to implement the walking of a biped robot on uneven terrain. It was assumed that the ground condition on the basis of ground reaction forces measured sensors on the soles of the feet during walking. The robot could maintain balanced walking through control of the ankle joints using a fuzzy algorithm.

REFERENCES

[1] M. Vukobratovic and D. Juricic, "Contribution to the synthesis of biped gait," IEEE Trans. on Bio-Medical Engineering, vol. 16,pp. 1-6, 1969.

[2] K. Nishiwaki, S. Kagami, Y. Kuniyoshi, M. Inaba, and H. Inoue, "Online generation of humanoid walking motion based on a fast generation method of motion pattern that follows desired ZMP," *Proc. of IEEE/RSJ Int. Conf. on Intelligent Robots and System*, vol. 3, pp. 2684-2689,2002.

[3] D. Djoudi and C. Chevallereau, "Stability analysis of a walk of a biped with control of the ZMP," *Proc. of IEEE/RSJ Int. Conf. on Intelligent Robots and Systems*, pp. 2461-2467, 2005..

2018 Changwon International Conference on Intelligent Robot and Convergence Industry (CICIRO 2018)
Dec 13(Thusday) ~ Dec 14(Friday), 2018 Changwon International Hotel, Changwon, Korea

A Robust Neural Network Control of Robot System for Process Automation

Ki-Won Jang1, Jong-Hoon Kim1, Woo-Song Lee2, Kyung-Wha Yoon3, Uhn-Joo Na4 Sung-Hyun Han4

[1] TESS Co., Ltd, Changwon, Korea (legna911@naver.com)
[2] SUNJIN Technology Co., Ltd., Changwon, 82331, Korea (elflws@nate.com)
[3] School of Mechanical Engineering, Kyungnam University, Changwon, 51767, Korea (shhan@kyungnam.ac.kr)

Abstract: In this paper, we present two kinds of robust control schemes for robot system which has the parametric uncertainties. In order to compensate these uncertainties, we use the neural network control system that has the capability to approximate any nonlinear function over the compact input space. In the proposed control schemes, we need not derive the linear formulation of robot dynamic equation and tune the parameters. We also suggest the robust adaptive control laws in all proposed schemes for decreasing the effect of approximation error. To reduce the number of neural of network, we consider the properties of robot dynamics and the decomposition of the uncertainty function. The proposed controllers are robust not only to the structured uncertainty such as payload parameter, but also to the unstructured one such as friction model and disturbance. The reliability of the control scheme is shown by computer simulations and experiment of robot manipulator with 8 axis.

Keywords: Tracking control, decomposition, neural network, robot dynamics, uncertainty

1. INTRODUCTION

In the recent decade, increasing attention has been given to the tracking control of robot manipulators. Tracking control is needed to make each joint track a desired trajectory. A lot of research has dealt with the tracking control problem: [1]–[4] were based on VSS (variable structure system) theory, [5]–[10] on adaptive theory, and [11]–[12] on Fuzzy logic. Robots have to face many uncertainties in their dynamics, in particular structured uncertainty, such as payload parameter, and unstructured one, such as friction and disturbance. It is difficult to obtain the desired control performance when the control algorithm is only based on the robot dynamic model. To overcome these difficulties, in this paper we propose the adaptive control schemes which utilize a neural network as a compensator for any uncertainty. To reduce the error between the real uncertainty function and the compensator, we design simple and robust adaptive laws based on Lyapunov stability theory. In the proposed control schemes, the NN compensator has to see many neural because uncertainties depend on all state variables. To overcome this problem, therefore, we introduce the control schemes in which the number of neural of the NN compensator can be reduced by using the properties of robot dynamics and uncertainties. By computer simulations, it is verified that the NN is capable to compensate the uncertainties of robot manipulator. This paper is organized as follows. Section 2 presents NN System. In Section 3, several properties of robot dynamics are introduced. In Section4, the adaptive control scheme is proposed, where the NN is utilized to compensate the uncertainties of the robot manipulator. The robust adaptive law is also designed. The algorithms that reduce the number of neural are proposed based on the properties of robot dynamics and uncertainties in Section 5. The decomposition algorithm of uncertainty function and results of computer simulations for the control scheme and experiment on dual-arm robot are also drawn in Section 6. In Section 7, we obtain the conclusions and discussion.

2. CONTROLLER DESIGN

2.1 Multiple Layers of Neurons

A network can have several layers. Each layer has a weight matrix ***W***, a bias vector ***b***, and an output vector ***a***. To distinguish between the weight matrices, output vectors, etc., for each of these layers in the figures, the number of the layer is appended as a superscript to the variable of interest. You can see the use of this layer notation in the three-layer network shown below, and in the equations at the bottom of the figure.

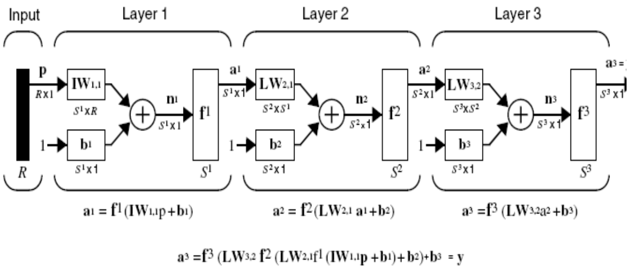

Fig. 1. MLP neural network

2.2 Dynamic, Nonlinear MLP Neural Network

This neural network consist of a number of layers and delay. The input and output of this network is dynamic and nonlinear.

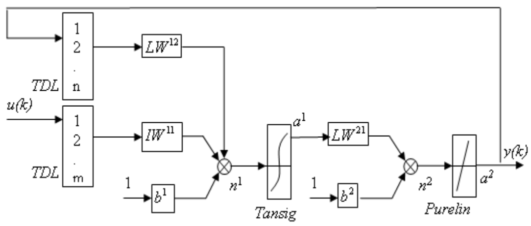

Fig. 2. Structure of dynamic, nonlinear neural network

To create adaptive characteristic for neural network controller, we design a neural network compensator following equation below:

$$y = \Theta^T \zeta(x) \quad (1)$$

Where $\zeta(x)$ is output of neural network and Θ is matrix of adaptive parameters

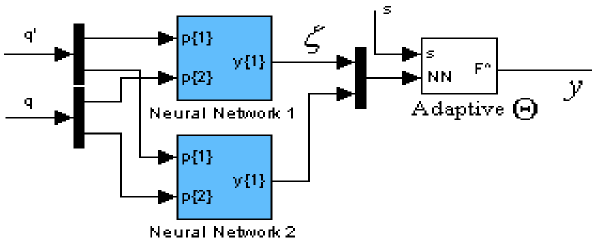

Fig. 3. The structure of adaptive neural network

3. DYNAMIC MODELING AND CONTROL OF ROBOT SYSTEM

A robot manipulator is defined as an open kinematic chain of rigid links. Each degree of freedom of the manipulator is powered by independent torques. Using the Lagrangian formulation, the equations of motion of an -degree-of-freedom manipulator can be written as

$$D(q)\ddot{q} + C(q,\dot{q})\dot{q} + G(q) + F_r(\dot{q}) + \tau_d = \tau \quad (2)$$

where $q \in R^n$ is the generalized coordinates; $D(q) \in R^{n\times n}$ is the symmetric, bounded, positive-definite inertia matrix; vector $C(q,\dot{q})\dot{q} \in R^n$ presents the centripetal and Coriolis torques; $\tau_d \in R^n$, $G(q) \in R^n$, $F_r(\dot{q}) \in R^n$ and $\tau \in R^n$ represent the gravitational torques, friction, disturbance, and applied joint torques, respectively.

The robot model (2) is characterized by the following structural properties.

Property 1: There exists a vector $\alpha \in R^m$ with components depending on manipulator parameters (masses, moments of inertia, etc.), such that

$$D(q).\ddot{q}_r + C(q,\dot{q})\dot{q}_r + G(q) + F_r(\dot{q}) + \tau_d = \varphi(q,\dot{q},\ddot{q})\alpha \quad (3)$$

where $\varphi(q,\dot{q},\ddot{q}) \in R^{nxm}$ is called the regressive matrix.

This property means that the dynamic equation can be linearized with respect to a specially selected set of manipulator parameters.

Property 2: Using a proper definition of matrix $C(q,\dot{q})$, both $C(q,\dot{q})$ and $D(q)$ are not independent and satisfy

$$x^T(\dot{D} - 2C)x = 0, \qquad \forall x \in R^n \quad (4)$$

that is, $(\dot{D} - 2C)$ is a skew-symmetric matrix.

This property is simply a statement that the so-called fictitious forces, defined by $C(q,\dot{q})\dot{q}$, do not work on the system. This property is utilized in stability analysis.

Property 3: The friction in the dynamic equation (2) is of the form

$$F_r(\dot{q}) = F_v\dot{q} + F_d(\dot{q}) \quad (5)$$

with F_v the coefficient matrix of viscous friction and $F_d(\dot{q})$ a dynamic friction term. Since friction is a local effect, $F_r(\dot{q}) = F_v\dot{q} + F_d(\dot{q})$ is uncoupled among the joints. The friction is dependent on only angular velocity $\dot{q}$.

This property is utilized in this paper in order to reduce the number of neural in the neural network compensator.

The considered tracking problem is stated as follows: Knowing desired trajectories $q_d \in R^n$, $\dot{q}_d \in R^n$, with some or all the manipulator parameters unknown, determine a control law τ and a sliding surface $s = 0$ such that sliding mode occurs on the sliding surface, the tracking error $\tilde{q} = q - q_d$ has a prescribed transient response and it goes to zero asymptotically as $t \to \infty$.

A. Simple Adaptive Control Law

The sliding surface $s = 0$ is chosen as a hyperplane

$$s = \dot{\tilde{q}} + \Lambda\tilde{q} \quad (6)$$

where Λ is a positive-definite matrix whose eigenvalues are strictly in the right-half complex plane and $\tilde{q}$ is the tracking error vector.

If the sliding mode exists on $s = 0$, then from the theory of VSS, the sliding mode is governed by the following linear differential equation whose behavior is dictated by the sliding hyperplane design matrix Λ :

$$\dot{\tilde{q}} = -\Lambda\tilde{q} \quad (7)$$

Obviously, the tracking error transient response is then determined entirely by the eigenvector structure of the matrix Λ.

In order to derive the sliding mode control law, which forces the motion of the error to be along the sliding surface $s = 0$, a vector of self-defined reference variables is introduced for the succinct formula expression in the sequel, that is,

$$\dot{q}_r(t) = \dot{q}_d(t) - \Lambda\tilde{q}(t) \quad (8)$$

Consider now the uncertainties of robot manipulator, (2) can be rewritten as

$$D(q)\ddot{q} + C(q,\dot{q})\dot{q} + G(q) + F(q,\dot{q},t) = \tau \quad (9)$$

Where $F(q,\dot{q},t) = F_r(\dot{q}) + \tau_d$. However, in this paper, this uncertainty function vector has to be replaced by $F(q,\dot{q},t)$

So (9) can be rewritten as

$$D(q)\ddot{q} + C(q,\dot{q})\dot{q} + G(q) + F(q,\dot{q},\ddot{q},t) = \tau \quad (10)$$

we let a Lyapunov function candidate be

$$V(t) = \frac{1}{2}(s^T D s + \sum_{i=1}^{n} \tilde{\Theta}_i^T \Gamma_i \tilde{\Theta}_i) \quad (11)$$

Where $\tilde{\Theta}_i = \Theta_i^* - \Theta_i, \Theta^*$ is the j th column vector of the optimal parameter matrix Θ^* and Γ_i is a strictly positive real constant.

Differentiating $V(t)$ with respect to time yields

$$\dot V(t) = s^T D\dot s + \frac{1}{2}s^T\dot D s + \sum_{i=1}^{n}\Theta_i^T\Gamma_i\dot\Theta_i$$
$$= -s^T(D\ddot q_r + C\dot q_r + G + F - \tau) + \sum_{i=1}^{n}\tilde\Theta_i^T\Gamma_i\tilde\Theta_i \qquad (12)$$

Where $F(q,\dot q,\ddot q,t)$ is a completely unknown nonlinear function vector. Therefore, we replace $F(q,\dot q,\ddot q,t)$ by a Neural network $\hat F(q,\dot q,\ddot q|\Theta)$ .Let us define the control law as

$$\tau = D(q).\ddot q_r + C(q,\dot q)\dot q_r + G(q) + \hat F(q,\dot q,\ddot q\,|\,\Theta) - K_D s \quad (13)$$

Where $K_d = diagK_i, \quad i = 1,2,...,n,$ and

$$\hat F(q,\dot q,\ddot q\,|\,\Theta) = \begin{bmatrix}\Theta_1^T\zeta(q,\dot q,\ddot q)\\ \Theta_2^T\zeta(q,\dot q,\ddot q)\\ ....\\ ....\\ .....\\ \Theta_n^T\zeta(q,\dot q,\ddot q)\end{bmatrix} \qquad (14)$$

Letting the optimal parameter matrix of the NN, we can define the minimum approximation error vector

$$w = F(q,\dot q,\ddot q,t) - \hat F(q,\dot q,\ddot q|\Theta). \qquad (15)$$

Therefore,

$$\dot V = -s^T K_D s - s^T w + \sum_{l=1}^{m}\left(\dot{\tilde\Theta}_l^T\Gamma_l\dot{\tilde\Theta}_l - s_l\tilde\Theta_l^T\zeta(q,\dot q,\ddot q)\right) \quad (16)$$

where $\tilde\Theta_i = \Theta_i^* - \Theta_i$ and $\zeta(q,\dot q,\ddot q)$ is a neural network basis function. Therefore, the adaptation laws are

$$\dot\Theta_i = -\Gamma_i^{-1}s_i\zeta(q,\dot q,\ddot q), \qquad i = 1,2,...,n \qquad (17)$$

Then

$$\dot V(t) = -s^T K_D s - s^T w \qquad (18)$$

Because the term $s^T w$ is of the order of the minimum approximation error and from the universal approximation theorem, it is expected that w should be very small, i.e., $w \le \varepsilon$, if not equal to zero in the adaptive neural network system. The proposed control scheme is shown in Fig. 4.

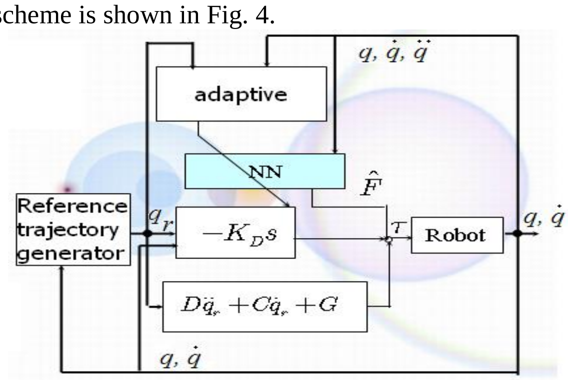

Fig. 4. the structure of the control systems

B. Robust Adaptive Control Law

Equation (16) contains the term $s^T w$; in this subsection, we propose the robust control law to reduce the approximation error. So we add a term to (13) as follows:

$$\tau = D(q).\ddot q_r + C(q,\dot q)\dot q_r + G(q)$$
$$+ \hat F(q,\dot q,\ddot q\,|\,\tilde\Theta) - K_D s - W.sign(s) \qquad (19)$$

Where

$$W = diag\left[w_{M1}, w_{M2}, w_{M3},.... w_{Mn}\right]$$
$$w_{Mi} \ge |w_l|, i = 1,2,...., n$$

Now consider the Lyapunov candidate (11) as well as (17) and (19) and, after straightforward manipulation, we obtain the time derivative as follows:

$$\dot V(t) = -s^T Ds_i \le 0$$

A. Friction

From Section III, we can see that the friction is dependent on $\dot q$ and uncoupled among the joints.

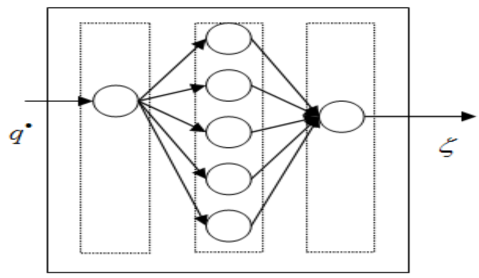

Fig. 5. The structure of a neural network as fiction compensator $\hat F(\dot q\,|\,\Theta) = \Theta^T\zeta$

Simple Control Law:

$$\tau = D(q).\ddot q_r + C(q,\dot q)\dot q_r + G(q) + \hat F(\dot q\,|\,\Theta) - K_D s \qquad (20)$$

Robust Control Law:

$$\tau = D(q).\ddot q_r + C(q,\dot q)\dot q_r + G(q) + \hat F(\dot q\,|\,\Theta)$$
$$- K_D s - W sign(s) \qquad (21)$$

Adaptive Law:

$$\dot\theta_i = -\Gamma_i^{-1}s_i\zeta^i(\dot q), \qquad i = 1,2,...,n \qquad (22)$$

B. Disturbance

From (7), considering only disturbance,

$F(q,\dot q,t) = \tau_d(t)$, the resulting control and adaptive laws are as follows.

Simple Control Law:

$$\tau = D\ddot q_r + C\dot q_r + G + \hat F(q,\dot q|\theta) - K_D s \qquad (23)$$

Robust Control Law:

$$\tau = D\ddot q_r + C\dot q_r + G + \hat F(q,\dot q|\theta) - K_D s - Wsign(s) \quad (24)$$

Adaptive Law:

$$\dot\Theta_i = -\Gamma_i^{-1}s_i\zeta^i(q,\dot q), \qquad i = 1,2,...,n \qquad (25)$$

Therefore we use the structure of the neural network as friction, disturbance compensator following:

4. EXPERIMENT AND RESULTS

We also apply real-time adaptive control based on neural network compensator to dual-arm robot shown in figs. 6 – 8. Because the characteristics of two arms are the same, so we show the results into one arm is enough.

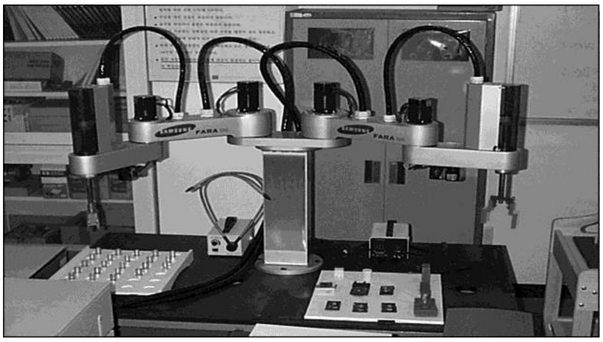

Fig. 6. Experimental set-up

All the algorithm calculation is calculated by Matlab and Simulink matlab on host computer and push into dual-arm robot which is shown in the Fig. 7. The desired trajectories are

$q_{1d} = q_{2d} = 15\pi \sin(\frac{2\pi}{300\pi} t - \frac{2\pi}{3})$ and the results of robust adaptive control are shown below

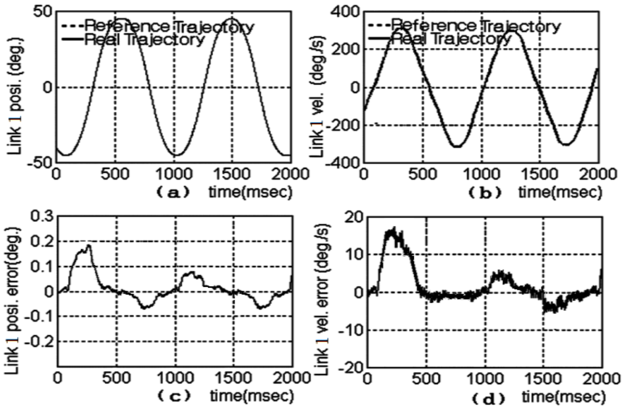

Fig. 7. (a)-(d) Experimental results for the position and velocity tracking of adaptive controller at the first joint.

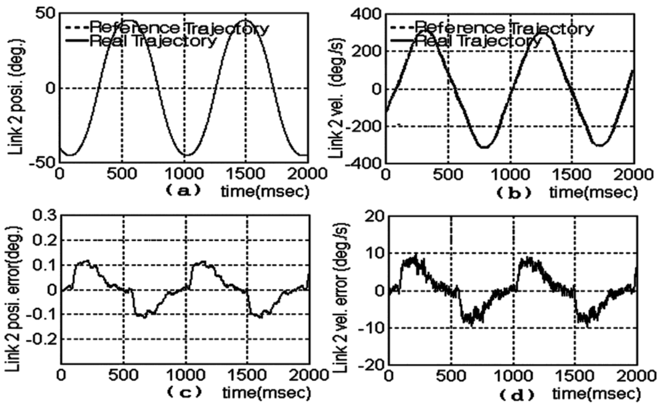

Fig. 8. (a)-(d) Experimental results for the position and velocity tracking of adaptive controller at the second joint.

7. CONCLUSIONS

In the results, we can see that the control objective is well accomplished and the neural network compensate the uncertainties. Especially, we observe that Fig. 10. is more better than Fig. 11. Because the robust control laws have the signum function $W\,\mathrm{sgn}(s)$. In all cases, robust control schemes are more effective than simple. The simulation and experimental results show that the neural network compensator - adaptive controller is robust to the payload variation, inertia parameter uncertainty and change of reference trajectory.

In addition, the proposed control technology needs to apply to robot manipulators include more joints, and degree of freedom. The research continues on the more general algorithms of the number and structure of neural network and it should be studied further for standard specification in manufacturing process.

REFERENCES

[1] G. Jumarie, "Tracking control of mechanical systems via sliding Lagrangian," J. Intell. Robotic Syst., vol. 13, pp. 181–199, 1995.

[2] C. Y. Su and T. P. Leung, "A sliding mode controller with bound estimation for robot manipulators," IEEE Trans. Robotics Automat., vol. 9, no. 2, pp. 208–214, 1993.

[3] J. E. Slotin and S. S. Sastry, "Tracking control of nonlinear systems using sliding surfaces, with application to robot manipulators," Int. J. Contr., vol. 38, no. 2, pp. 465–492, 1983.

[4] J. J. E. Slotine and W. Li, Applied Nonlinear Control. Englewood Cliffs, NJ: Prentice-Hall, 1991.

[5] F. L. Lewis, C. T. Abdallah, and D. M. Dawson, Control of Robot Manipulators. London, U.K.: Macmillan, 1993.

[6] M. W. Spong, Robot Dynamics and Control. New York: Wiley, 1989.

[7] W. C. Ham, "Adaptive nonlinear control of one-link flexible arm," in IEEE/RSJ Int. Conf. Intelligent Robots and Systems, vol. 1, Yokohama, Japan, 1993, pp. 3–7.

[8] "Adaptive control based on explicit model of robot manipulators," IEEE Trans. Automat. Contr., vol. 38, pp. 654–658, 1993.

[9] "Adaptive control based on speed gradient algorithm for robot manipulators," in Int. Conf. Industrial Electronics Control and Instrumentation, vol. 2, Bologna, Italy, 1994, pp. 776–781.

[10] B.K. Yoo, W.C. Ham "Adaptive Control of Robot Manipulator Using Fuzzy Compensator". IEEE transaction on Fuzzy System. VOL. 8. NO. 2. April 2000.

A Study on the Trajectory Control and Control of Robot Arm with Seven Joint

Du-Beum Kim ,Keun-Hwan Dong ,Geo-Seung Choi2, Byung-Seuk Yoon3, Sung-Hyun Han4

[1] Department of Advanced Engineering., Kyungnam University, Changwon, 51767, Korea
(E-mail : kms21018@naver.com)
[2]SAMHYUN CO. Ltd., Changwon, 51398, Korea (E-mail : gschoi@samhyun.co.kr)
[3]Dongmyeongjeong-gi Co., Ltd., Changwon, 51561, Korea (E-mail : bsyoon@naver.com)
[4] SMEC co., Ltd. Gimhae City, 50969, Korea
(Tel : +82-10-4582-8264; E-mail : won@esmec.com)
[5]School of Mechanical Engineering, Kyungnam University, Changwon, 51767, Korea
(Tel: +82-10-3585-5111; E-mail: shhan@kyungnam.ac.kr)

Abstract: In this study, we proposed robust control schemes for robot system which has the parametric uncertainties in forging process. In order to compensate these uncertainties, we use the neural control algorithm that has the capability to approximate any nonlinear model over the precise input space. In the proposed control schemes, it is not necessary to drive the linear formulation of robot dynamic equation and tune the parameters. We also suggest the robust adaptive control laws in all proposed schemes for decreasing the effect of approximation error. To reduce the number of neural of network, we consider the properties of robot dynamics and the decomposition of the uncertainty function. The proposed controllers are robust not only to the structured uncertainty such as payload parameter, but also to the unstructured one such as friction model and disturbance. The reliability of the control scheme is shown by computer simulations and experiment of robot manipulator with 6 axis in forging process.

Keywords: Robust control, decomposition, neural network, robot dynamics, uncertainty .

1. INTRODUCTION

To overcome these difficulties, in this paper we propose the adaptive control schemes which utilize a neural network as a compensator for any uncertainty. To reduce the error between the real uncertainty function and the compensator, we design simple and robust adaptive laws based on nonlinear stability method. In the proposed schemes, the compensator has to see many neural because uncertainties depend on all state variables. To overcome this problem, therefore, we introduce the control schemes in which the number of neural of the NN compensator can be reduced by using the properties of robot dynamics and uncertainties.

2. PATH PLANNING AND CONTROL

A robot manipulator is defined as an open kinematic chain of rigid links. Each degree of freedom of the manipulator is powered by independent torques. Using the Lagrangian formulation, the equations of motion of an -degree-of-freedom manipulator can be written as

$$D(q)\ddot{q}+C(q,\dot{q})\dot{q}+G(q)+F_r(\dot{q})+\tau_d = \tau \quad (1)$$

where $q \in R^n$ is the generalized coordinates; $D(q) \in R^{n\times n}$ is the symmetric, bounded, positive-definite inertia matrix; vector $C(q,\dot{q})\dot{q} \in R^n$ presents the centripetal and Coriolis torques; $\tau_d \in R^n$, $G(q) \in R^n$, $F_r(q) \in R^n$ and $\tau \in R^n$ represent the gravitational torques, friction, disturbance, and applied joint torques, respectively.

The robot model (2) is characterized by the following structural properties.

This property is utilized in this paper in order to reduce the number of neural in the neural network compensator.

The considered tracking problem is stated as follows: Knowing desired trajectories $q_d \in R^n$, $\dot{q}_d \in R^n$, with some or all the manipulator parameters unknown, determine a control law τ and a sliding surface $s = 0$ such that sliding mode occurs on the sliding surface, the tracking error $\tilde{q} = q - q_d$ has a prescribed transient response and it goes to zero asymptotically as $t \to \infty$.

A. Simple Adaptive Control Law

The sliding surface $s = 0$ is chosen as a hyperplane

$$s=\dot{\tilde{q}}+\Lambda\tilde{q} \quad (5)$$

where Λ is a positive-definite matrix whose eigenvalues are strictly in the right-half complex plane and $\tilde{q}$ is the tracking error vector.

If the sliding mode exists on $s = 0$, then from the theory of VSS, the sliding mode is governed by the following linear differential equation whose behavior is dictated by the sliding hyperplane design matrix Λ :

$$\dot{\tilde{q}}=-\Lambda\tilde{q} \quad (6)$$

Obviously, the tracking error transient response is then determined entirely by the eigenvector structure of the matrix Λ .

In order to derive the sliding mode control law, which forces the motion of the error to be along the sliding surface $s = 0$, a vector of self-defined reference variables is introduced for the succinct formula expression in the sequel, that is,

$$\dot{q}_r(t)=\dot{q}_d(t)-\Lambda\tilde{q}(t) \quad (7)$$

Consider now the uncertainties of robot manipulator, (1) can be rewritten as

$$D(q)q + C(q,q)q + G(q) + F(q,q,t) = \tau \quad (8)$$

Where $F(q,\dot{q},t) = F_r(\dot{q}) + \tau_d$. However, in this paper, this uncertainty function vector has to be replaced by $F(q,\dot{q},t)$

So (9) can be rewritten as

$$D(q)\ddot{q} + C(q,\dot{q})\dot{q} + G(q) + F(q,\dot{q},\ddot{q},t) = \tau \quad (9)$$

we let a Lyapunov function candidate be

$$V(t) = \frac{1}{2}(s^T Ds + \sum_{i=1}^{n} \tilde{\Theta}_i^T \Gamma_i \tilde{\Theta}_i) \quad (10)$$

Where $\tilde{\Theta}_i = \Theta_i^* - \Theta_i$, Θ^* is the *j* th column vector of the optimal parameter matrix Θ^* and Γ_i is a strictly positive real constant.

Differentiating $V(t)$ with respect to time yields

$$\dot{V}(t) = s^T D\dot{s} + \frac{1}{2} s^T \dot{D} s + \sum_{i=1}^{n} \tilde{\Theta}_i^T \Gamma_i \dot{\tilde{\Theta}}_i$$

$$= -s^T (D\dot{q}_r + Cq_r + G + F - \tau) + \sum_{i=1}^{n} \Theta_i^T \Gamma_i \Theta_i \quad (11)$$

Where $F(q, \dot{q}, \ddot{q}, t)$ is a completely unknown nonlinear function vector. Therefore, we replace $F(q, \dot{q}, \ddot{q}, t)$ by a Neural network $\hat{F}(q,\dot{q},\ddot{q}|\Theta)$ .Let us define the control law as

$$\tau = D(q).\ddot{q}_r + C(q,\dot{q})\dot{q}_r + G(q) + \hat{F}(q,\dot{q},\ddot{q} \mid \Theta) - K_D s \quad (12)$$

Where $K_d = diag K_i$, $i = 1, 2, ..., n$, .

3. EXPERIMENT AND RESULTS

We also apply real-time adaptive control based on neural network compensator to dual-arm robot shown in figs. 1. Because the characteristics of two arms are the same, so we show the results into one arm is enough.

Fig. 1. Experimental set-up

All the algorithm calculation is calculated by Matlab and Simulink matlab on host computer and push into dual-arm robot which is shown in the Fig. 2. The desired trajectories are

$$q_{1d} = q_{2d} = 15\pi \sin\left(\frac{2\pi}{300\pi} t - \frac{2\pi}{3}\right)$$

and the results of robust adaptive control are shown below

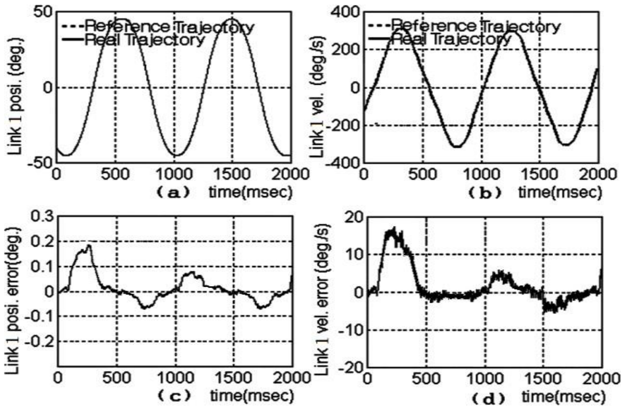

Fig. 2. (a)-(d) Experimental results for the position and velocity tracking of adaptive controller at the first joint.

4. CONCLUSIONS

In this paper, we have illustrated that the control objective is well accomplished and the neural network compensate the uncertainties. In addition, the proposed control technology needs to apply to robot manipulators include more joints, for forging process automation.

ACKNOWLEDGEMENT

This study was performed by project of the robot business belt construction enterprise..

REFERENCES

[1] J. E. Slotin and S. S. Sastry, "Tracking control of nonlinear systems using sliding surfaces, with application to robot manipulators," Int. J. Contr., vol. 38, no. 2, pp. 465–492, 1983.

[2] J. J. E. Slotine and W. Li, Applied Nonlinear Control. Englewood Cliffs, NJ: Prentice-Hall, 1991.

[3] F. L. Lewis, C. T. Abdallah, and D. M. Dawson, Control of Robot Manipulators. London, U.K.: Macmillan, 1993.

[4] M. W. Spong, Robot Dynamics and Control. New York: Wiley, 1989.

[5] W. C. Ham, "Adaptive nonlinear control of one-link flexible arm," in IEEE/RSJ Int. Conf. Intelligent Robots and Systems, vol. 1, Yokohama, Japan, 1993, pp. 3–7.

[6] "Adaptive control based on explicit model of robot manipulators," IEEE Trans. Automat. Contr., vol. 38, pp. 654–658, 1993.

2018 Changwon International Conference on Intelligent Robot and Convergence Industry (CICIRO 2018)
Dec 13(Thusday) ~ Dec 14(Friday), 2018 Changwon International Hotel, Changwon, Korea

A Robust Control of Mobile Robot by Voice Command for FA

Yang-Keun Jeong 1 , Hee-Jin Kim 2, Woo-Song Lee 3, Yeon-Guk Noh 4, Geo-Seung Choi 5, Sung-Hyun Han 6

[1] Shinla Information Technology Co., Ltd., Changwon, 51390, Korea (shintech@hanmail.net) * Corresponding author
[2] Department of Mechanical engineering, Graduate School of Industry & Business administration Graduate School Kyungnam University, Changwon, 51767, Korea (jizhen79@nate.com)
[3] SUNJIN Technology co., Ltd., Changwon, 82331, Korea (elflws@hanmail.net)
[4] SFNT Co., Ltd., Changwon, 631-821, Korea (ykno1339@naver.com)
[5] SAMHYUN Co., Ltd, Changwon, 51398, Korea(gschoi@samhyun.co.kr)
[6] Department of Mechanical Engineering, Kyungnam University Changwon, 51767 Korea (shhan@kyungnam.ac.kr)

Abstract: Generally, it is possible to control the walking information based on the mobile robot's own postures, because a type of motion and gesture produces almost the same pattern of noise every time. In this paper, we describe a voice recognition control technology for mobile robot system which can robustly recognize voice by adults and children in noisy environments. We prove the performance of robot control system in a communication robot placed in a real noisy environment. Voice is captured using a wireless communication.

Keywords: Robust voice recognition, Side-lobe canceller, Navigation system

1. INTRODUCTION

Each kind of robot motion or gesture produces almost the same noises every time it is performed. By recording the motion and gesture noises in advance, the noises are easily estimated. By using this, we introduce a new method under robot motor noise. These methods can utilize pre-recorded noises as described later. Since each of these techniques has advantages and disadvantages, whether it is effective depends on the types of motion and gesture. The result of an experiment of isolated word recognition under a variety of motion and gesture noises suggested the effectiveness of this approach.

2. ROBOT SYSTEM

In this study, a sonar array composed of 16 ultrasonic sensors cannot be fired simultaneously due to cross talk. Instead, we adopt a scheduled firing method where sensors are activated in sequence of $\{s_1, s_{12}, s_2, s_{11} \ldots\}$. The arrangement of the ultrasonic sensors in upper layer and the sensors are marked as dots in the figure. The distances e_j $(j = 1, 2, \ldots 12)$ from the origin of the robot frame {R} to obstacles detected by the sensor s_j, can be defined as $e_j = \delta_j + R_r$. Here, R_r is the radius of the robot and the δ_j, is the range value measured by the sensor s_j .

$$u(t) = (v(t), \Delta\theta(t))^T = (v(t), w(t), Tms)^T \tag{1}$$

3. EXPERIMENT

The proposed robot has the maximum travel speed of 0.55 m/s and the maximum steering rate of 3.0rad/sec. Experiments are performed in an indoor with the first experiment for voice recognition without objects and second experiment for both of them: voice recognition and obstacles avoidance.

4. CONCLUSION

This paper proposed the integration of robust voice recognition and navigation system capable of performing autonomous navigation in unknown environments. In order to evaluate the performance of the overall system, a number of experiments have been undertaken in various environments.

REFERENCES

[1] M. Blanchet, J. Boudy, and P. Lockwood, "Environment adaptation for speech recognition in noise," in Proc. of EUSIPCO-92, vol. VI,1992, pp. 391–394.

A Robust Motion Control of Bipped Robot with 28 Joints

Hyun-Min Kim[1], Min-Seong Kim[2], Hyun-Woo Song[3], Yang-Keun Jung[4]

[1] Department of Advanced Engineering., Kyungnam University, Changwon, 51767, Korea
(E-mail : khm9153@nate.com)
[2] Department of Advanced Engineering., Kyungnam University, Changwon, 51767, Korea
(E-mail : kms21018@naver.com)
[3] Department of Mechatronics Engineering., Kyungnam University, Changwon, 51767, Korea
(E-mail : thgudn@naver.com)
[4] Shinla Information Technology CO., Ltd., Changwon City,
51390, Korea (E-mail : shintech@hanmail.net)

Abstract : This paper deals with the stable walking for a humanoid robot, on uneven terrain, A humanoid robot necessitates achieving posture stabilization since it has basic problems such as structural instability. In this paper, a stabilization algorithm is proposed using the ground reaction forces, which are measured using FSR (Force Sensing Resistor) sensors during walking, and the ground conditions are estimated from these data. From this information the robot selects the proper motion pattern and overcomes ground irregularities effectively. In order to generate the proper angel of the joint. The performance of the proposed algorithm is verified by simulation and walking experiments on a 24-DOFs humanoid robot.

Keywords Force sensing resistor, fuzzy algorithm, humanoid robot, stabilization

1. INTRODUCTION

In this paper, a real-time walking stabilization method utilizing a fuzzy algorithm under uneven terrain is proposed. We focused most of our interest on landing phase. The ground reaction forces, measured by FSR sensors on the sole, are used to assess the ground condition and the robot posture. Simulation and experiment results for the proposed method are given in Section 3, followed by conclusions in the final section.

2. STABILIZATION

2.1 Walking pattern

Basically, a robot walks with the trajectory generated previously assuming even terrain. If different values from the expected sensor are measured during walking, the robot should be deployed using the stabilization algorithm. Fig.1 presents the walking algorithm.

When the robot is walking, it measures the ground reaction forces in real-time and utilizes them as inputs to the controller. When the control of the robot is interrupted by an unexpected situation or a unit step has ended, the new trajectory should be generated according to the changed situation. The newly verification based on the ZMP criterion. Once the stability of the trajectory is guaranteed, the robot becomes able to resume the walking.

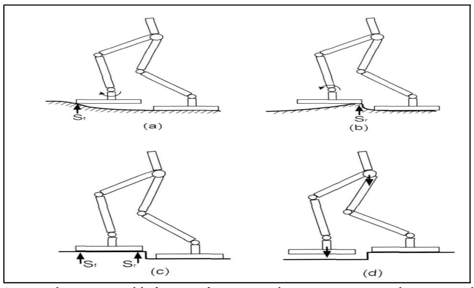

Fig. 1. The walking irregular ground condition.

2.2. Stabilization algorithm

In order to ensure that the robot walks stably, the motion should basically be stable and smooth. In addition, the robot must be able to detect approaching situations, and to control itself accordingly. When this control concept is applied, the robot is able to walk stably coping with unexpected external disturbances.

A robot can face unexpected situations during walking such as projecting ground, depressed ground, and projected ground as described in Fig.1.

3. EXPERIMENT AND RESULT

3.1 Humanoid robot and sensor system

The simulation is based on a humanoid robot. The robot has a height of about 950mm, a weight of roughly 35kg, and 24 DOFs. The robot determines a walking pattern using the ground reaction forces measured from the sole.

The robot measures these forces using FSR sensors fixed at the sole, and the obtained data is employed as the input of the stabilization algorithm. FSR sensors are generally used for measuring the dynamic force by the variation of resistance in the force or pressure acting on the surface. FSR sensors are economical, thin, light, and easy to use. In addition, Moving-Average Filter is applied to reduced influence of the disturbance by sensor noise. Equation (1) shows the Moving-Average Filter.

$$R(n)\frac{\sum_{i=0}^{k} f(n-i)}{k} \qquad (1)$$

In (1),,k, and R(n) are the raw sensor data at n time, orders of filter, and filtered data, respectively.
Four sensors are equipped at 4 corners of each foot. In order to minimize impact and deformation, and also to distribute repulsive power, the sole is composed of a bakelite plate and a rubber plate. The sensors are fixed between the two plates.

The robot walks according to a basic trajectory. In basic walking, a stride is 0.12m, velocity is 0.04m/s, and the ground is regarded as being flat. The robot steps on projected ground of 11mm in height with the tie if the swing leg. When the control algorithm is not applied, the sensor data is presented as given in Fig.2, The robot pushes the ground continuously, and the heel does not contact until the end of the stride.

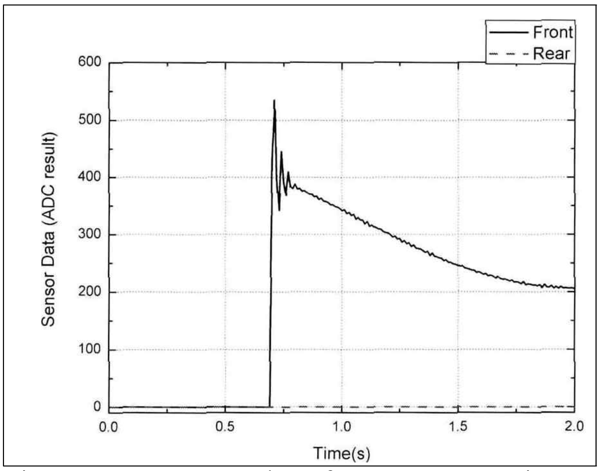

Fig. 2. FSR sensor data for uneven terrain

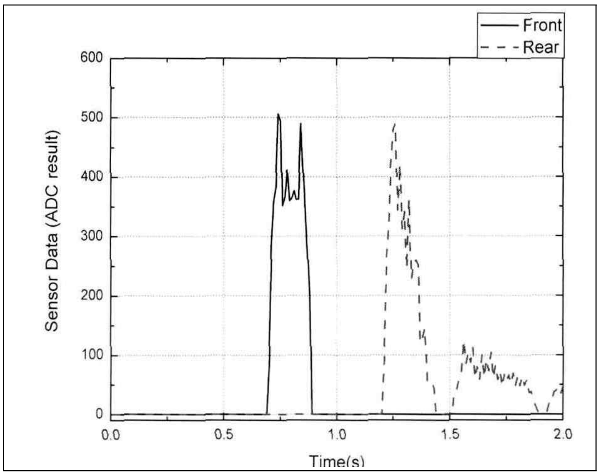

Fig. 3. Controller input for constant control.

4. CONCLUSION

This work was supported (National Robotics Research Center for Robot Intelligence Technology, Kyungnam University) by Ministry of Knowledge Economy under Human Resources Development Program for Convergence

REFERENCES

[1] M. Vukobratovic and D. Juricic, "Contribution to the synthesis of biped gait," IEEE Trans. on Bio-Medical Engineering, vol. 16,pp. 1-6, 1969.

[2] K. Nishiwaki, S. Kagami, Y. Kuniyoshi, M. Inaba, and H. Inoue, "Online generation of humanoid walking motion based on a fast generation method of motion pattern that follows desired ZMP," Proc. of IEEE/RSJ Int. Conf. on Intelligent Robots and System, vol. 3, pp. 2684-2689,2002.

[3] D. Djoudi and C. Chevallereau, "Stability analysis of a walk of a biped with control of the ZMP," Proc. of IEEE/RSJ Int. Conf. on Intelligent Robots and Systems, pp. 2461-2467, 2005..